Resource allocation in *Eucalyptus*

By

Courtney Eugene Campany

A thesis submitted in fulfilment of the requirements

for the degree of Doctor of Philosophy

WESTERN SYDNEY
UNIVERSITY

Hawkesbury Institute
for the Environment

2016

Acknowledgements

“I am the Lorax. I speak for the trees. I speak for the trees for the trees have no tongues.”

Dr. Seuss

I dedicate this thesis to my mother, for she has been my inspiration to become a scientist for as long as I can remember. Her passion for the natural world is infectious and her ability to pass her scientific knowledge to others is inspirational. It is because of you that I flip over rocks to see what is hiding underneath.

I would equally like to acknowledge my father for instilling in me the work ethic and drive that has carried me to this point. Without his undying support I might never have achieved the level of success I have been afforded.

À Caroline, rien de tout ça n’aurait été possible sans que tu sois à mes côtés. Tu as été un roc quand j’avais besoin d’ancrage et une lumière quand mon chemin semblait perdu.

I am sincerely grateful to my principal supervisor, Dr. Remko Duursma, and my supervisory committee, Prof. Mark Tjoelker and Prof. Belinda Medlyn, for their excellent mentoring and support.

Statement of Authentication

The work presented in this thesis is, to the best of my knowledge and belief, original except as acknowledged in the text. I hereby declare that I have not submitted this material, either in full or in part, for a degree at this or any other institution.

Table of Contents

LIST OF TABLES

LIST OF FIGURES

Figure 2.6. Total carbon mass for harvested and modeled seedlings versus predicted total carbon gain after 120 days (a) and reductions in final seedling carbon mass, both modeled and observed, as a function of the reduction in leaf photosynthesis across treatments (b).

Figure 2.S1. Sensitivity testing of the seedling growth model to different carbon allocation strategies including; constraints of leaf mass fraction to treatment specific final harvest values (a) and increases in respiration of non-leaf tissue components by 50 % (b).

Figure 3.1. Bars represent the local light environment for sun and shade leaves during six gas exchange campaigns from October 2013 to April 2014.

Figure 3.2. (a) AC_i curves for sun and shade leaves at elevated (ET) and ambient (AT) temperature treatments.

Figure 3.3. The response of A_n to g_s (a) and g_m (b) for sun leaves measured at high light and shade leaves measured at both low and high light under their respective elevated and ambient temperature treatments.

Figure 3.4. The mean ± 1 standard error of g_s (a), g_m (b) and A_n (c) of sun leaves and shade leaves at both low and high light pooled across six measurement dates.

Figure 3.5. (a) Response of instantaneous transpiration efficiency (ITE) to VPD for sun leaves and shade leaves at both low and high light with elevated and ambient temperature treatments. (b) The relationship between leaf $\delta^{13}C$ and leaf N_a for sun leaves at high light and shade leaves at low light.

Figure 3.6. Relationship between the observed discrimination of $^{13}CO_2$ measured during photosynthesis (Δ_o) and measured C_i/C_a for sun leaves measured at high light and shade leaves measured at both low and high light.

Figure 3.7. The mean ± 1 standard error of (a) intercellular CO_2 concentration (C_i), (b) CO_2 concentration in the chloroplasts (C_c) and (c) CO_2 drawdown from substomatal cavities to sites of carboxylation of sun leaves and shade leaves at both low and high light (C_i-C_c).

Figure 3.S1. . Daily maximum and minimum temperature (a), daily maximum VPD (b) and total daily PPFD (c) for each chamber across the experiment duration.

Figure 3.S2. Photosynthetic CO_2 response (AC_c) curves for sun and shade leaves at elevated and ambient temperature treatments.

Figure 3.S3. Response of A_n (a), g_m (b) and C_i-C_c to leaf temperature for sun leaves and shade leaves at low and high light.

LIST OF ABBREVIATIONS

A_n	Net leaf photosynthesis rate
aC_a	Ambient CO_2 treatment
AC_i	Photosynthetic CO_2 response curves
A_{max}	Leaf net photosynthesis at saturating light and CO_2 concentration
A_{sat}	Leaf net photosynthesis at saturating light
AT	Ambient air temperature treatment
C	Carbon
$[CO_2]$	CO_2 concentration
C_a	Atmospheric CO_2 concentration
C_{ab}	Aboveground standing crop C mass
C_{day}	Predicted daily carbon assimilation
C_i	Intercellular CO_2 concentration (or partial pressure)
C_c	Chloroplastic CO_2 concentration (or partial pressure)
$C_{r,T}$	Total C mass of roots
E	Leaf transpiration
eC_a	Elevated CO_2 treatment
ET	Elevated air temperature treatment
FACE	Free-air CO_2 enrichment experiments
F_c	Net aboveground carbon uptake
$F_{c,r}$	Residual belowground C flux
free	freely-rooted
FRLD	Fine root length density

g_s	Stomatal conductance
g_m	Mesophyll conductance
ITE	Leaf level instantaneous transpiration efficiency
J_{max}	Maximum rate of photosynthetic electron transport
K_l	Leaf-specific hydraulic conductance
LA	Leaf area
LMA	Leaf mass per unit area
LMF	Leaf mass fraction
N	Nitrogen
N_a	Leaf nitrogen on an area basis
N_f	TNC-free leaf nitrogen content
PPFD	Photosynthetic photon flux density
Q_{10}	Rate of change in respiration due to 10 °C increase in temperature
R	Leaf dark respiration rate
RMF	Root mass fraction
SLA	Specific leaf area
SLA_f	TNC-free Specific leaf area
SMF	Stem mass fraction
TBCA	Total belowground C allocation
TNC	Total non-structural carbohydrate
TDL	Tunable diode laser
V_{cmax}	Maximum rate of rubisco carboxylation
VPD	Vapour pressure deficit
VPDB	Standard Vienna Pee Dee Belemnite

WUE	Water-use efficiency
WTC	Whole-tree chambers
$\delta^{13}C$	C isotope ratios of ^{13}C to ^{12}C expressed relative to standard VPDB
Δ	C isotope discrimination during C3 photosynthesis
Ψ_l	Midday leaf water potential
Ψ_{pd}	Predawn leaf water potential
σ_s	Self shading parameter

Abstract

Plants must utilize external resources including light, CO_2, water and mineral nutrients to support photosynthetic carbon (C) gain. This photoassimilate is then allocated within the plant as the essential C resource for growth, maintenance and storage. Theory and observations suggest that C allocation and leaf physiology are optimized to maintain functional balance for external resource capture and to maximize C gain. However, the impacts of a changing climate may disrupt the proposed balance of C allocation between above and belowground pools. Variation in resource distribution and leaf physiology within tree canopies is also not fully understood, thus all canopy leaves may not follow theories of leaf optimal behavior. This lack of understanding regarding C uptake and the fate of assimilated C inhibits our ability to precisely test the coordination between canopy photosynthesis and growth. To address these broad ecological questions, this PhD research utilized a diverse set of experiments which manipulated resource availability and climate factors on *Eucalyptus* tree species. My goal was to measure aspects of resource allocation and C uptake across different scales, from leaf to whole tree, to improve understanding of the physiological processes which determine tree growth and the sensitivity of these processes to changing environments.

First, I determined whether manipulations of soil volume would limit growth in *Eucalyptus tereticornis* seedlings by disrupting the balance between source and sink activity. Seedlings were grown in a large range of container sizes and planted flush to the soil alongside naturally planted freely-rooted seedlings (free). Aboveground growth of seedlings in containers was negatively affected compared to free seedlings soon after

the experiment started. Despite large reductions in total growth across soil volume treatments, relative partitioning of mass to leaves, stems and roots was similar for all seedlings after 120 days. Leaf photosynthetic capacity decreased in containers compared to free seedlings, and was correlated to both leaf nitrogen (N) content and starch accumulation. Although belowground sink limitation resulted in a reduction of net leaf photosynthesis (A_n), a mass balance model concluded that these reductions were not large enough to explain observed growth responses. As A_n and growth were not tightly coordinated, the model predicted excess photosynthetic C not attributed to biomass in potted seedlings. Quantifying the fate of this excess C will be essential in evaluating feed-backs between sink strength and leaf C uptake in future studies.

Second, I investigated how light gradients within *Eucalyptus tereticornis* tree canopies affect the distribution of resources that define photosynthetic capacity of sun and shade leaves. Trees were grown in climate-controlled whole tree chambers under prevailing ambient and warmed (+3 °C) treatments and leaf gas exchange was coupled with online C isotope discrimination to measure A_n, stomatal conductance (g_s) and mesophyll conductance (g_m) of sun and shade leaves. Photosynthesis rates were reduced by ca. 40 % in shade leaves associated with a 75 % reduction in photosynthetically active radiation compared to sun leaves. Photosynthetic capacity (ca. 20 % lower V_{cmax} and J_{max}) and leaf N were also lower in shade leaves than sun leaves; however, g_s was similar. Leaf C_i, estimated from both leaf $\delta^{13}C$ and gas exchange, was higher in shade leaves than sun leaves. Here, the optimization theory hypothesis that C_i should be optimized throughout the canopy was rejected because water use efficiency was lower in

shade leaves, compared to sun leaves. When light intensity was increased from low light to high light for shade leaves, both g_s and g_m increased rapidly (within minutes), leading to increases in A_n greater than sun leaves at the same high light environment. This rapid response of g_m with light likely enables shade leaves to respond quickly to sunflecks and possibly represents a new mechanism underpinning leaf gas exchange responses to light. This capacity of shade leaves to adjust their physiological behavior and increase C uptake when sunflecks occur likely plays significant role in whole tree C uptake for some tree species, albeit at the cost or reduced water-use efficiency. These findings reveal that plant resources within a canopy may be distributed to utilize sunflecks and the dynamic physiological responses of shade leaves to altered light environments must be accounted for when up-scaling leaf level measurements to predict whole canopy C gain.

Finally, I examined how net aboveground C uptake correlated to tree biomass growth and whether elevated [CO_2] and drought treatments altered C allocation patterns above or belowground in *Eucalyptus saligna* trees. Trees were grown in climate-controlled whole tree chambers (WTCs) over a period of two years under treatments of two [CO_2] (380 ppm and 620 ppm) and two watering regimes (well-watered and a four-month drought) in factorial combination. Additionally, we utilized a novel approach to calculate total belowground C allocation (TBCA) for each WTC as the residual between the measured aboveground net CO_2 uptake and aboveground C mass. Measured cumulative aboveground net C uptake correlated positively to whole tree C mass production and leaf area over the final eleven months of the experiment. Contrary to

previous studies, cumulative TBCA was unaffected by either elevated CO_2 or drought treatments. As a fraction of total aboveground net C uptake, TBCA was also found to remain relatively stable across daily time steps for all trees. Increases in C allocation to leaves were detected in elevated CO_2 treatments, while the effects of a 4 month drought were negligible on C allocation in aboveground tissues. These results reveal how climate change factors impact the investment of photosynthetic C in a *Eucalyptus* tree species and provide evidence that belowground processes may not be as sensitive to global change factors as previously thought.

In conclusion, this PhD research addressed interrelated questions regarding resource allocation in *Eucalyptus* tree species by linking leaf physiology to whole canopy C gain and allocation of photosynthetic C to whole tree growth. This study confirms that the distribution of photosynthetic resources constrain canopy C uptake, yet within canopy leaf physiology does not follow prevailing optimal theory regarding water use. Results from this work reveal how quantifying the fate of photosynthetic C among tissue pools, beyond biomass production, is imperative to accurately assess the impacts of environmental change on tree productivity. This research offers critical empirical data needed to refine process based models which predict canopy C gain from rates of A_n and forest growth models where C allocation is represented. Ultimately, this work contributes valuable information regarding the physiological and growth responses of *Eucalyptus* tree species essential for reconciling the impacts of resource availability and global climate change on Australian ecosystems and the productivity of *Eucalyptus* plantation forests.

Chapter 1

General Introduction

1.1 Overview

1.1.1 Resource allocation in plants

Plants require resources including light, CO_2, water and mineral nutrients to support growth and reproduction. Resource acquisition requires an energy supply, appropriate tissues for uptake and a transport system to deliver resources to their required destination (Grace 1997). The uptake of nutrients from roots is necessary for leaf growth. Leaves then fix the C, via net photosynthesis (A_n), required for growth of the entire plant. This assimilated C from source leaves, in the form of simple sugars, is in itself an essential C resource that must be allocated to the growth and maintenance of tissues or is diverted to a storage pool of carbohydrates. As a result, growth is driven by several simultaneous processes, including A_n, C investment among organs, resource acquisition and metabolic costs (Körner 2006, Fourcaud et al. 2008). Gaining an understanding of the sensitivity of these processes to environmental change is crucial for predicting future terrestrial C cycling (Friedlingstein et al. 1999), as there is currently little consensus on how C allocation should be modeled (Franklin et al. 2012, De Kauwe et al. 2014).

1.1.2 Resource allocation theory

Theoretically, growth under resource limitation will be maximized when investment into the acquisition of any single resource from the environment leads to an equivalent increase in growth (Bloom et al. 1985). The two critical assumptions of allocation theory are that the resource in question is in fixed supply and that allocation among competing functions is mutually exclusive (Bazzaz et al. 2000). Thus, trade-offs between different tissue C sinks will exist as resources are invested within the plant. Allocation of newly acquired resources to different tissues will then affect subsequent rates of capture of CO_2 and soil resources (Shipley and Meziane 2002). In resource-saturated environments plants should maximize growth by allocating resources to support leaf growth to increase C acquisition (Monsi and Saeki 2005). Resource availability, however, is rarely saturated in natural ecosystems. For example, tree growth can be limited by the availability of carbon within the plant (carbon limitation) or by the tree's ability to use available carbon via nutrient shortages (Wiley and Helliker 2012). As a result, shifts in allocation of external resources and assimilated C to different tissue or ecosystem components can occur. Debate still exists regarding which of these limiting resources most strongly limit plant growth or how they regulate carbon availability.

Shifts in resource allocation within plants have led to two main theories regarding allocation strategies. First, the balanced growth hypothesis suggests that individual plant tissues should provide a 'balanced internal economy' as each component supplies resources for the other (Davidson 1969). This functional equilibrium between tissues can then be adaptive if conditions limit A_n or soil nutrient uptake (Cannell et al. 1985), such

that plants should allocate resources to the organ that is capturing the resource most limiting growth (Shipley and Meziane 2002). Changes in plant resource allocation are also theorized to be a function of allometric trajectories of plant development, independent of changes in nutrient supply (Müller et al. 2000). In this strategy, investment into leaf mass increases with both stems and root, but not proportionally, as a greater allocation of biomass to the stem exists as a simple function of plant size (Zens and Webb 2002). When constrained by ontogeny, plants are more likely to adjust tissue morphology, chemistry, metabolism or turnover to alter resource capture (Reich et al. 2002).

1.1.3 Tree canopy resource gradients

Incident PPFD declines exponentially with cumulative leaf area index from the top of the tree downward, creating steep light gradients within tree canopies (Monsi and Saeki 2005). Leaf photosynthesis responds strongly and non-linearly to irradiance (Evans 1995). As costs and limitations of light harvesting prevent plants from exposing all leaves to full sun (Niinemets 2010), it follows that a substantial portion of canopy C assimilation should occur in leaves with the highest exposure to light. Consequently, the distributions of resources required for A_n are partially defined by canopy light gradients. As the photosynthetic capacity of leaves is related to its N content (Field and Mooney 1986), a larger investment in N to the upper canopy should yield a larger return from whole canopy C assimilation (Ellsworth and Reich 1993). The supply of water also imposes limits on photosynthetic C gain through direct limitations on leaf level physiology. The stomatal resistance to CO_2 uptake is a function of the balance between transpiration losses and leaf water potentials (Farquhar and Sharkey 1982) and sun

leaves frequently experience greater water limitations in the upper canopy (Sellin et al. 2008, Niinemets 2012). Thus, photosynthetic N investment in the upper canopy will be ineffective in enhancing A_n if water supply is insufficient (Niinemets 2012, Peltoniemi et al. 2012). Overall, the allocation of soil resources within the canopy constrains leaf physiology and photosynthetic capacity, thereby regulating the efficiency of CO_2 uptake.

1.1.4 Fate of assimilated carbon

Carbon allocation represents the fraction of gross primary productivity distributed to different tissue components above and belowground. In trees, C allocation encompasses investment into tissue biomass production as well as fluxes including respiration, exudation and turnover rates (Litton et al. 2007). The fate of this assimilated C is regulated by the delicate balance between leaf C uptake (source) and the C sink strength of the different biomass pools. For example, the sensitivity of C source and sink activities to water and nutrient availability could lead to an imbalance between C supply and C used for tissue growth and respiration (Fatichi et al. 2014). Additionally, imbalances between source and sink activity can lead to investment into carbohydrate synthesis as a transient C storage sink (Paul and Foyer 2001).

As woody plants have competing tissue carbohydrate sinks, growth should principally depend on the allocation of leaf C assimilate among different sink organs (Kozlowski 1992, Lacointe 2000). In response to changing environmental conditions, however, trees may adaptively shift tissue C allocation to balance growth, storage and C loss. Due to conservation of mass, it is conceivably possible to track photosynthates from leaf C uptake to their eventual destination in above and belowground pools. Although mass

balance approaches can be used to quantitatively assess tree C allocation, few studies so far have been able to provide direct empirical measurements of C allocation among component pools (Klein and Hoch 2015). Improving our understanding of tree C allocation will require novel experimental infrastructure capable of quantifying net canopy photosynthesis and the fate of C into growth, storage and C loss pools.

Tree C allocation strategies drive acquisition of the essential resources (light, nutrients and water) that limit forest productivity (Litton et al. 2007). Thus, understanding potential shifts in plant C allocation are necessary to understand the consequences of climate change on vegetation (Sevanto and Dickman 2015). In a higher CO_2 vegetation may increase C storage, but predictions of the change in C storage depend on how allocation processes are represented (De Kauwe et al. 2014). Under climate warming enhanced growth is expected though increases in C allocation aboveground to leaves and shoots, which may vary by plant functional type (Way and Oren 2010). In drought scenarios, increases in C allocation to storage and are expected in order provide hydraulic safety margins (McDowell et al. 2011, Epron et al. 2012, Sala et al. 2012). However, the degree to which these expected outcomes are affected by interactions between these climate change factors is largely unknown. For Australian forests, which are characterized by relatively poor resource availability, investigation of C allocation patterns will be essential to predict the susceptibility of these ecosystems to changing climates.

1.1.5 Eucalyptus tree species as model for research

Research on *Eucalyptus* trees is ecologically important for Australia as it is the most dominant tree genus (Boland et al. 2006). *Eucalyptus* forests are the continent's most common forest type, covering about three-quarters of Australia's native forests (92 million hectares) and occurring in all but the continent's driest regions (SOFR 2013). *Eucalyptus* tree species are also economically important globally as they are commonly cultivated in plantations due to fast growth. Despite the fact that only a few *Eucalyptus* species have natural ranges outside continental Australia (Pryor and Johnson 1981), *Eucalyptus* trees are grown in plantations in over 90 countries (Booth 2013). This is because *Eucalyptus* species have been shown to exhibit both adaptive plasticity and genetic specialization to spatial variation in climate (Byrne et al. 2013). Currently, the global plantation area of eucalypts totals nearly 20 million hectares, accounting for around 15 % of the world's total plantation forests (IUFRO 2015). Consequently, this iconic Australian tree species is an excellent model to investigate strategies of resource allocation in trees facing global climate change.

1.2 Current Knowledge Gaps

1.2.1 Resource allocation in trees

The distribution of assimilated C is a primary determinant of plant growth (Friedlingstein et al. 1999), yet our knowledge of the mechanisms by which allocation is regulated is poor (Poorter, Niklas, et al. 2012). A key issue with drawing generalized

conclusions about the plasticity of C allocation in trees is with the inconsistency in terminology used to define C allocation to specific tissue or ecosystem components (Litton et al. 2007). Biomass partitioning, as the relative distribution of biomass between different tissue components, should not be confused with the allocation of newly fixed photosynthates to different organs. This is because the measured biomass at any time point represents the cumulative result of potentially dynamic C allocation over time (Poorter et al. 2015). This dynamic C allocation includes not only tree parts such as leaves, stems and roots but also respiration, exudation, turnover and transient C storage pools. As C allocation integrates all of these processes, it is extremely difficult using current methods to assess C allocation in whole trees. Disentangling the effects of resource supply on plant C allocation patterns is often assessed across "snapshots" in time, which should be done with caution (Reich et al. 2002). This is because of plants have developmental shifts in biomass partitioning, independent of resource supply, as they age (Müller et al. 2000, Poorter et al. 2015). Additionally, supplies of light and soil resources fluctuate continuously, making equilibrium with C allocation at any "snapshot" highly unlikely (Shipley and Meziane 2002).

As accurately measuring tree C allocation remains a difficult task, especially belowground, drawing conclusions that are applicable to whole plants or ecosystems remains a challenge. Currently, the representation of C allocation lags behind photosynthesis (A_n) in process-based forest models (Friedlingstein et al. 1999, Franklin et al. 2012, Iversen and Norby 2014) and our understanding of how global change impacts C allocation is incomplete (Litton et al. 2007, Warren et al. 2012). This knowledge gap of C allocation patterns in trees is of major concern due to the potential

for forest ecosystems to sequester C in a changing climate. This deficiency requires more empirical data to derive basic principles that drive patterns of tree C allocation in changing environments. However, this will require novel experiments and approaches to better quantify shifts in C allocation above and belowground in future studies.

1.2.2 Coupling of photosynthesis and tree growth

On short timescales, A_n and total respiratory losses may not correlate with growth because of the dynamics of tissue C storage pools. As plant growth is commonly defined as irreversible changes in size, transient storage pools represents the fraction of available C that does not currently contribute to biomass production (i.e. tissue elongation).
On longer timescales, however, A_n and tissue respiration determine net plant C balance and must correlate to growth. This had led to the long standing debate over how strongly plant growth is controlled by either source or sink activity (Sweet and Wareing 1966, Körner 2013). To date studies manipulating either source activity (CO_2 fumigation or defoliation) or sink activity (fruit removal, girdling or low growth temperatures) have not resulted in consensus when addressing this debate. This uncertainty arises from the difficulty in measuring the balance between C uptake and the fate of assimilated C among pools with long (biomass) or short (carbohydrate storage, respiration, exudation) retention times. When shifts in carbohydrate storage, tissue respiration or turnover rates occur, rates of C assimilation may not correlate with biomass production at a given time point (Rocha et al. 2006, Litton et al. 2007, Gough et al. 2008). To assess this balance will likely require integration of empirical and modelling approaches to assess leaf physiological and whole plant responses to manipulations of source-sink activity. To

address this knowledge gap, new approaches are needed to test how interactions between source and sink activity affect the fate of assimilate C across different temporal scales.

1.2.3 Within canopy resource utilization

Due to the relationships between light, N and leaf photosynthetic capacity, it is commonly assumed that a limited availability of N should be distributed proportional to light availability within tree canopies. Observed canopy distribution of N is often less steep than optimal theory suggests, however, with shade leaves having more N than expected based on average light gradients (Peltoniemi et al. 2012). Additionally, constraints on water supply from the soil to the upper canopy may negatively impact the distribution of photosynthetic N to canopy light availability (Niinemets 2012, Peltoniemi et al. 2012). Whether insufficient hydraulic supply results in the observed sub-optimal canopy N gradients has yet to be empirically tested. Assessing leaf C gain as a function of light availability is also made difficult by frequent light fluctuations within a canopy, via sunflecks. Sunflecks cause temporal variation in PPFD that is not taken into account when considering what is optimal for a plant in terms of distributing resources along a gradient of light availability.

Leaves have been proposed to exhibit optimal physiological behavior in order to efficiently utilize and transport resources to maximize A_n (Thornley 1972). In trees, leaf physiology often focuses on full sun leaves and relationships between leaf physiological behavior and the availability of N, water and light between sun and shade leaves requires further attention. For example, stomatal conductance (g_s) has been hypothesized to be distributed within a canopy to utilize supplies of light, N and water to maximize A_n

(Peltoniemi et al. 2012). In shade leaves, stomata might be expected to be more closed to efficiently use water with generally low A_n. To date, however, no clear picture has emerged on the relationship between g_s and A_n within canopies (see Jifon and Syvertsen 2003, Tissue et al. 2006, Sellin and Lubenets 2010).

Additionally, mesophyll conductance (g_m) also limits A_n and complex relationships may exist between canopy light gradients, leaf N and g_m. Unfortunately, a scarcity of values for g_m within tree canopies (see Lloyd et al. 1992, Piel et al. 2002, Warren et al. 2003b, 2007) hinders our ability to relate individual leaf physiological behavior to optimal canopy C uptake. As the CO_2 drawdown from the atmosphere to the site of carboxylation includes g_s and g_m, relationships between A_n with light availability, N and water within canopies will require the integration of both physiological variables in future experiments. Incorporation of g_m into process based tree growth models, similar to the progress made with g_s, should be made a priority. Whether the limitations of g_m on both leaf and canopy C gain can be parameterized accurately, however, has yet to be reported.

1.3 Thesis Objectives

The overall research goal is to evaluate how trees adjust their growth and physiology to maximize resource uptake and C gain. Specifically, this PhD research addresses knowledge gaps of how tissue C allocation, source and sink regulation and resource distribution affect the coordination between A_n and whole tree growth. In order to investigate key mechanisms that drive patterns in resource allocation in trees this

research was carried out across multiples scales, from leaf isotope discrimination across the photosynthetic CO_2 flux pathway to tissue specific biomass partitioning to total belowground C allocation. Understanding how resource allocation is correlated with individual leaf physiological behavior within tree canopies is crucial in accurately determining the capacity for whole canopy C assimilation, which is the essential resource for tree growth. Aspects of this research use manipulations of key global change factors, including elevated CO_2, warming and drought to investigate the plasticity of observed physiological and growth responses to future climate scenarios. An improved understanding of how C is allocated within trees will supply much needed empirical data for process-based forest models where C allocation is currently poorly represented.

This research focuses on two Australian tree species, *Eucalyptus tereticornis* and *Eucalyptus saligna*, which have important roles in both native forests ecosystems and as commercial plantation timber. For example, *Eucalyptus tereticornis* is part of the critically endangered Cumberland Plain ecological community and *Eucalyptus saligna* is part of the critically endangered Blue Gum High Forest ecological community, with both communities having fragmented geographic distributions in the Sydney Basin bioregion (Hughes 2011). Both of these species are part of the "big nine" *Eucalyptus* species group which accounts for more than 90 % of planted *Eucalyptus* forests worldwide (Stanturf et al. 2013). As a result, the core findings of this PhD research have both conservation and commercial applications in addressing the productivity of these two important tree species in the face of global climate change. For example, considerable uncertainty

remains as to the magnitude of CO_2 fertilization on this continent as much of the vegetation is already under nutrient and/or water limitation (Hughes 2003).

This research was conducted using the state of the art Whole Tree Chamber experiment as well as a novel field-based seedlings container study at Western Sydney University. Using the two *Eucalyptus* tree species, fundamental principles of common optimization theories were tested at several tree growth stages. Leaf-level data were combined with tissue biomass production and canopy C fluxes to develop a better understanding of how resources are allocated to optimize whole tree growth. Empirical data were also integrated with a seedling growth model to test how resource limitation impacts the coordination between A_n and growth. Specifically, this thesis aimed to address current knowledge gaps by answering the following main questions:

1. **Where does the carbon go?**

How will biomass partitioning and carbon allocation in *Eucalyptus* trees be affected by global climate change and belowground resource limitation?

2. **When do photosynthesis and growth not add up?**

What do mass balance approaches reveal about the coordination of growth and photosynthesis at different temporal scales?

3. **Are whole canopies optimized for carbon gain?**

How does resource availability within *Eucalyptus* tree canopies interact with dynamic physiology of sun and shade leaves to maximize canopy carbon gain?

1.4 Thesis Outline

Chapter 2 was designed to address thesis questions 1 & 2 by manipulating belowground sink strength in *Eucalyptus tereticornis* seedlings, via a range of container sizes, in a novel field-based experimental design. The effects of belowground resource limitation were then used to investigate patterns in biomass partitioning, leaf gas exchange and growth between container treatments and field grown seedlings. Empirically measured gas exchange parameters were then used to model daily C gain for each seedling to test the coordination between the reduction in A_n and biomass production of seedlings with soil volume restriction. The sensitivity of this model to different C allocation scenarios was used to speculate possible fates of photosynthetic C not accounted for in the default model. Results of this study are then used to address the ongoing debate over source or sink controls of A_n and growth. The flexibility of this mass balance modelling approach is used to highlight the importance of quantifying C allocation when evaluating the impacts of resource limitation on tree seedling growth.

Chapter 3 addressed thesis question 3 by combining leaf gas exchange with online C isotope discrimination to measure the responses of sun and shade leaf physiology to light availability. The distribution of leaf N and leaf hydraulic conductance within *Eucalyptus tereticornis* canopies was examined to test if the resources required for A_n were preferentially invested into sun leaves, as predicted by standard optimal theory, to maximize whole canopy C gain. The physiological capacity of shade leaves to respond to increases in light availability was quantified to determine if shade leaves “lie in wait” for sunflecks. Trees were grown in climate controlled WTCs under ambient and elevated

air (+3°C) temperature treatments to test the impacts of future climate warming on each of these processes. Rarely have relationships between A_n and both g_s and g_m been quantified within tree canopies, thus results from this experiment are used to reveal potential new mechanisms underpinning leaf gas exchange responses to light. Unexpected decreases in water-use efficiency in shade leaves were related to the capacity of inner canopy leaves to rapidly utilize sunflecks. Empirical data from this experiment improves our ability to predict whole canopy C gain by prioritizing both sun and shade leaf physiology, which may be optimized differently.

Chapter 4 addresses thesis questions 1 & 2 by quantifying high resolution net canopy photosynthesis measurements and C allocation in *Eucalyptus saligna* trees grown under drought and elevated CO_2 treatments in factorial combination. The unique WTC experimental facility measures cumulative net aboveground C fluxes which were compared to canopy leaf area and tree biomass production. A novel framework was also applied to calculate a more reliable estimate of the sensitivity of TBCA to global climate change. I then evaluated how potentially interacting climate change factors impacted C allocation to above and belowground pools through time. Results from this experiment emphasize the need to quantify individual components of tree C allocation and to separate impacts on measured biomass from those of total C allocation when assessing tree growth responses. As empirical measurements of C allocation are difficult to obtain, especially with belowground processes, these results provide much needed empirical data to validate process-based model where C allocation is represented.

Chapter 5 presents the synthesis and outlook of the major findings in my PhD research as they relate to each main thesis question. First, shifts in C allocation likely occurred as these two *Eucalyptus* species were impacted by changing environments, even though biomass partitioning of harvested trees remained relatively conserved. Combined results from Chapters 2 & 4 are used to discuss how observed responses of biomass partitioning and C allocation correspond to prevailing theory and how these mass balance approaches have improved our understanding of the investment of photosynthetic C in trees. Second, I show that coupling between total C gain and tree growth can be disrupted over shorter experimental time frames, while over longer time scales they are strongly correlated as a function of leaf area. Results from Chapter 2 use empirical data and modelling approaches to address the current debate over source and sink control over seedling growth, while Chapter 4 is used to discuss how unique measurements of net canopy photosynthesis correlate to tree productivity under future climate scenarios. Last, I show that sun and shade leaves exhibit different physiological behavior in order to utilize differential availability of external resources within *Eucalyptus tereticornis* canopies. Results from Chapter 3 are used to show that shade leaf physiology is likely optimized differently from sun leaves in order to respond to sunflecks, which has important consequence for current theories regarding how resources are allocated to optimize canopy C gain.

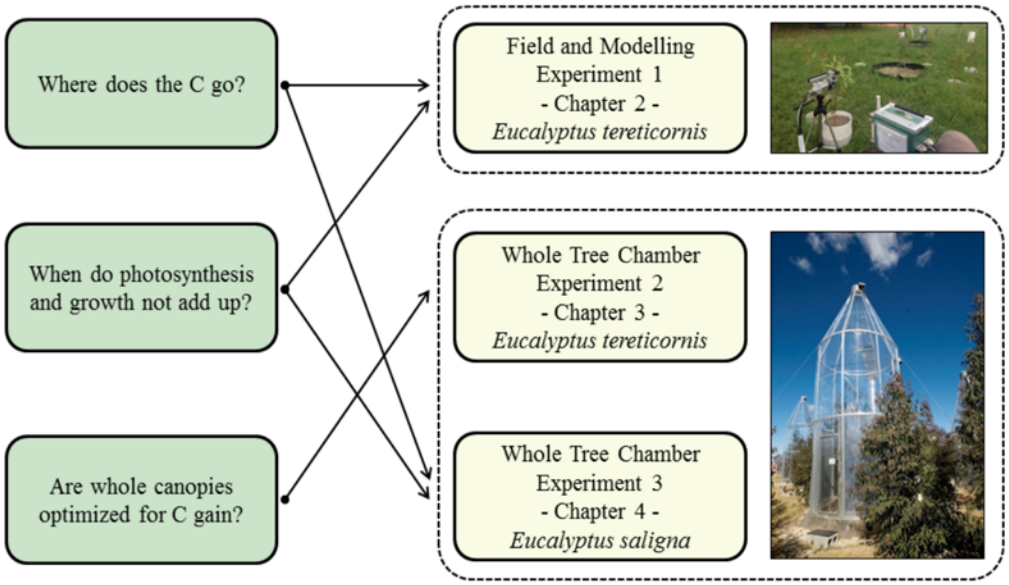

Figure 1.1. Each main thesis question linked to individual experiments designed to address current knowledge gaps. Experiment 1 was conducted with a novel field-based seedlings container study, while experiments 2 and 3 occurred in the Whole Tree Chamber experimental system.

1.5 Reproducible Research

Science and hypothesis testing is driven by data, yet it is a challenge to ensure that reported experimental data are appropriately described, standardized, archived and openly available (Hanson et al. 2011). Reproducibility of analyses serves as a minimum standard for judging scientific claims when full independent replication of a study is not possible, which should include making available the data and the computer code used to analyze the data (Peng 2011). Not only does creating reproducible research increase the reliability and credibility of one's findings, but it encourages the engagement of the scientific community to advance new research ideas. Every aspect of this PhD research attempts to adhere to these key principles of reproducibility. Raw data and code for each experimental chapter are located in an easily accessible online repository. This entire thesis is also compiled as a reproducible document, including R code (R Development Core Team 2011) to analyze data, generate text and create tables/figures, which are all made available for open access. As a result, all necessary information required to reproduce this thesis, in its entirety, are located in repositories at https://github.com/CourtneyCampany.

Chapter 2

Belowground sink limitation alters growth and carbon balance of *Eucalyptus* seedlings

2.1 Abstract

Interpreting limitations to plant growth requires understanding the balance between carbon (C) source and sink activity. This study used manipulations of soil volume to test how growth is coupled to physiology, C allocation, and sink activity in *Eucalyptus tereticornis* seedlings. We grew individual seedlings in a large range of container sizes and planted containers flush to the soil alongside naturally planted freely-rooted (free) seedlings. We developed a seedling growth model that utilized leaf photosynthesis rates (A_n) to allocate daily C uptake towards mass growth of leaves, stems and roots. Reduced soil volume was expected to induce rapid negative effects on growth and physiology compared to free seedlings. It was hypothesized that the soil volume effect would be largest in the smallest containers, negatively impacting mass partitioning belowground. An accumulation of leaf non-structural carbohydrates, resulting from reduced belowground sink strength, was expected to correlate to reductions in photosynthetic capacity. We observed a negative effect of container volume on aboveground growth soon after the experiment started. Although growth was consistently different across soil volumes, dry mass partitioning to leaves, stems and roots was unchanged after 120 days.

Photosynthetic capacity was significantly reduced in containers compared to free seedlings, and was related to both reduced leaf nitrogen content and starch accumulation. We then asked whether the observed reductions in A_n explained the observed differences in seedling biomass. Although belowground sink limitation resulted in a reduction of $A_{n,}$ the model concluded that these reductions were not large enough to explain observed growth responses. As A_n and growth were not tightly coupled, an unaccounted for pool of photosynthetic C was predicted in seedlings with soil volume restriction. These results highlight the need to further utilize mass balance approaches when evaluating plant C allocation and confirm that important feedbacks exist between belowground sink strength and leaf C uptake.

2.2 Introduction

Understanding plant growth and its relationship to C assimilation requires knowledge of the mass balance that must be achieved between C uptake and subsequent allocation to growth, storage, and respiration. As woody plants have highly integrated systems of competing carbohydrate sinks (Kozlowski 1992), growth should principally depend on the allocation of photosynthate among different tissues and organs. At long enough time scales leaf photosynthesis (A_n) and respiratory losses together determine net C balance and will correlate to plant growth. At shorter temporal scales, however, growth can instead be mediated by tissue C storage pools. This has led to the current debate on how strongly plant growth is controlled by either source or sink activity. Consequently, plant growth cannot always be simply determined by A_n, making it complex to understand and challenging to model (Fourcaud et al. 2008). Despite a wealth of studies, large

uncertainties still remain regarding the coordination of C supply and growth of woody species.

In woody species, the coordination of A_n and growth has been studied with manipulations of C source activity. Examples included elevated CO_2 experiments, for example FACE (reviewed in Ainsworth and Long 2005), and partial defoliation experiments. Elevated CO_2 has been shown to increase A_n (Drake et al. 1997, Ainsworth and Rogers 2007) and across four FACE experiments this resulted in a stimulation of 23 % in forest biomass production (Norby et al. 2005). Evidence from a wide range of elevated CO_2 experiments, however, also reveals that even with an average photosynthetic enhancement of over 30 %, the biomass growth rate only increases by around 10 % (Kirschbaum 2011). In partial defoliation experiments, increases in A_n of the remaining foliage are commonly shown, yet are attributed to various mechanisms, including reduction in end-product inhibition (Iglesias et al. 2002, Zhou and Quebedeaux 2003, Handa et al. 2005), enhanced biochemical activity (Ovaska, Sari, et al. 1993, Layne and Flore 1995, Pinkard et al. 2011), increased stomatal conductance (Layne and Flore 1995), enhanced leaf nutrient status (Turnbull et al. 2007, Pinkard et al. 2011) and regulatory sugar signaling (Eyles et al. 2013). However, increases in A_n in defoliation experiments did not always produce increased growth due to reductions in meristem sink strength (Palacio et al. 2012), C limitation to mycorrhizal colonization (Markkola et al. 2004), or an overall decrease in whole plant C gain (Ovaska, Walls, et al. 1993). These manipulations of C source activity expose unresolved issues with how changes in A_n do not always correspond with proportional responses in growth.

Alternatively, manipulating plant tissue C sinks is often used to investigate the correlation between A_n and growth. This is because metabolic signaling networks, relaying information on C and N status of different tissues, can regulate photosynthetic activity (Paul and Foyer 2001). If sink inhibition of A_n occurs, a close coordination between declines in A_n and growth should be expected. Whether photosynthetic down regulation is evident in woody species has been tested through fruit removal and phloem girdling. In these studies, down regulation of A_n was frequently correlated to carbohydrate accumulation resulting from reduced tissue sink strength (Iglesias et al. 2002, Urban and Alphonsout 2007, Haouari et al. 2013). However, reductions in A_n were also attributed to biochemical limitations prior to carbohydrate accumulation (Nebauer et al. 2011), irreversible photo-oxidative damage (Duan et al. 2008) and stomatal limitation (Li et al. 2005). These mixed results are not surprising as we still know little about the balance between assimilation, storage and growth across temporal scales in plants (Smith and Stitt 2007). As these manipulations likely impact source as well as sink activity simultaneously, affect water transport, are very extreme, or are specific to the occurrence of large fruiting sinks, they tell us little about source-sink coordination in typical growing conditions for woody species.

An alternative experimental approach is to reduce belowground C sink strength in tree seedlings by manipulating rooting volume, by varying the container size (Arp 1991, NeSmith and Duval 1998, Poorter, Bühler, et al. 2012). Possible advantages of this approach are that it allows a large range of treatment levels, can be easily compared to

naturally planted seedlings and may mimic natural conditions as seedlings compete for space or reach bedrock. Seedlings undergo many physiological and morphological changes in response to rooting volume, including biomass partitioning, A_n, water relations, nutrient uptake and respiration (NeSmith and Duval 1998, Poorter, Bühler, et al. 2012 and references therein). Inadequate rooting volume may decrease C sink strength by progressively restricting root growth in growing plants (Thomas and Strain 1991). Container size studies frequently exhibit photosynthetic down-regulation, likely as a result of sink limitation (Arp 1991, McConnaughay and Bazzaz 1991, Gunderson and Wullschleger 1994, Sage 1994, Maina et al. 2002, Ronchi et al. 2006). A meta-analysis by Poorter, Bühler, et al. (2012) concluded that A_n is the process likely to be the strongest affected by pot size and may best explain the effects on biomass seen in the large number of studies where containers are used. This conclusion arises because plants grown in small containers are shown to accumulate leaf starch while having lower C exchange and assimilate export rates (Robbins and Pharr 1988). However, evidence in support for a trade-off between C storage and growth in trees is, to date, inconclusive (Palacio et al. 2014). Based on these previous studies, using container size as a sink-strength manipulation can be used to empirically test the extent to which growth and A_n are coordinated.

This study utilizes a novel field design to investigate the coordination between growth and A_n in *Eucalyptus tereticornis* Sm. seedlings, by manipulating container size and thus rooting volume. Seedlings were maintained under well-watered conditions in order to isolate the effect of restricted soil volume. We used freely-rooted seedlings as a control

for the container size treatments. Empirical results were combined with a simple plant growth model to simulate seedling growth with a C mass balance approach, which was then compared to observed harvested seedling mass. The model used whole-plant C gain, scaled from instantaneous rates of leaf A_n, to quantify seedling dry mass production over the 120 day experiment.

Our hypotheses were as follows:

1). The manipulations of container size were expected to induce a belowground sink limitation compared to free seedlings. We hypothesized that declines in seedling growth would be largest in the smallest containers.

2). As the finite pool of rooting volume and soil nutrients will decline faster in trees growing in small containers, we expected reductions in partitioning to fine root mass relative to tree size with decreasing container size.

3). Reduced sink strength was expected to lead to accumulation of leaf non-structural carbohydrates, and a resulting down regulation of A_n. We therefore expected a correlation between carbohydrate accumulation and photosynthetic capacity as a function of soil volume.

4). Last, observed seedling mass was expected to correspond to growth model mass predicted from a simple C balance model taking into account measured rates of photosynthesis.

2.3 Materials and Methods

2.3.1 Experimental design

This experiment was located at the Hawkesbury Forest Experiment site in Richmond, NSW, Australia. Plots were located in an open cover paddock that was converted from native pasture grasses. Top soils at this site are an alluvial formation of low-fertility sandy loam soils (380 and 108 mg kg^{-1} total N and phosphorus respectively) with low organic matter (0.7 %) and low water holding capacity. At this site a soil hard layer exists at ~1.0 m with a transition to heavy clay soils. The climate for the region is classified as sub-humid temperate.

Eucalyptus tereticornis seedlings, 20 weeks old and approximately 40 cm tall in tube stock, were chosen from a single local Cumberland plain cohort. Six additional seedlings were harvested before planting to measure initial leaf area and dry mass of leaves, stems and roots. Previous container experiments have confirmed that species with tap roots (similar to *E. tereticornis*) use the center of the container as the medium for thick roots leaving the periphery of the soil as the most active sites for fine root proliferation (Biran and Eliassaf 1980a, 1980b). By using a species with tap root growth and manipulations of container length rather than width, we believed that a more realistic test of growth inhibition through constrained soil volume would be achieved.

Six container volumes were used ranging from 5 L to 35 L, with a 22.5 cm diameter, and lengths ranging from 15 to 100 cm. Containers were constructed of PVC pipe and were

filled with local top soil (described above). Soil in each container was packed to achieve a target soil bulk density that matched local soil conditions of 1.7 g cm^{-3}. A Imidacloprid (BAYER CropScience) insecticide tablet was planted 5 cm below the roots of each seedling. Containers were planted flush with the soil surface inside metal sleeves, designed to minimize excess air space between the container and outside soil while also allowing for container removal. This allowed for soil temperatures in containers to reflect conditions of naturally planted (free) seedlings. Each experimental block (n=7) contained a complete replicate set of six container volumes as well as one free seedling, with 1 m^2 spacing. For each free seedling, used as the control, a 1 m^2 subplot was excavated to the hard layer and replaced with the same soil used in each container. This ensured that any possible feedbacks from soil disturbance would be similar between seedlings in containers and free seedlings. A border of root exclusion material was buried 0.25 m deep and extended 0.25 m above the ground surface around each subplot to exclude local vegetation, which was further kept out by periodic weeding.

Plants were watered weekly or when needed to maintain soil moisture at field capacity (13-15 %). Drain systems were built into each pot to prevent pooling of water throughout the experiment. Pooling of water could lead to an anaerobic environment around the root that could hinder the uptake of water through reduced root conductance (Poorter et al. 2009), an undesired experimental artifact. A collection compartment in the bottom of containers, containing gravel covered by root exclusion mesh, was used to collect excess water for 20, 25, and 35 l containers. Plastic tubing (6 mm diameter) was inset into the gravel layer and extended through the top of the container. A lysimeter

pump was then used to suction excess water, through the tubing, as needed. For small containers (5, 10, and 15 L) a simple bottom plug was used to drain excess water from the gravel compartment. Each container was inspected after every watering and rainfall event to determine if pooling had occurred.

2.3.2 Growth and morphology metrics

Seedlings were planted in summer (January 21st 2013) and stem height, diameter at 15 cm and leaf count were measured weekly thereafter. Once the growth rate of individual plants had significantly declined a full biomass harvest was completed and the experiment ended (May 21st 2013). Dry mass of leaves, stems, roots and total leaf area (LI-3100C Area Meter; LI-COR, Lincoln, NE, USA) were measured for each seedling. Mean individual leaf area for each harvested seedling was calculated by dividing total measured leaf area by total leaf count of only fully expanded leaves. Mean individual leaf area was then used to interpolate total seedling leaf area through time with weekly leaf counts. Root mass was collected by removing the roots system and passing soil from each container through a 1 mm sieve, washing, separating into fine and coarse roots (<2 mm and >2 mm diameter, respectively) and then drying to a constant mass. Roots of seedlings in containers were not considered pot bound, as clusters of roots along the soil-container interface were not observed. Roots from the free seedlings were collected by excavating each 1 m^2 subplot to the hard layer and keeping only roots within the subplot. For each seedling, a sub-sample of washed fine roots was analyzed for root length using WhinoRhizo software (Regent Instruments Inc., Quebec, QC, Canada). Specific root length (SRL) is reported as the root length divided by the dry mass of each sub-sample

(m g^{-1}). Fine root length density (FRLD) for seedlings in containers is reported as the total fine root length divided by the volume of each container (m dm^{-3}).

2.3.3 Photosynthetic parameters

Leaf gas exchange measurements were performed fortnightly at saturating light (A_{sat}) and saturating light and [CO_2] (A_{max}) on new fully expanded leaves. Measurements were initiated only after sufficient new leaf growth occurred (March 05th, 2013), approximately 6 weeks following planting, and continued until the biomass harvest. Leaf level gas exchange was measured with a standard leaf chamber (2 x 3 cm) equipped with blue-red light emitting diodes using a portable gas exchange system (LI-6400, LI-COR, Lincoln, NE, USA). A_{sat} measurements were made at PPFD of 1800 μmol m^{-1} s^{-1} and [CO_2] of 400 μl l^{-1} and A_{max} with [CO_2] of 1600 μl l^{-1} and PPFD of 1800 μmol m^{-1} s^{-1}. This choice of light level to achieve light saturation is consistent with other studies on *Eucalyptus* species (Kallarackal and Somen 1997, Pinkard et al. 1998, Crous et al. 2013, Drake et al. 2014). These measurements were conducted during midday (10:00-14:00 h) with leaf temperature maintained at 25 °C. After CO_2 and water vapor flux values stabilized in the leaf chamber, net CO_2 assimilation rate and stomatal conductance (g_s) were logged 5 times and averaged for both A_{sat} and A_{max}.

Photosynthetic CO_2 response (AC_i) curves were measured at 25 °C on a random subset of each container size (n=3) after new leaves were first produced (March 13-14th, 2013) and prior to the final harvest (May 14-15$_{th}$, 2013). Each AC_i curve was started at the reference [CO_2] of 400 μl l^{-1} and then consisted of 12 additional steps from [CO_2] of 50 to 1800 μl^{-1} at 25 °C at saturating light (above). From these curves the photosynthetic

parameters, J_{max} and V_{cmax}, were quantified using the biochemical model of (Farquhar et al. 1980) and fit with the 'plantecophys' package (Duursma 2015) in R (R Development Core Team 2011) using default parameters.

Leaf dark respiration rates (R) was measured on each seedling during the same dates as AC_i curves. Freshly detached leaves were collected at least 1 hour after sundown and placed inside a conifer chamber attached to the Licor 6400. This method increases the measureable surface area of each leaf, beyond the standard leaf chamber, to accurately quantify R. Measurements were taken at a reference [CO_2] of 400 μl l^{-1} while leaf temperature was maintained at current ambient conditions. Reported values of R are standardized rates at 25 °C using a Q_{10} value (1.86) developed for these seedlings in a separate experiment (Drake et al. unpublished). Leaf area and dry mass were recorded for each leaf during gas exchange campaigns. 3

2.3.4 Leaf water potential

Predawn (Ψ_{pd}) and midday (Ψ_l) leaf water potentials were measured for each seedling using a PMS 1505D pressure chamber (PMS Instruments, Albany, OR, USA) on fully expanded leaves during the same time period as AC_i and R. Leaves were detached and immediately stored inside foil covered bags before water potential measurements were performed. Ψ_{pd} was measured before sunrise and Ψ_l at midday 13:00-14:30 h. These measurements were used as a measure of static water stress on the seedlings (Sellin 1999) and to ensure that the bulk soil water availability was high enough for plants to avoid water stress as they became larger and roots filled the soil volume.

2.3.5 Leaf, root and soil chemistry

Leaves used in each gas exchange measurements and subsamples of harvested roots were dried to a constant mass and milled for analysis of N content, $\delta^{13}C$, and total non-structural carbohydrates (TNC). Pre-planting soil samples (n=6) and subsamples of soil from each container following harvest were sieved to remove organic material, air dried and milled for analysis of N. Nitrogen concentrations of leaf and soil samples were determined using a Carlo Erba CE1110 elemental analyzer with thermal conductivity and mass spectromic detection (of N_2 and CO_2). The percentage of N in the sample was calculated by comparison with certified standards. Leaf $\delta^{13}C$ was analyzed with an Delta V Advantage coupled to a Flash HT and Conflo IV isotope ratio mass spectrometer. Leaf samples were flash combusted at 1000°C to convert to CO_2, feed to the mass spectrometer and isotopic signatures are reported relative to the standard Vienna Pee Dee Belemnite scale.

Leaf total non-structural carbohydrate (TNC) concentration was analyzed on dried and milled leaf samples using a total starch assay kit (Megazyme International, Wicklow, Ireland) and includes the starch and soluble sugar concentrations (mg g^{-1}). Starch was quantified using a thermostable α-amylase and amyloglucosidase assay (McCleary et al. 1997) and soluble sugars were determined following the anthrone method (Ebell 1969). Complete methods of the TNC assay are described in (Mitchell et al. 2013). TNC-free specific leaf area (SLA_f, m^2 kg^{-1}) for leaves sampled during gas exchange campaigns, were calculated by first subtracting the TNC content from individual dry leaf mass

before dividing leaf area by leaf mass or the leaf N content. Similarly, TNC-free leaf N (N_f, %) was calculated on all gas exchange leaves from leaf mass without TNC content.

2.3.6 Seedling growth model

We developed a simple seedling growth model that utilized leaf A_n rates to allocate daily C assimilate towards biomass production of stems, leaves, fine roots and coarse roots. The model begins with mean initial tissue component biomass ($leaf_i$, $stem_i$ and $root_i$) and a starting leaf area (LA_i) measured prior to planting. The initial biomass of roots was divided evenly between fine and coarse roots. The daily net biomass production of seedlings (P_i) is then given by

(1)

$$P_i = L\left(\frac{C_{day,i}\ \sigma_s}{\epsilon_c}\right) - R$$

where L is total plant leaf area (m^2), $C_{day,i}$ is the predicted daily C assimilation (g C g $mass^{-1}$ d^{-1}, explained below), σ_s is a self-shading parameter (explained below), ϵ_c is a biomass conversion efficiency parameter (g C g $mass^{-1}$) and R is the mass based total respiration of all tissue components (g C d^{-1}). Total respiration was calculated as

(2)

$$R = \Sigma(R_c\ M_c)$$

where R_c is tissue respiration rates of fine roots, coarse roots or stems (Table 2.S1, g C g $mass^{-1}$ d^{-1}) and M_c is the standing biomass of each component (g). Tissue respiration

rates were not directly measured in this experiment, so published or local default values from *Eucalyptus* species were used. Leaf respiration is represented in the calculation of C_{day} (described below). The change in individual component biomass (M_c), here solved on a daily time step, is given by

(3)

$$\frac{dM_c}{dt} = A_c\ P_i\ -\ (\Lambda_c\ M_c)$$

where A_c is the component specific biomass partitioning to whole plant biomass (%) and Λ_c is component specific turnover rate (yr^{-1}). Because we did not observe branch turnover, Λ_{stem} was assumed to equal 0. Total seedling biomass, per time step, was then equal to the sum of all biomass components; leaves, stems, fine roots and coarse roots.

C_{day} was predicted by using a coupled photosynthesis - stomatal conductance model (Farquhar et al. 1980, Medlyn et al. 2011) with the 'plantecophys' package (Duursma 2015) with the mean photosynthetic parameters (J_{max}, V_{cmax}, R and g_1) for each treatment and meteorological data from an onsite weather station. J_{max} and V_{cmax} were estimated from AC_i curves (explained above), R was empirically measured and the g_1 parameter, describing the plants water-use strategy, was generated by fitting the optimal stomatal conductance model from (Medlyn et al. 2011) with observed g_s values. Methods of the coupled leaf gas exchange model are described in Duursma et al (2014). Combined with the meteorological parameters; PPFD, air temperature, and relative humidity, at 15 min intervals, leaf A_n rates (μmol CO_2 m^{-2} s^{-1}) were then predicted for each soil volume

treatment. C_{day} was calculated by converting predicted rates to mass C gain over 15 min time steps (g m^{-2}) and then summed for 24 h. This resulted in 120 unique values of C_{day} for each soil volume treatment, one value for each day of the experiment. Thus, each daily time step for model runs included a value of C_{day} that represented both treatment specific photosynthetic parameters and meteorological constraints across the duration of the experiment.

It was further necessary to calculate a self-shading parameter (σ_s) when scaling leaf A_n with total plant leaf area. Accurately modelling canopy photosynthesis requires inclusion of the heterogeneous nature of light availability that occurs from self-shading and the limitations this then imposes on leaf A_n (De Pury and Farquhar 1997, Marchiori et al. 2014). This was accomplished by utilizing 61 previously digitized *Eucalyptus* seedlings, covering 5 total species which include *E. tereticornis*, from Duursma et al. (2012) to run in 'YplantQMC' package (Duursma 2014) in R to build a 3D plant structure based on digitized metrics of plant allometry and crown structure. Using the same treatment specific physiological parameters listed above, 'YplantQMC' outputs total A_n, using total leaf area, for seedlings assuming self-shading as well as for a full sun large horizontal leaf. The ratio of total A_n with self-shading to horizontal leaf was then used to calculate σ_s for each of the 61 digitized seedlings, independently for each of the seven soil volume treatments. Next, the linear relationship between σ_s and total leaf area was determined across digitized seedlings, within each treatment. For the growth model, σ_s was then predicted for each daily time step using the previous days cumulative leaf area and this

value was then applied to $C_{day,i}$. All default parameters used in model simulations are reported in Table 2.S1.

We then utilized this model to test the hypothesis that the effects of belowground sink limitation on rates of leaf A_n were sufficient to accurately predict overall seedling biomass production after 120 days. Each model run utilized changes in A_n and leaf mass fraction (LMF), with values of stem and root respiration rates, to generate total seedling mass and leaf area after 120 days. Cumulative net leaf C gain for each treatment was equal to the sum of each value of $C_{day,i}$ over 120 days and final seedling C was assumed to equal half of the final dry mass for both modeled and observed seedlings.

First, a default model was fitted with mean photosynthetic parameters from the free seedlings and then optimized to produce a LMF which correctly predicted both the leaf mass and total biomass of the harvested free seedling (M_{free}). This optimized LMF was then used to constrain model runs with soil volume treatment specific C_{day}, while keeping tissue respiration and turnover parameters constant, to determine if changes in leaf A_n alone could predict biomass of seedlings in containers (M_{pots}). Next, model sensitivity to different C allocation scenarios, including observed treatment specific LMF and up-regulation of non-leaf tissue respiration by 50 % of default values (M_{S1} and M_{S2}, respectively), was used to test for improvement of biomass predictions compared to measured harvest biomass. For all cases, seedling biomass production was compared between model output and harvested seedlings with treatment specific mean C_{day} by first scaling values to the free seedling control.

2.3.7 Data analysis

Differences in measured variables with soil volume were analysed by mixed-effects models in R with individual containers and experimental blocks as random effects and soil volume treatment as a categorical fixed effect with seven levels. Tukey's post-hoc tests were performed in conjunction with ANOVA to determine which specific paired comparisons among soil volume treatments were different. A linear mixed effect model of A_{mass} and leaf chemistry was performed using the 'nlme' package (Pinheiro et al. 2015) in R. Explained variance (R^2) of mixed models were computed as in (Nakagawa and Schielzeth 2013), in which the marginal R^2 represents variance explained by fixed factors and the conditional R^2 by both fixed and random factors. Tests of allometric relationships between log-transformed biomass components were implemented using standardized major axis regression in the 'smatr' package in R (Warton et al. 2012). All tests of statistical significance were conducted at an α level of 0.05.

2.4 Results

2.4.1 Growth and morphology

Plant height, diameter and leaf area diverged between container volumes soon after start of the experiment (Figure 2.1a-c). First, seedling leaf area significantly diverged between soil volumes ($P < 0.029$) during the 5^{th} week of the experiment. Following this period both height (8^{th}) week) and then diameter (9^{th} week) significantly deviated across soil volumes ($P < 0.045$ & 0.035, respectively). The large reductions in height gain and total leaf area in smaller compared to larger containers continued throughout the experiment. In this field study, colder temperatures and reductions in total PPFD per day

(Figure 2.2) likely slowed the growth of seedlings in the final weeks of the experiment. Seedlings maintained diameter growth throughout the experiment, although marginal with smaller soil volumes in the final month. Final seedling height significantly increased with increasing soil volume ($P < 0.001$). Increases in both final stem diameter ($P < 0.001$) and cumulative leaf area (both $P < 0.001$) were found with increasing soil volume and these differences were driven mainly by the largest container and the free seedling treatments.

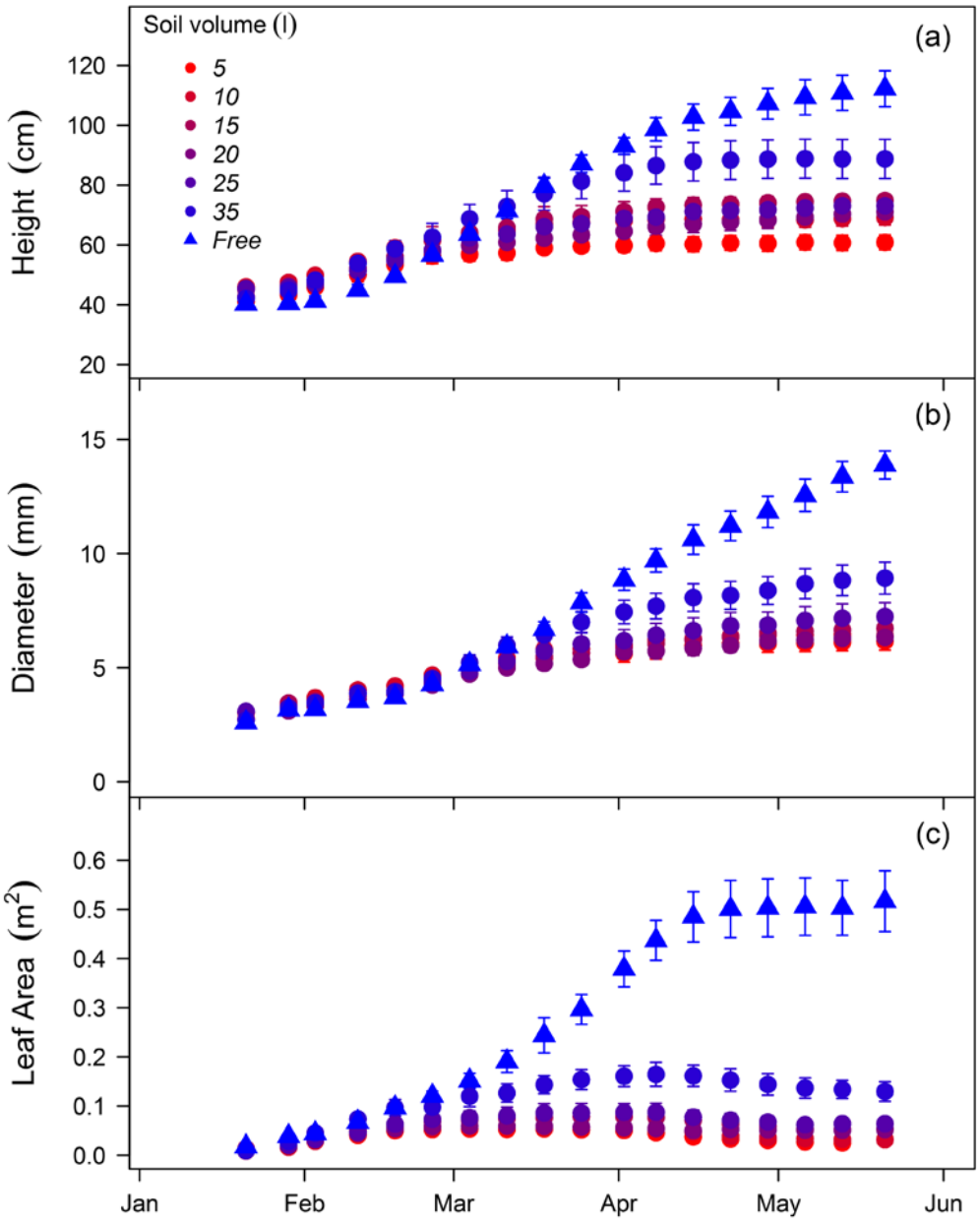

Figure 2.1. Soil volume treatment means ± standard error of height growth (a), diameter growth (b), and seedling leaf area estimated from leaf counts (c) measured weekly of *Eucalyptus tereticornis* seedlings across the experiment duration in 2013.

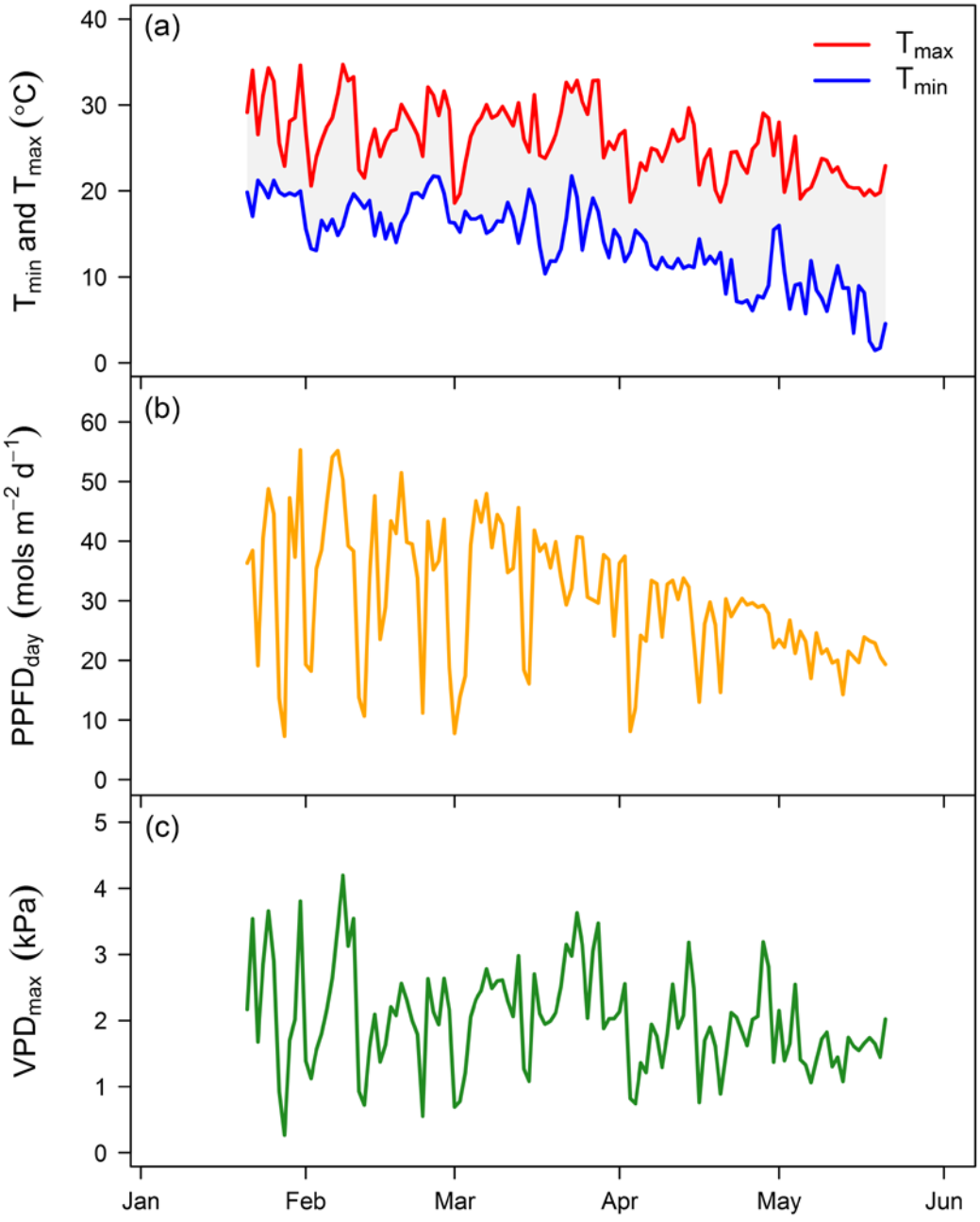

Figure 2.2. Daily maximum and minimum temperature (a), total daily PPFD (b), and daily maximum vapour pressure deficit (c) across the experiment duration in 2013.

Total seedling biomass at harvest was significantly different across container volumes ($P < 0.001$) and between container treatments and free seedlings ($P < 0.001$, Table 2.1). On average, harvested biomass of free seedlings was 84% higher than seedlings in containers. Plant biomass was positively correlated with total leaf area across all treatments ($R^2 = 0.97$, $P < 0.001$). Differences in biomass partitioning to leaves, stems and roots were not different across soil volumes after variation in seedling biomass across treatments was factored in the analysis (Figure 2.3a,b). Across all treatments, the final harvest root:shoot biomass ratio was conserved in these seedlings which exhibited a slightly higher shoot than root mass ($\bar{x} = 0.904$, 95% CI = [0.846,1.119]) and the ratio of leaf to fine root mass was also not different (Figure 2.3c).

Table 2.1.Responses of plant and leaf characteristics of *Eucalyptus tereticornis* seedlings to soil volume treatments. Each value reflects the mean (± 1 standard error) for each treatment. Seedling mass and leaf $\delta^{13}C$ values are from final harvest. Values of leaf starch, sugars, TNC-free nitrogen (N_f) and specific leaf area (SLA) represent overall means across measurement campaigns (n=6). Different letters represent significant differences between treatments. The volume effect P value represents the overall difference between seedlings with soil volume restriction and the control seedlings.

Volume (L)	**Seedling mass (g)**	**$SLA_{TNC\text{-}free}$ (m^2 kg^{-1})**	**Leaf Starch (%)**	**Leaf Sugars (%)**	**Leaf N_f (%)**	**Leaf $\delta^{13}C$ (‰)**
5	14.8 (1.82) a	11.8 (0.32) a	12.7 (0.97) b	6.4 (0.28) a	1.3 (0.03) a	-30.1 (0.26) a
10	20.0 (2.38) ab	11.7 (0.31) a	9.4 (0.75) ab	6.7 (0.25) a	1.5 (0.04) ab	-30.2 (0.25) a
15	25.4 (2.49) ab	12.7 (0.48) a	7.3 (0.73) a	7.2 (0.28) a	1.6 (0.07) ab	-30.3 (0.36) a
20	23.4 (1.63) ab	11.8 (0.37) a	9.5 (0.88) ab	6.6 (0.26) a	1.7 (0.06) ab	-29.7 (0.28) a
25	30.4 (5.49) ab	12.4 (0.40) a	9.8 (0.71) ab	6.9 (0.24) a	1.6 (0.07) ab	-29.7 (0.25) a
35	52.2 (9.55) b	13.5 (0.46) ab	9.8 (0.65) ab	6.8 (0.22) a	1.8 (0.08) b	-30.6 (0.38) a
Free	174.5 (18.02) c	15.1 (0.47) b	6.8 (0.65) a	7.4 (0.25) a	2.7 (0.09) c	-30.0 (0.34) a
Volume Effect (P value)	0.001	0.001	0.029	0.125	0.001	0.372

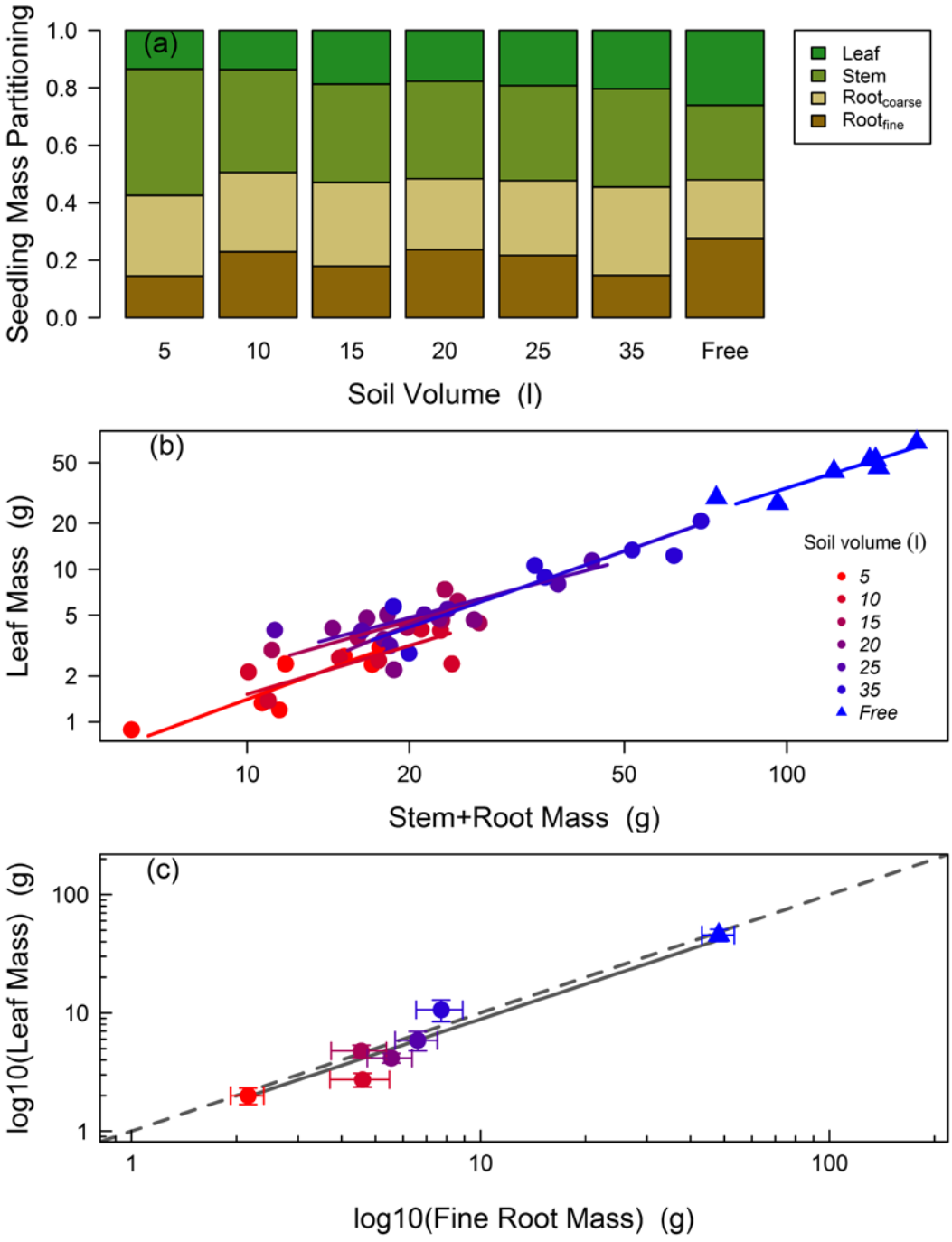

Figure 2.3. Soil volume treatment means of biomass partitioning to leaves, stems, and roots at harvest (a), bi-variate relationships between mass allocation to leaves and stems

+ roots (b) and leaf mass as a function of fine root biomass with ± standard error (c). For (b) lines represent standardized major axis fitting of the log-transformed allometric relationships of leaf mass fraction by treatment. For (c) the dashed line is the 1:1 relationship and the solid line represents the significant log-log model fit ($R^2 = 0.82$) with equation: log(x) = 0.983log(y) - 0.036.

Overall, SRL was higher in seedlings in containers compared to free seedlings but only in some of the container size treatments (Table 2.2, P = 0.009). Fine root length density was significantly higher in the two smallest container sizes and was the lowest in the largest container size (Table 2.2, P < 0.001). Over the duration of the experiment SLA_f was higher in free seedlings, but was not different across containers sizes (Table 2.1, P < 0.001) and this pattern was evident beginning in the first gas exchange measurement campaign (P < 0.001).

Table 2.2. Responses of root characteristics of *Eucalyptus tereticornis* seedlings to soil volume treatments. Each value reflects the mean (± 1 standard error) for each treatment. All values are from the final harvest. Values for fine root length density (FRLD) were only calculated for seedlings in containers as free seedlings had potentially unlimited soil volume to exploit. Different letters represent significant differences between treatments. The volume effect P value represents the overall difference between seedlings with soil volume restriction and the control seedlings, except for FRLD which represents only differences between seedlings in containers.

Volume (L)	**Root Nitrogen (%)**	**SRL (m g^{-1})**	**FRLD (m dm^{-3})**
5	0.78 (0.04) ab	73.0 (6.73) ab	36.4 (5.68) bc
10	0.75 (0.02) a	99.6 (8.70) b	45.9 (8.68) c
15	0.71 (0.02) a	74.6 (6.98) ab	20.9 (1.51) ab
20	0.76 (0.04) a	85.8 (7.37) ab	23.0 (3.09) ab
25	0.74 (0.02) a	82.5 (15.02) ab	24.7 (7.58) ab
35	0.77 (0.03) ab	63.1 (6.47) a	13.3 (1.98) a
Free	0.90 (0.03) b	50.9 (5.00) a	
Volume Effect (P value)	0.017	0.009	0.001

2.4.2 Leaf and root chemistry

Leaf N_f was significantly higher in free seedlings and the largest container volume compared to the smaller container volumes at the onset of gas exchange measurements (6th week, $P < 0.001$). Throughout the remainder of the experiment the smallest container volume had a significant reduction in leaf N_f compared to other soil volumes, while free seedlings maintained the highest leaf N_f (Table 2.1, $P < 0.001$). Leaf starch content in the smallest container was ca. double that of free seedlings ($P = 0.039$), while leaf soluble sugars did not differ across treatments throughout the experiment (Table 2.1). Differences in leaf starch between the free seedling and the smallest container were evident during the first gas exchange campaign ($P = 0.001$). Root N was higher in free seedlings compared to seedlings in containers but only for some of the container size treatments (Table 2.2).

2.4.3 Gas exchange and photosynthetic parameters

At the first measurement campaign, both A_{sat} and A_{max} were significantly higher in the free seedling treatment compared to seedlings in containers (both $P < 0.001$). Across all measurement campaigns mean A_{sat} (Figure 2.4) and A_{max} (Table 2.3) were consistently higher in free seedlings than in containers (26 % and 29 %, respectively). The relationships between photosynthetic capacity, leaf starch and leaf N on a mass basis was marginally significant ($P = 0.058$), but A_{max} on a mass basis was highly correlated to both leaf N content and leaf starch (both $P < 0.001$). We used predictions from the linear mixed effect model equation to visualize these relationship of A_{max} to either leaf N content or leaf starch at multiple bin levels (n=5) of the co-variate parameter (Figure

2.5). Across all measurement campaigns and treatments A_{max} was higher when leaf N was also higher, usually associated with low levels of leaf starch (Figure 2.5a). A_{max} was also lower when leaf starch was high as higher leaf N often did not coincide with high leaf starch (Figure 2.5b). These relationships were also analyzed when variables were expressed per unit leaf area and the interpretation of the results did not change, as SLA was similar between treatments. Overall, A_{max} was positively correlated with final harvest biomass across all seedlings ($P < 0.001$).

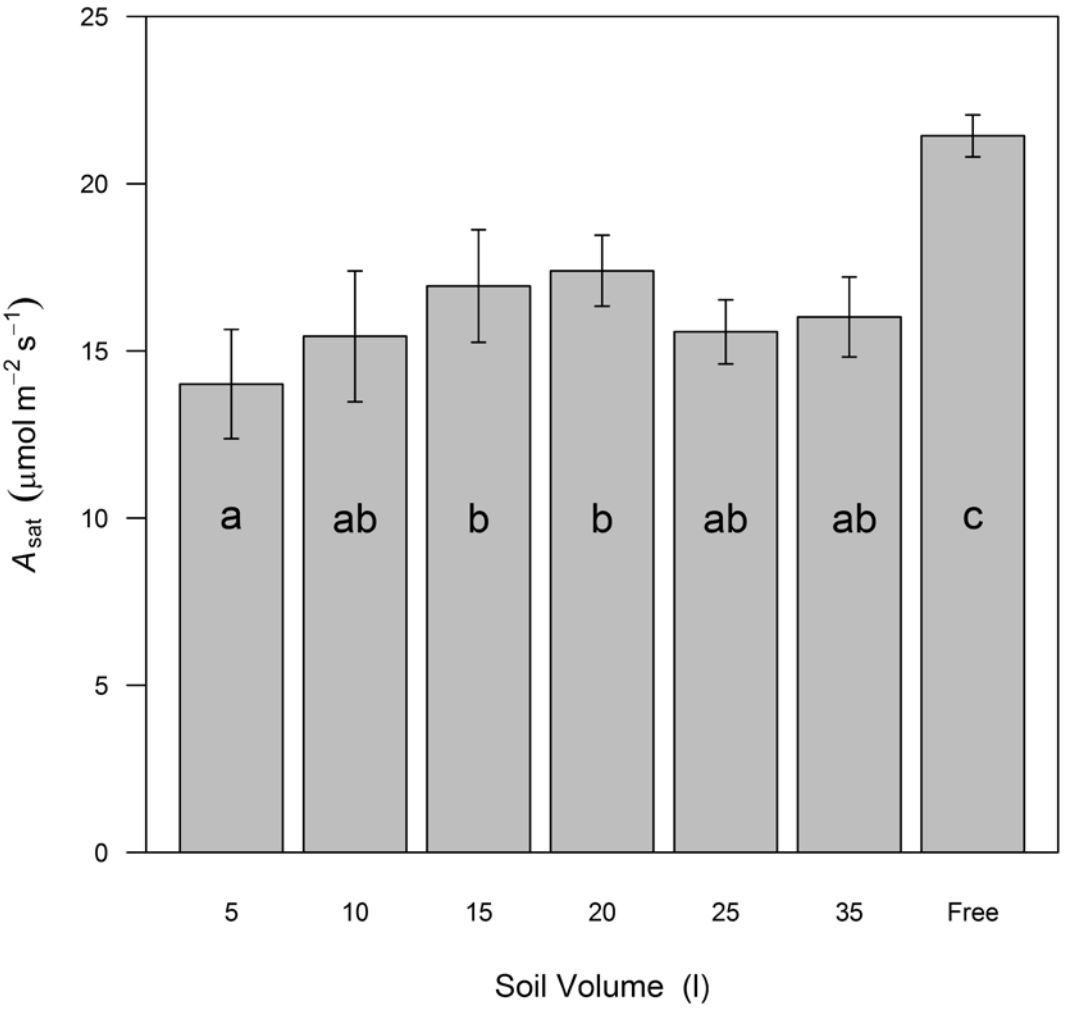

Figure 2.4. Soil volume treatment means ± standard error, across all measurement

campaigns (n = 6), of light saturated rates of photosynthesis at 25 °C. Different letters represent significant differences between treatments

Table 2.3. Responses of leaf level gas exchange variables of *Eucalyptus tereticornis* seedlings to soil volume treatments. Each value reflects the mean (± 1 standard error) for each treatment. A_{max}, R and g_s are each measured at 25 °C. Values of A_{max}, g_s and g_1 represent overall means across measurement campaigns (n=6). R, J_{max} and V_{cmax} values are means of two measurement campaigns at beginning and end of gas exchange measurements. Different letters represent significant differences between treatments. The volume effect P value represents the overall difference between seedlings with soil volume restriction and the control seedlings.

Volume (L)	**A_{max} (μmol m^{-2} s^{-1})**	**R (μmol m^{-2} s^{-1})**	**J_{max} (μmol m^{-2} s^{-1})**	**V_{cmax} (μmol m^{-2} s^{-1})**	**g_s (mol m^{-2} s^{-1})**	**g_1**
5	21.2 (0.9) a	0.61 (0.04) a	104.5 (3.3) a	63.3 (2.5) a	0.30 (0.009) a	5.1 (0.14) bc
10	22.3 (1.4) ab	0.79 (0.06) a	116.5 (7.5) a	69.4 (4.7) a	0.36 (0.009) ab	5.4 (0.10) cd
15	23.3 (1.2) ab	0.70 (0.05) a	125.4 (7.8) a	80.8 (5.1) ab	0.42 (0.010) ab	5.8 (0.14) d
20	26.1 (0.7) b	0.73 (0.11) a	131.5 (8.6) a	82.1 (4.7) ab	0.37 (0.011) ab	4.9 (0.12) ac
25	23.9 (0.9) ab	0.53 (0.13) a	132.8 (13.1) a	79.0 (8.7) a	0.30 (0.009) a	4.5 (0.14) a
35	25.0 (1.0) ab	0.61 (0.04) a	127.2 (6.1) a	82.4 (3.6) a	0.31 (0.011) a	4.4 (0.15) a
Free	33.1 (0.7) c	0.64 (0.07) a	169.0 (8.2) b	100.4 (3.3) b	0.44 (0.011) b	4.5 (0.14) ab
Volume Effect (P value)	0.001	0.269	0.004	0.005	0.007	0.001

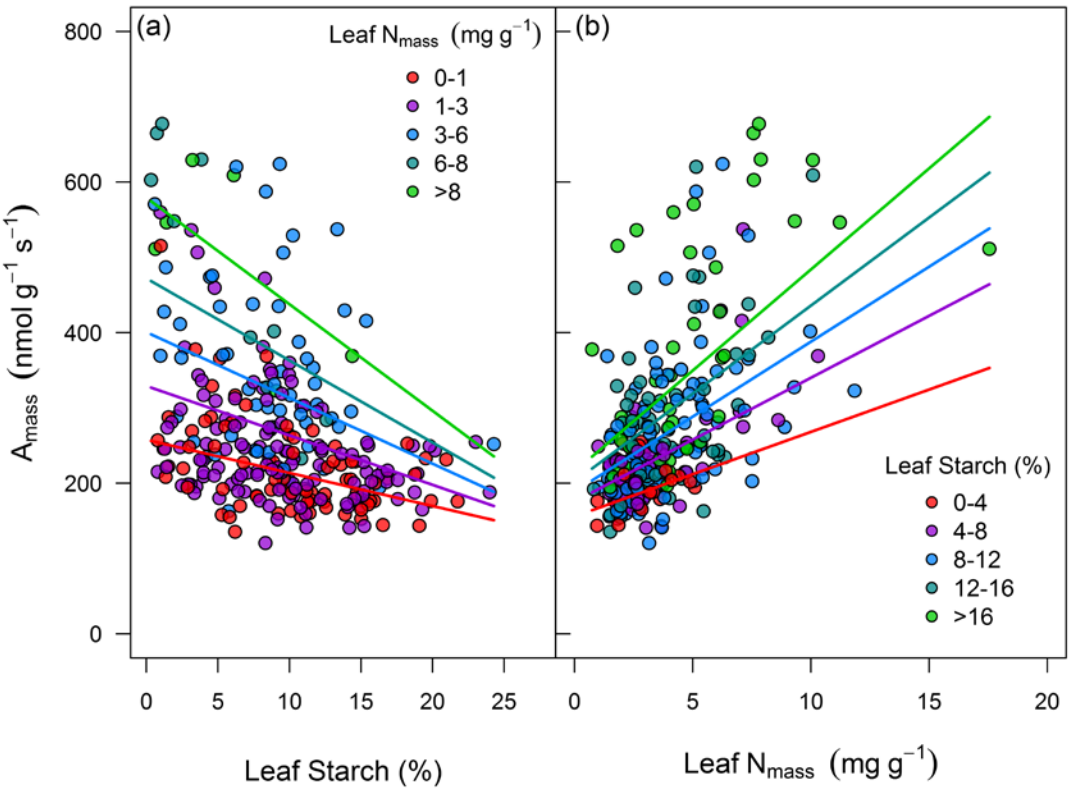

Figure 2.5. Photosynthetic capacity on a leaf mass basis, as a function of accumulation of leaf starch (a) and leaf nitrogen per unit mass without TNC (b). Colors represent bins levels (n = 5) of both leaf starch and nitrogen grouped from low to high. Lines represents predictions, for each bin level, from the linear mixed effects model equation of A_{mass} as a function of starch and nitrogen. The marginal R^2 (fixed effects only) was 0.37 and the conditional R^2 (fixed and random effects) was 0.48 for the complete model.

Both J_{max} and V_{cmax} were significantly higher in free seedlings (30 % and 26 %, respectively) than container-grown seedlings with little variation between container volume treatments (Table 2.3). Overall, the J_{max}:V_{cmax} ratio was relatively conserved across all treatments (1.6±0.02), which is consistent with findings across many tree

species (Medlyn 1996, Leuning 1997, Medlyn et al. 1999, Warren et al. 2003a, Crous et al. 2008). Leaf dark respiration rates were not significantly different across soil volumes (Table 2.3). The g_1 parameter, generated for each seedling from the Medlyn et al (2011) optimal stomatal conductance model, was lowest in the free seedling treatment and was marginally different across soil volume treatments (Table 2.3).

Neither Ψ_{pd} nor Ψ_l were different across treatments, with mean values of -0.27 and -1.2 MPa across all seedlings, respectively. Although g_s in free seedlings was generally higher than those in containers (Table 2.3, $P < 0.001$), the mean rates for all seedlings were high at 0.37 mol m^{-2} s^{-1} and did not change throughout the course of the experiment. Additionally, leaf $\delta^{13}C$ at final harvest was not different across treatments (Table 2.1). Combined these indices provide strong evidence that water stress was not apparent on these seedlings throughout the experiment. Soil N at harvest was not different across soil volumes ($\overline{x}$ = .045 %), with minimal decreases from pre-planting values ($\overline{x}$ = .049 %). This indicates that nutrient leaching from free seedlings or from draining of containers following natural rainfall events did not differ between treatments.

2.4.4 Modelling seedling biomass

The default model (M_{free}), successfully optimized a LMF (21.6 %) which then allowed the model to predict mean harvest total biomass of free seedlings within 1.2 %. Using this optimized LMF, the total biomass of modeled seedlings for each soil volume treatment (M_{pots}) were on average 23±2.4 g C more than measured seedling biomass when compared against predicted total net leaf C gain (Figure 2.6a). As a result, seedling

C mass was overestimated by an average of 50±8.7 % in modeled seedlings across the soil volume treatments when non-photosynthetic parameters were kept constant (Figure 2.6b). As a result, the observed reductions in leaf A_n with decreasing soil volume when integrated across the 120 day experiment were not large enough to explain the reduction in observed seedling biomass across the container size treatments.

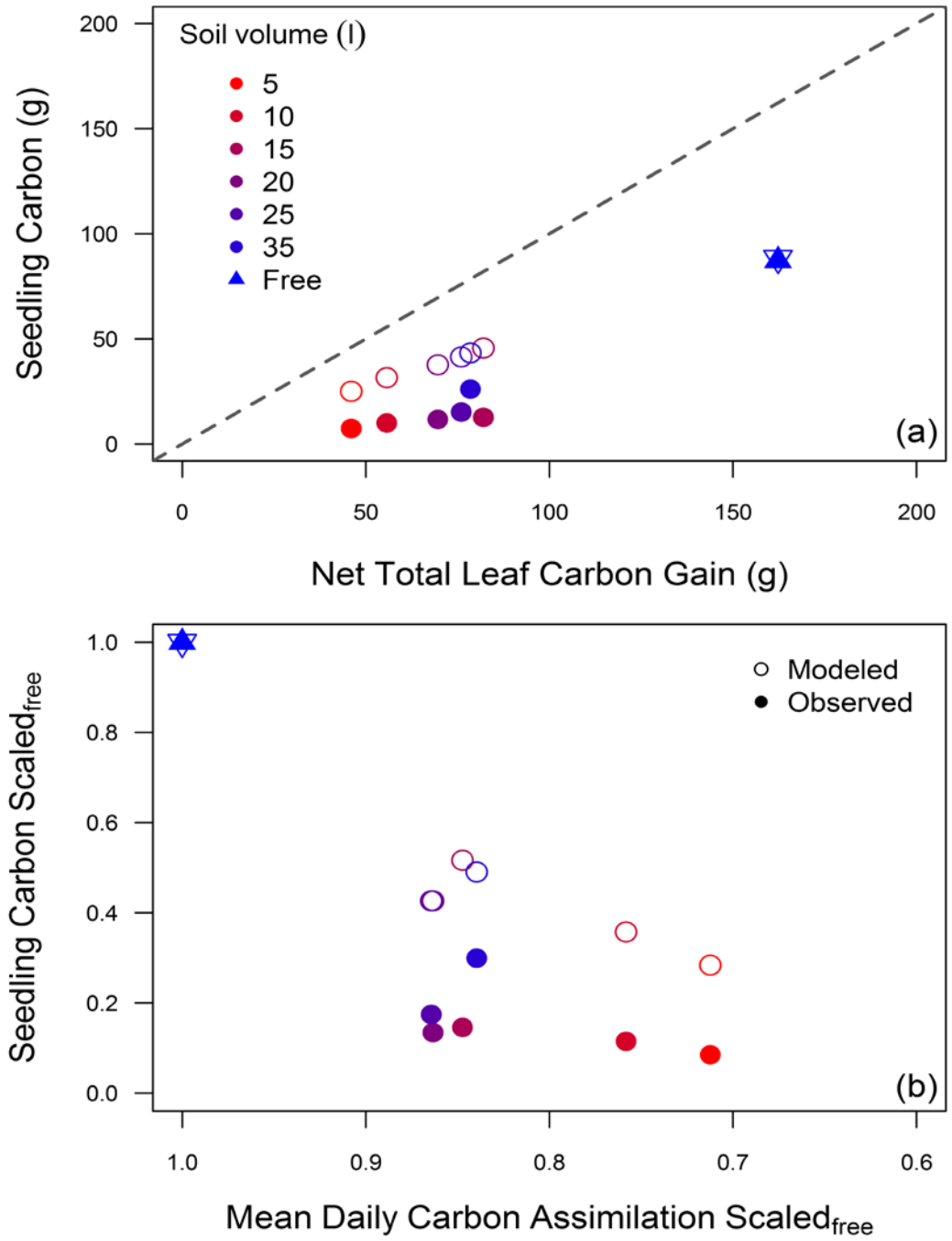

Figure 2.6. Total carbon mass for harvested and modeled seedlings versus predicted total carbon gain after 120 days (a) and reductions in final seedling carbon mass, both modeled and observed, as a function of the reduction in leaf photosynthesis across

treatments (b). For (a) the dashed 1:1 identifies the difference between net total leaf carbon gain and gross seedling production. For (b) both seedling carbon mass and daily carbon assimilation were first scaled to the free seedling control.

Next, we performed a series of model simulations to test possible C allocation scenarios to account for the over predictions of seedling C mass. Testing the sensitivity of the model to observed treatment-specific LMF from the final harvest (M_{S1}), which were each lower than the optimized LMF value (see Figure 2.3a), improved model predictions of seedling C mass but still overestimated seedling total C by 32±11.1 % (Figure 2.S1a). Using harvest values of LMF, however, does not capture the observed increase in leaf turnover of seedlings in small containers (Figure 2.1c). Thus, the use of harvest LMF values for seedlings in containers in M_{S1} likely underestimates daily C allocation to leaves over the final months of the experiment. Increases of 50 % in non-leaf tissue respiration (M_{S2}) improved biomass estimates slightly but overestimated mass C by an average of 46±9.3 % in seedlings with soil volume restriction (Figure 2.S1b). With M_{S2}, non-tissue respiration rates would need to be increased by ca. 250% in order for mass balance to be achieved.

2.5 Discussion

This study utilized a novel field design to manipulate belowground sink limitation and physically restrict *Eucalyptus tereticornis* seedling biomass production. We addressed questions regarding the coordination of A_n and growth by complementing empirical results with a C mass balance model. We found that reductions in leaf A_n across

container sizes, when integrated across the 120 day experiment, were alone insufficient to account for observed reductions in total plant biomass production.

2.5.1 Reductions in growth and physiology under sink limitation

Soon after seedlings became established both height and diameter growth were negatively affected by decreasing soil volume. This led to the large reductions in biomass in small containers, compared to freely rooted seedlings. We analyzed the relationship between biomass growth and soil volume and found an increase of 34 % with a doubling of container volume, consistent with the meta-analysis of Poorter, Bühler, et al. (2012). These growth reductions were expected, as the impedance of root growth can cause reductions in overall plant growth and activity (McConnaughay and Bazzaz 1991, Young et al. 1997). It has been shown that roots subjected to environmental stress may send inhibitory signals to the shoots that affect g_s, cell expansion, cell division and the rate of leaf appearance (Passioura 2002). Here, this was likely evident in a large divergence in leaf area between seedlings in containers and free seedlings through time, with the eventual cessation of new leaf growth in seedlings in small containers.

Decreases in A_{sat} occurred at the same time as reductions in height and diameter of seedlings in containers. This initially suggests a strong link between growth and an apparent down regulation of A_n. However, there are several possible mechanisms that can explain reduced A_n in small containers including nutrient content, water or reduced sink strength (Poorter, Bühler, et al. 2012). It was therefore necessary to examine each

of these factors to determine if the induced belowground sink limitation actually triggered photosynthetic down regulation.

With high rates of g_s, non-limiting leaf water potential (Ψ_{pd}) and consistent leaf $\delta^{13}C$ across soil volume treatments there was little evidence that water stress caused the reduction in A_n. This finding is consistent with other container size studies without drought treatments. For example, reduced A_{max} in cotton seedlings grown at elevated CO_2 was attributed to sink-limited feedback inhibition from inadequate rooting volume, not decreased g_s (Thomas and Strain 1991). Additionally, severe reductions in A_n in coffee plants were not attributed to impacts of container size on leaf water potentials or g_s (Ronchi et al. 2006). It is likely that reductions in A_n of well-watered seedlings observed in our study of *E. tereticornis* seedlings was instead the result of limiting soil nutrients or space restriction on belowground sink strength.

Here, reductions in A_n were positively correlated with decreases in leaf N and leaf N was considerably reduced for seedlings in containers. As leaf N reductions were detected with TNC-free leaf mass, this suggests that physical root restriction or decreased supply likely affected seedling N uptake instead of TNC dilution in leaves in the smallest containers. Root N at the end of the experiment was on average higher in free seedlings but not consistently higher than every container volume treatment. Unrestricted mycorrhizal recruitment could have instead facilitated the increases in leaf N in free seedlings, but this effect is unknown. Combined with the fact that soil N declined evenly across all treatments, there was no clear mechanism present to identify changes in root N

uptake between free seedlings and seedlings in containers. In these already low fertility soils, it is possible that seedlings in containers simply grew into increasing N limitation which negatively affected belowground sink strength. Although no clear feedback could be determined between the available soil N pool and decreases in leaf N, the effects of belowground sink limitation on A_n of seedlings in containers was evident throughout the experiment. Future experiments, in which soil N treatments are added, may be able to elucidate the apparent feedbacks between N uptake by roots and leaf N content.

As both rooting space and resources were finite in containers, the inability of seedlings to maintain the capacity of the belowground C sink resulted in the buildup of C assimilate in leaves. The feedback inhibition of A_n from starch accumulation has been proposed, yet it is still not known whether there is a starch threshold that triggers the down-regulation process (Nebauer et al. 2011). Here, declines in A_{max} were correlated with higher starch content throughout the experiment. This agrees with a study on a deciduous conifer by Equiza et al. (2006) where photosynthetic downregulation from reduced sink strength was correlated with starch content. As starch content in leaves of plants grown in the smallest containers was nearly double that of free seedlings in our study, this suggests the response of A_n to sink inhibition was regulated by this accumulation, as hypothesized.

2.5.2 Biomass partitioning under sink limitation

As biomass partitioning is likely controlled by the source and sink strength of all organs (Poorter, Niklas, et al. 2012), it was important to determine which tissue components were most affected by the container size treatments. It was necessary to distinguish if

growth was affected beyond ontogenetic constraints, by correcting for size, as biomass distribution is strongly size-dependent (Gould 1966, Lleonart et al. 2000). In this study, there was no significant difference in root, leaf, or stem biomass partitioning with reduced soil volume compared to free seedlings, outside of ontogenetic drift (Figure 2.3a,b). This is a surprising result as shifts in partitioning have been noted specifically for nutrient limitation (McConnaughay and Coleman 1999, and references therein). Surprisingly, a constant ratio of fine root mass to leaf mass was observed across all treatments suggesting a functional partitioning response to optimize resource gain did not occur.

The lack of detected shifts in partitioning to fine roots provides evidence against an optimal foraging strategy for seedlings in containers. This could be because lateral root development is affected by inanimate obstacles and avoiding growth towards container walls could improve the efficiency of resource allocation (Falik et al. 2005). The sensitivity of roots to their own exudates near obstructions may prevent further growth (Semchenko et al. 2008). Here, we found that FRLD was highest in smallest containers suggesting that root restriction likely occurred as simple function of available rooting space. Additionally, physical restriction of root proliferation could have impacted root development and morphology prior to shifts in mass partitioning. Here, increases in SRL were detected in several of the soil volume treatments. This is not surprising as plants in containers have been shown to have different root morphology to field grown plants (NeSmith and Duval 1998). The poor soil quality used in our experiment and root restriction, however, likely decreased the capacity of this morphological response to increase N uptake. Alternatively, root exudation may have increased with reduced

rooting volumes to facilitate N uptake in favour of increasing partitioning to root biomass.

2.5.3 Do reductions in photosynthesis explain reductions in seedling growth?

Our model used a simple approach to drive seedling growth with measured reductions in leaf A_n, via soil volume effects, while treating C use efficiency, respiration and C allocation as fixed processes. Contrary to expectation, the model consistently overestimated seedling growth in containers when parameterized with an optimized LMF for free seedlings. Although reductions in both A_{max} and biomass were strongly correlated among treatments, as hypothesized by Poorter, Bühler, et al. (2012), we provide evidence that the negative effects of sink limitation on A_n do not fully explain reduced seedling growth. These findings are important as this model reflects classical approaches in tree growth and production modelling that are driven by inputs of C assimilation and processes such as respiration are considered proportional to biomass (Le Roux et al. 2001) or growth rate (Tjoelker et al. 1999). It is possible that the overestimation of growth was due to an initial overestimation of A_n, however, the robust empirical based methods used to generate photosynthetic parameters (J_{max}, V_{cmax}, R and g_1) make this unlikely. Instead, our results indicate a need to evaluate how oversimplified representations of processes other than A_n affect models which distinguish the fate of assimilate C within a plant. Doing so will provide valuable input to future models as assimilate allocation is a key component in carbon-balance driven plant growth models (Lacointe 2000). To address this issue, we utilized the flexibility of this model to test plausible fates of the pool of simulated non-biomass C unaccounted

for with observed mass balance. Similar to Lohier et al. (2014) we manipulated processes contributing to modeled seedling C mass balance, including changes to leaf C allocation or non-leaf tissue respiration, to quantitatively test their respective influences on model predictions.

Using measured LMF from the harvest, instead of the optimized seedling control (M_{S1}), improved biomass predictions and provided insight into how sink limitation can impact leaf C allocation beyond A_n. The sensitivity of the model to shifts in LMF could represent leaf loss throughout the experiment that could not be explicitly quantified in this field study. As TNC accumulation can lead to accelerated leaf senescence (Paul and Foyer 2001), this could explain the observed decline in total leaf area of seedlings in small containers. Future empirical and modelling studies should focus on how feedbacks from sink activity affect both rates of A_n and the fate of C allocated to growth, respiration and C storage in leaves. It will be the interactions between these two components that will determine the total C gain available for plant growth.

Increasing rates of non-leaf respiration (M_{S2}) improved biomass predictions but to a far lesser extent than changes to leaf C allocation. We also show that very large increases in non-leaf respiration rates would have been required to accurately predict observed seedling biomass. Although the fraction of photosynthate used in respiration is known to vary among species and is sensitive to changes in growth rates (Lambers et al. 2008), results from M_{S2} highlight a lack of knowledge regarding how respiration rates of individual tissues, within a single plant, maybe be differentially affected by

environmental change. This is noteworthy, as C balance is a delicate equilibrium between fluxes of A_n and respiration, partial accounting of C dynamics can easily lead to erroneous conclusions (Valentini et al. 2000). These results imply that using fixed rates of respiration in models likely underestimates plant responses to sink limitation. Thus, we agree with Delucia et al. (2007) that it is likely inappropriate to assume that respiration is a constant fraction of gross primary production in models. Our findings reveal that a combination of different mechanisms, beyond A_n, are likely at play in driving the observed seedling biomass response to sink manipulation. However, the degree to which these mechanisms will regulate growth will undoubtedly shift across different experimental manipulations and plant species.

2.5.4 Conclusions

With a novel field-based design we detected a massive effect of container volume on seedling growth when compared with naturally planted seedlings. This is important as manipulations of plants grown in containers are often used to draw conclusions about growth and physiological principles, but how these results actually reflect field-grown plants has seldom been studied. Although biomass partitioning was conserved, our empirical and model results suggest that the amount of photosynthate allocated to non-biomass pools such as TNC or respiration were likely altered by sink inhibition. The debate over how rates of photosynthesis affect plant growth or to what degree these rates are instead controlled by growth has existed for decades (Sweet and Wareing 1966). Our combined empirical and modelling approach shows that when non-photosynthetic parameters were kept constant, changes in A_n were not able to fully to predict changes in growth, an important distinction often missed in studies that manipulate source/sink

activity. Körner (2013) suggests that it is the norm for sink activity to feedback onto source activity, causing growth to control A_n through the demand for C. Although this may be true, our results imply that quantifying the fate of assimilated C into known pools of growth, storage and C loss are needed prior to addressing this debate. Our modelling results agree with conclusions from Valentine and Mäkelä (2005) where the problem with predicting tree growth is a problem in forecasting the assimilation and allocation of C and other constituents. The approach used here has the flexibility to account for multiple drivers of C allocation and provides an avenue to address future questions regarding the impact of environmental change on plant growth.

2.6 Supporting Information

Table 2.S1.Seedling growth model default parameters.

Variable	Description	Default Value	Units	Source
Leaf area_i	initial leaf area	0.035	m^2	this study
Leaf mass_i	initial leaf mass	3.45	g	this study
Stem mass_i	initial stem mass	1.51	g	this study
Root mass_i	initial root mass	0.99	g	this study
ϵ_c	biomass conversion efficiency	0.65	g C g $mass^{-1}$	Mäkelä (1997)
$R_{\text{coarse root}}$	coarse root respiration	0.00124	g C g $root^{-1}$ d^{-1}	Marden et al. (2008)
$R_{\text{fine root}}$	fine root respiration	0.01037	g C g $root^{-1}$ d^{-1}	Ryan et al. (2010)
R_{stem}	stem respiration	0.00187	g C g $stem^{-1}$ d^{-1}	Drake et al. (unpublished)
C_{day}	daily leaf carbon assimilation	5.4 - 7.6	g C m^{-2} d^{-1}	this study
Λ	leaf or root turnover	1	yr^{-1}	theoretical

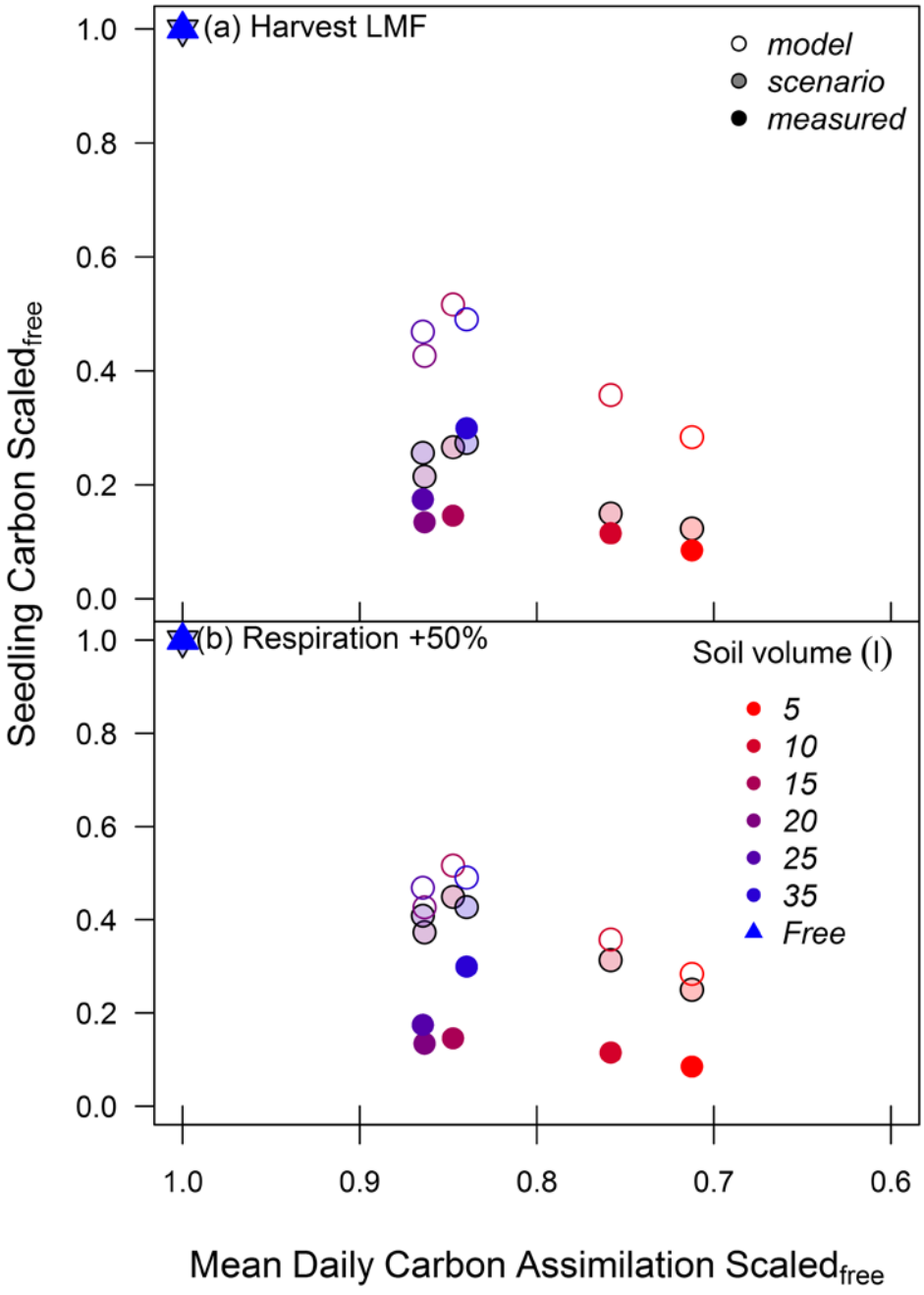
(a) Harvest LMF
model
scenario
measured
(b) Respiration +50%
Soil volume (l)
5
10
15
20
25
35
Free
Seedling Carbon Scaled$_{free}$
Mean Daily Carbon Assimilation Scaled$_{free}$
1.0
0.8
0.6
0.4
0.2
0.0
1.0
0.9
0.8
0.7
0.6

Figure 2.S1. Sensitivity testing of the seedling growth model to different carbon allocation strategies including; constraints of leaf mass fraction to treatment specific final harvest values (a) and increases in respiration of non-leaf tissue components by 50 % (b). Open and filled symbols represent default model and harvest values, while shaded symbols represent model sensitivity to each scenario by soil volume treatment. Both seedling carbon mass and daily carbon assimilation were first scaled to the free seedling control.

Chapter 3

Rapid response of mesophyll conductance to light availability allows shade leaves to take advantage of sunflecks

3.1 Abstract

Light gradients within tree canopies play a major role in the distribution of plant resources that define photosynthetic capacity of individual leaves. A lack of empirical data relating photosynthesis to leaf physiological behavior within tree canopies, however, impedes our ability to assess the contribution of shade leaves to canopy carbon gain. To investigate the CO_2 diffusion pathway of sun and shade leaves, leaf gas exchange was coupled with online carbon isotope discrimination to measure net leaf photosynthesis (A_n), stomatal conductance (g_s) and mesophyll conductance (g_m) in *Eucalyptus tereticornis* trees grown in climate controlled whole tree chambers. Compared to sun leaves, shade leaves had lower A_n, g_m, V_{cmax}, J_{max} and leaf nitrogen but but g_s was similar. When light intensity was increased from low light to high light for shade leaves both g_s and g_m increased rapidly, leading to increases in A_n greater than sun leaves at the same photosynthetic photon flux density. Here we show that dynamic physiological responses of shade leaves to altered light environments has important implications for upscaling leaf level measurements and predicting whole canopy carbon gain. We argue that the rapid response of g_m with light enables shade leaves to respond quickly to sunflecks. Evidence that g_m not only varies within a canopy but can be up-

regulated over short time intervals possibly represents a new mechanism underpinning leaf gas exchange responses to light.

3.2 Introduction

Light availability is one of the most important environmental drivers of leaf carbon (C) uptake in trees. Predicting C uptake of forests usually involves upscaling leaf level measurements to assess whole canopy function. Due to the costs and limitations of efficient light harvesting, plants cannot expose all leaves to full sun (Niinemets 2010), making simple upscaling based on solar irradiance problematic. Incident photosynthetic photon flux density (PPFD) declines exponentially with cumulative leaf area index, creating a steep light gradient from the canopy top to bottom (Monsi and Saeki 2005). Consequently, structural and functional properties of leaves are modified to efficiently use light (Vogelman et al. 1996, Niinemets and Valladares 2004), as changing irradiance strongly affects rates of leaf photosynthesis (A_n) (Evans 1995). To estimate whole canopy C gain it is thus necessary to account for the non-linear response of A_n to light by distinguishing between shaded and sunlit leaves (De Pury and Farquhar 1997, Linderson et al. 2012).

The distribution of resources required for A_n, including leaf nitrogen (N) and supply of water, are also partially defined by canopy light gradients. As A_n has a saturating response with light and maximum rates depend in part on N-rich photosynthetic machinery, it has been argued that leaf N should be proportional to PPFD along the

canopy light gradient to maximize canopy C gain at a given total canopy N (Field 1983, Field and Mooney 1986, Peltoniemi et al. 2012). Changes in chlorophyll per unit N, chlorophyll a:b ratios, electron transport capacity per unit chlorophyll, and ratios of electron transport capacity to Rubisco activity can also occur in response to changes in irradiance (Evans and Poorter 2001). Sun leaves frequently experience greater water limitations in the upper canopy, despite effective vascular systems developed for high radiation loads and transpiration (Sellin et al. 2008, Niinemets 2012). Higher rates of A_n and stomatal conductance (g_s) can only be sustained if the leaf specific hydraulic conductance (K_l) is also large enough to avoid low leaf water potentials (Hubbard et al. 2001). Optimal photosynthetic N investment in the upper canopy will be ineffective in enhancing A_n if water supply is insufficient (Niinemets 2012, Peltoniemi et al. 2012), thus K_l should also be higher in the upper canopy to supply sunlit leaves with sufficient water (Burgess et al. 2006, Sellin and Kupper 2007 , Sellin et al. 2008).

Rates of photosynthesis in C_3 plants are limited by the [CO_2] available for fixation by Rubisco within the chloroplast and this [CO_2] is a function of the drawdown of CO_2 from the atmosphere to the site of carboxylation (Warren 2008). This drawdown consists of multiple resistance pathways to CO_2 diffusion which include CO_2 diffusion from the atmosphere through stomata (stomatal conductance, g_s) and then from these intercellular air spaces into the chloroplast (mesophyll conductance, g_m). Based on optimal theory, regulation of g_s within a tree canopy should act to efficiently utilize available supplies of light, N and water to maximize A_n (Peltoniemi et al. 2012). This is because stomata are hypothesized to exhibit an optimal behaviour to maximize C gain while simultaneously

minimizing water loss through transpiration (Cowan and Farquhar 1977). Mesophyll conductance can also impose limitations on A_n as large g_s (Warren 2008, Ubierna and Marshall 2011), reducing the efficiency of leaf N use in A_n (Niinemets 2007) if g_m constrains CO_2 supply to the chloroplast. Part of the variation in photosynthetic capacity between sun and shade leaves has been proposed to be due to differences in g_m (Piel et al. 2002, Warren et al. 2007), yet the trade-offs that constrain this diffusion pathway are yet to be explicitly quantified. It is likely that leaf anatomical costs associated with minimizing the length, diameter and tortuosity of the g_m diffusion pathway are necessary to maintain a high g_m (Hassiotou et al. 2009). Stomatal and mesophyll conductance should not be considered independent of each other (Griffiths and Helliker 2013), but a lack of empirical data currently hinders our ability to interpreting their coupled responses to A_n across sun and shade leaves.

Additionally, accounting for short term light fluctuations within a canopy, via sunflecks, makes assessing shade leaf behaviour difficult. How shade leaves utilize sunflecks for short term C gain depends on the combined response time of g_s and g_m and the underlying photosynthetic biochemistry acclimated to a low light environment (Pearcy 1990, Tausz et al. 2005). The utilization of sunflecks is first limited by delayed responses of stomata opening, which may take minutes, effectively limiting the maximum assimilation rate that can be achieved (Piearcy 1990, Vico et al. 2011, Way and Pearcy 2012). Mesophyll conductance has been shown to respond to environmental factors (e.g. CO_2, temperature or vapor pressure deficit) at timescales of minutes, possibly faster than g_s (Flexas et al. 2008 and references therein), yet short term response

to light availability are unclear. For example, g_m was found to be independent of light intensity in wheat leaves (Tazoe et al. 2009) but was responsive to light in tobacco (Flexas et al. 2007). Anatomical parameters which regulate g_m with changing irradiance such as chloroplast surface area (Terashima et al. 2006) and mesophyll thickness (Boardman 1977) are also unlikely to adjust during short light fluctuations. The physiological behaviour of shade leaves to maximize C gain must be assessed as both a degree of acclimation to local irradiance and as a potential response to transitory light availability.

Climate warming may also affect the physiological behaviour of leaves within a canopy. This is because leaves can be exposed to different heat, water and high light stresses as temperature and vapour pressure deficit (VPD) vary with canopy light availability (Baldocchi et al. 2002, Niinemets and Valladares 2004, Niinemets 2007). How these stresses affect the diffusion of CO_2, through either g_s or g_m, will have implications for upscaling A_n for sun and shade leaves. Additionally, light saturated rates of A_n are limited by the maximum rate of Rubisco carboxylation (V_{cmax}) or the maximum rate of photosynthetic electron transport (J_{max}) across a range of temperatures, yet their temperature dependencies are not the same (Farquhar et al. 1980, Medlyn et al. 2002). How these parameters are differentially affected by warming may impact constraints of N distribution and leaf photosynthetic capacity across light gradients. The impacts of warming on plant physiological processes are vast, yet differentiating their impacts on leaf physiology within a canopy will be essential to evaluate whole tree responses to a changing climate.

In this study we use *Eucalyptus tereticornis* Sm. trees, planted in climate controlled whole tree chambers with ambient and elevated temperature (ambient +3°C) treatments, to empirically evaluate the distribution of nitrogen and water supply and leaf physiological behaviour of sun and shade leaves. Our hypotheses are as follows:

1. If whole tree canopies are optimized for C gain, then leaf N, hydraulic conductance and biochemical photosynthetic capacity are predicted to be higher in sun leaves compared to shade leaves.

2. Stomatal conductance is proportional to A_n across sun and shade leaves under similar leaf VPD and g_m scales positively with photosynthetic capacity.

3. As shade leaves were expected to develop lower biochemical photosynthetic capacity, increases in A_n following sunfleck simulations were not expected to reach rates of full sun leaves.

4. Climate warming would decrease g_s and leaf C gain in sun leaves more so than shade leaves during summer months, as increased evaporation demand from higher temperatures and irradiance lead to stomatal closure.

3.3 Materials and Methods

3.3.1 Whole tree chamber experimental design

Twelve *Eucalyptus tereticornis* seedlings, chosen from a single local Cumberland plain cohort, were planted in March 2013 into 12 whole-tree chambers (WTC) at the Hawkesbury Forest Experiment site near Richmond, NSW, Australia. Each chamber has a height of 9 m and seedlings were grown for 15 months. A detailed description of the WTC operation and design is available in Barton et al. (2010). Six chambers were set to match outside ambient air temperatures (AT) while the remaining 6 experienced an elevated air temperature treatment of +3°C (ET, Figure 3.S1). Mixing fans in each chamber maintained air movement to minimize leaf boundary layer, resulting in leaf temperatures in each WTC close to those of outside control trees (Barton et al. 2010). Overall, minimal WTC effects on tree performance were previously detected across a range of structural characteristics and physiological parameters compared to outside trees (Medhurst et al. 2006).

Trees grew quickly and developed large canopies, with height growth reaching the top of the WTCs over the experiment duration. Trees were watered weekly with 70 L from March 2013 to November 2013. From October 2013 to the end of the experiment trees were watered every 15 days with the mean monthly rainfall amount for Richmond, NSW. In February 2013 half of the chambers (3 each of AT and ET) were subjected to a drought treatment by withholding watering. Due to a limited range of data for the drought treatment only well-watered trees are reported, which reduces the sample size of

WTC (n=6 to n=3) for the final 3 months of the experiment. This limited amount of data is attributed to small sample sizes as well as a difficulty in generating a sufficient CO_2 drawdown inside the leaf cuvette, due to drought conditions, needed to accurately measure g_m.

Before seedlings were planted into each chamber they were maintained under well-watered conditions in 25 L pots and kept inside each chamber. This allowed for seedlings to gain sufficient size before planting while also allowing them to acclimate to chamber temperature treatments. Seedlings were planted into each chamber after mean seedling height reached ca. 100 cm. The top soils at this site, used in both pots and chambers, are an alluvial formation of low-fertility sandy loam soils (380 and 108 mg kg-1 total N and phosphorus respectively) with low organic matter (0.7 %) and low water holding capacity. A root exclusion barrier extended from chamber walls to the hard layer (ca. 1 m) and roots were allowed to grow freely below the barrier. Leaf gas exchange measurements were initiated in October 2013 when trees had both ample height growth and canopy development for realistic canopy light gradients to be measured. At this point, trees under AT treatment had a mean diameter of 28.2±1.1 mm, height of 348±15.1 cm and a leaf area of 3.9±0.1 m^2. For ET treatments, trees had a mean diameter of 34.1±2.1 mm, height of 418.3±23.1 cm and a leaf area of 6.2±0.2 m^2. Leaf area was calculated based on complete leaf counts and mean leaf size from a subsample.

3.3.2 Leaf gas exchange, online carbon isotope discrimination and mesophyll conductance

Leaf gas exchange measurements were performed six times, beginning in October 2013 and monthly from December 2013 to April 2014. Measurements were taken on a representative sun and shade leaf for each tree during each measurement campaign. The newest fully expanded leaf from the branch apex was chosen for gas exchange measurements and sun leaves were measured in the upper third of the canopy. Here, shade leaves are defined as inner-canopy leaves developing on secondary branches in a low light environment. Shade leaves were always measured in the lower canopy, but leaves were sampled on subsequent higher branches across measurement campaigns to minimize confounding effects of leaf age. As shade leaves most likely developed slower this assured that older leaves in the bottom canopy were avoided.

Prior to gas exchange measurements photosynthetic photon flux density (PPFD) was recorded as a point measurement at the individual leaf level and a spatially averaged measurement at the canopy position for each selected leaf. A hand-held quantum sensor (LI-COR, Lincoln, NE, USA) was used to record leaf level PPFD to ensure that chosen leaves were positioned in the desired light environment, either full sun or full shade. A ceptometer (AccuPAR LP-80, Decagon Devices, Pullman, USA) was then used to measure a spatially averaged PPFD at the canopy height of each chosen leaf type. Each ceptometer reading integrated an array of 80 sensors over a total length of 84 cm. Five ceptometer readings were recorded at different locations within the canopy, but at the same height and close to each selected leaf. The mean of these readings was assumed to

represent the local light environment of sun and shade leaves for each tree. All measurements of PPFD and gas exchange were performed on sunny days between 10:00-14:30 h.

Leaf level gas exchange was measured with a standard (2 x 3 cm) leaf cuvette using a portable gas exchange system (LI-6400XT, LI-COR, Lincoln, NE, USA). This system was coupled with a tunable diode laser (TDL; TGA100,Campbell Scientific, Inc., Logan, UT, USA) for concurrent measurements of online C isotope discrimination. The CO_2 in the leaf cuvette was set at ambient atmospheric [CO_2] (400 ppm) with a flow rate of 200 μmol s^{-1}. We did not explicitly control relative humidity within the leaf cuvette. Two identical gas exchanges systems were run simultaneously, one in each of an AT or ET WTC. Leaf temperatures were controlled at the current AT or ET WTC air temperature, thus observed VPD is based on leaf temperatures in the cuvette. PPFD in the cuvette was set to match the individual light environment of each leaf type (explained above). Periods of high irradiance were simulated for shade leaves by increasing the leaf cuvette PPFD (LI-COR red/blue light source) to match the light environment of the full sun leaf in the same tree. The maximum sunfleck response of shade leaves was then recorded once CO_2 and water vapor fluxes re-stabilized in the leaf cuvette (ca. 25 min).

Once CO_2 and water vapor flux values were stable for each leaf measurement, the sample and reference gas lines were diverted to the TDL via T-junctions inserted into the reference gas tube and match valve outlet of the LI-6400. The gas streams were dried

by passing through napion gas dryers in the respective gas lines, and then $^{12}CO_2$ and $^{13}CO_2$ concentrations were measured for each gas stream by the TDL. Reference, sample and two calibration gases were run on alternating 80 s loops (20 s each), one for each AT and ET leaf at a matched canopy position, for a total of 12 min. This allowed for 4-5 measurements per leaf and data were averaged over the last 10 s of reference line and samples line gas streams for calculations. The two calibration gases were drawn from compressed air tanks (330 and 740 ppm CO_2) in order to correct for gain drift of the TDL on each measurement cycle. Photosynthesis, g_s, transpiration, VPD and intercellular [CO_2] (C_i) were auto-logged every 15 s for each gas exchange system over the same 12 min interval.

Using online C isotope discrimination measurements, the difference between the observed discrimination and what is predicted for light saturated gas exchange is proportional to g_m (Griffiths and Helliker 2013). First, leaf C isotope discrimination was calculated by comparing the isotopic composition of the reference gas entering the leaf cuvette ($\delta^{13}C_e$) with the sample gas ($\delta^{13}C_o$) such that:

(1)

$$\delta = \left(\frac{R_s}{R_{stnd}} - 1\right) 1000$$

where R_s is the isotopic ratio of the sample and R_{stnd} is the isotopic ratio of the standard Vienna Pee Dee Belemnite (VPDB). Next, the observed discrimination (Δ_o) is calculated from Evans et al. (1986):

(2)

$$\Delta_o = \frac{\xi(\delta^{13}C_o - \delta^{13}C_e)}{1000 + \delta^{13}C_e - \xi(\delta^{13}C_o - \delta^{13}C_e)}$$

where:

(3)

$$\xi = \frac{C_e}{C_e - C_o}$$

and ξ is the ratio of the CO_2 entering the well mixed leaf cuvette to the CO_2 draw down in the gas stream by the leaf.

Second, C isotope discrimination during C_3 photosynthesis (Δ) is the resultant discrimination from CO_2 diffusion from the atmosphere to the site of carboxylation, consisting of a series of fractionation steps described in Evans et al. (1986). In this experiment, a modified form of this equation presented in Evans and von Caemmerer (2013) with ternary effect corrections by Farquhar and Cernusak (2012) was used such that:

(4)

$$\Delta_o = \Delta_i - \Delta_{gm} - \Delta_e - \Delta_f$$

where Δ_o is the observed discrimination and Δ_i, Δ_{gm} , Δ_e and Δ_f are the contributions to fractionation if $C_i = C_c$, g_m, respiration and photorespiration, respectively. The equations for each are as follows:

(5)

$$\Delta_i = \frac{1}{1-t}a' + \frac{1}{1-t}((1+t)b - a')\frac{C_i}{C_a}$$

(6)

$$\Delta_{gm} = \frac{1+t}{1-t}\left(b - a_i - \frac{eR_d}{A+R_d}\right)\frac{A}{g_m C_a}$$

(7)

$$\Delta_e = \frac{1+t}{1-t}\left(\frac{eR_d}{(A+R_d)C_a}(C_i - \Gamma_*)\right)$$

(8)

$$\Delta_f = \frac{1+t}{1-t}\left(f\frac{\Gamma_*}{C_a}\right)$$

where the different fractionation factors include; diffusion through water (a_i, 1.8‰), Rubisco carboxylation (b, 29‰), the photorespiratory fractionation (f, 16.2‰) and the combined fractionation through the boundary layer and the stomata (a'). a' is defined by:

(9)

$$a' = \frac{a_b(C_a - C_i) + a(C_s - C_i)}{C_a - C_i}$$

where C_s is the CO_2 partial pressure at the leaf surface, a_b is the fractionation from boundary layer diffusion (2.9‰) and a is the fractionation due to diffusion in air (4.4‰) (Evans et al. 1986). C_a and C_i are the atmospheric and intercellular partial pressures and Γ_* is the compensation point in the absence of mitochondrial respiration in the light (R_d). In this experiment both Γ_* and R_d were derived using a standard Arrhenius function with parameters for *Eucalyptus globulus* from Crous et al. (2012). The ternary effect corrections (t) are described by:

(10)

$$t = \frac{(1 + a')E}{2g_{ac}^t}$$

where E denotes the transpiration rate and g_{ac}^t is the total conductance to CO_2 diffusion to both the boundary layer and stomatal conductance.

The g_m can then be calculated as:

(11)

$$g_m = \left(\frac{1 + t}{1 - t}\left(b - a_i - \frac{eR_d}{A + R_d}\right)\frac{A}{C_a}\right) / \left(\Delta_i - \Delta_o - \Delta_e - \Delta_f\right)$$

The CO_2 diffusion from the intercellular airspace to the chloroplast, g_m, is given by its relationship to the leaf photosynthesis rate (A_n) by:

(12)

$$g_m = \frac{A_n}{C_i - C_c}$$

where C_c is the chloroplast CO_2 partial pressure. Once g_m was calculated C_c and the drawdown of CO_2 from the intercellular air spaces to the site of carboxylation were then estimated using Equation 12. Examples of this approach to measure gas exchange and C isotope discrimination are presented in Evans and Von Caemmerer (2013). The variation in Δ_o between sun and shade leaves and the simulated sunfleck where then compared as a function of C_i:C_a.

3.3.3 Biochemical parameters of photosynthesis

Photosynthetic CO_2 response (AC_i) curves were measured at 25 °C for one sun and shade leaf for each WTC prior to the initiation of the drought treatment. Each AC_i curve began at the reference [CO_2] of 400 μl l^{-1} and then consisted of 12 additional steps from [CO_2] of 50 to 1800 μl l^{-1} at 25 °C at saturating light (1800 μmols m^{-1} s^{-1}). From these curves the photosynthetic parameters, J_{max} and V_{cmax}, were quantified using the biochemical model of (Farquhar et al. 1980) and fit with the 'plantecophys' package (Duursma 2015) in R (R Development Core Team 2011) using default parameters.

3.3.4 Leaf chemistry and hydraulic parameters

Following gas exchange measurements each leaf was collected, measured for leaf water potential (explained below), scanned for leaf area, dried and weighed. These leaves were then milled and analyzed for leaf N content and δ^{13}C. Leaf samples were analysed on a Delta V Advantage coupled to a Flash HT and Conflo IV (Thermo Fisher Scientific, Bremen, Germany) in dual-reactor setup. Samples were flash combusted at 1000°C and converted to CO_2 and N_2 and then subjected to stable isotope ratio mass spectrometry. Leaf N is reported on an area basis (N_a, g m^{-2}) and isotopic signatures of dry matter are reported relative to VPDB.

Predawn (Ψ_{pd}) and midday (Ψ_l) leaf water potentials (MPa) were measured for sun and shade leaves during each gas exchange campaign using a PMS 1505D pressure chamber (PMS Instruments, Albany, OR, USA). The leaf closest to the leaf used for gas exchange was sampled for measurement of Ψ_{pd}. Predawn leaf water potential was measured before sunrise on the same day as gas exchange measurements. Leaves used for gas exchange were immediately sampled for Ψ_l once measurements were completed. All leaves were detached and immediately stored inside foil covered bags before water potential measurements were performed. The degree to which leaf cuvette conditions, especially for shade leaves, modified Ψ_l is unknown. Leaf water potential and transpiration (E, mmol^{-2} m^{-2} s^{-1}) from gas exchange in the leaf cuvette were then used to calculate leaf-specific hydraulic conductance (K_l, mmol m^{-2} s^{-1} MPa) with the equation:

(13)

$$K_l = \frac{E}{\Psi_{pd} - \Psi_l}$$

Leaf level instantaneous transpiration efficiency (ITE) was calculated as A_n divided by E. The g_1 parameter, describing the plants water-use strategy, was estimated from ITE to VPD response curves by fitting a rearranged optimal g_s model for ITE (Medlyn et al. 2011) using non-linear regression (see Duursma et al. 2013). Small values of g_1 indicate that transpiration is costly in C terms and plants are then likely to exhibit conservative water use, whereas large values imply a lower C construction cost and decreased water-use efficiency (Lin et al. 2015).

3.3.5 Data analysis

Differences in experimental parameters to either the warming treatment or leaf type were analysed by mixed-effects models in R (R Development Core Team 2011) with WTC as a random effect. Explained variance (R^2) of mixed models were computed as in (Nakagawa and Schielzeth 2013), in which the marginal R^2 represents variance explained by fixed factors and the conditional R^2 by both fixed and random factors. Confidence intervals (95 %) of mixed effect linear models were generated using bootstrapping methods with 999 simulations, using the bootMer function in the 'lme4' package (Bates et al. 2015). For non-linear relationships, confidence intervals were estimated by fitting a generalized additive model to the data with the 'mgcv' package, using WTC as a random effect. All tests of statistical significance were conducted at an α of 0.05.

3.4 Results

3.4.1 Leaf resource distribution

Across six measurement campaigns over the 7 month period PPFD was reduced on average by >75% in the shade (Figure 3.1). Leaf-specific hydraulic conductance (K_l) was similar across sun and shade leaves (Table 3.1). This was because Ψ_{pd}, Ψ_l (Table 3.1) and E (Table 3.2) did not differ between leaf types. Leaf N_a was approximately 20% higher in sun leaves compared to shade leaves (Table 3.1). Leaf mass per area was not different between leaf types. No effect of the warming treatment was detected with PPFD, Ψ_{pd}, Ψ_l, K_l, E, N_a or LMA either within or across leaf types ($P > 0.05$).

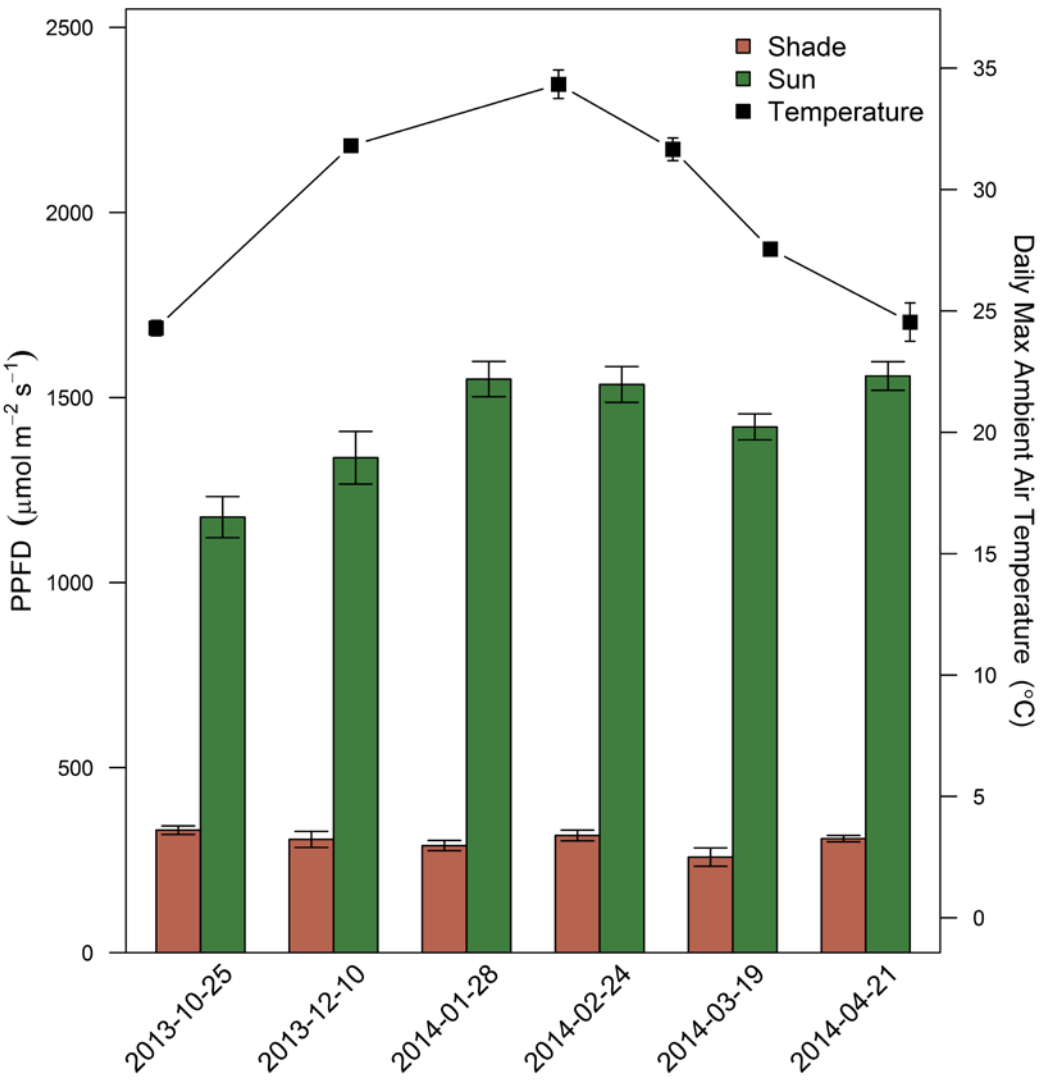

Figure 3.1. Bars represent the local light environment for sun and shade leaves during six gas exchange campaigns from October 2013 to April 2014. Means ± 1 standard error represent integrated PPFD, measured with a ceptometer, at the canopy height of each selected leaf. Each date represents the starting date for each measurement campaign. Points represent the mean (± 1 standard error) daily maximum air temperature during each campaign period.

Table 3.1. *Eucalyptus tereticornis* leaf morphological and physiological traits between full sun and shade leaves under ambient and elevated temperature treatments. Leaf mass per area, N_a, $\delta^{13}C$, Ψ_{pd}, Ψ_l and K_l values represent treatment mean (± 1 standard error) across measurement campaigns (n=6). Values of V_{cmax} and J_{max} are treatment means (± 1 standard error) from AC_i curves measured in each chamber at saturating light with units of μmol m^{-2} s^{-1}. Units of LMA and Leaf N_a are g m^2, K_l is mmol m^{-2} s^{-1} MPa, WP is MPa and $\delta^{13}C$ is ‰. Different letters represent significant differences between leaf type and temperature treatments. The P value represents the overall effect between each unique combination of leaf type and temperature treatment for each trait.

Leaf	**Temperature**	**LMA**	N_a	V_{cmax}	J_{max}	**K**	Ψ_{pd}	Ψ_l	$\delta^{13}C$
Sun	AT	114.1 (4.5) a	2.63 (0.08) b	96.0 (6.7) b	141.6 (7.5) b	1.69 (0.18) a	-0.32 (0.03) a	-1.60 (0.10) a	-28.1 (0.18) b
	ET	109.9 (4.8) a	2.60 (0.09) b	95.5 (6.6) ab	148.3 (11.8) b	1.79 (0.15) a	-0.32 (0.02) a	-1.70 (0.09) a	-28.3 (0.17) b
Shade	AT	118.3 (4.4) a	2.13 (0.07) a	73.3 (6.4) a	102.1 (6.9) a	1.70 (0.13) a	-0.27 (0.02) a	-1.50 (0.09) a	-29.9 (0.17) a
	ET	113.1 (4.3) a	1.88 (0.06) a	77.6 (4.9) ab	106.2 (6.5) a	1.78 (0.14) a	-0.30 (0.02) a	-1.60 (0.11) a	-30.4 (0.22) a
P value		0.781	0.001	0.028	0.002	0.973	0.3486	0.6385	0.001

Table 3.2. *Eucalyptus tereticornis* leaf gas exchange variables for sun and shade leaves under ambient and elevated temperature treatments. Each value reflects the mean (± 1 standard error) for each treatment across gas exchange campaigns (n=6). Units for A_n and E are μmol m^{-2} s^{-1}, for g_s and g_m are mol m^{-2} s^{-1} and for VPD is kPa. Different letters represent significant differences between leaf type, light environment and temperature treatments. The P value represents the overall effect between each unique combination of leaf type, light environment and temperature treatment for each variable.

Leaf	**Light**	**Temperature**	A_n	g_s	g_m	**ITE**	E	**VPD**	C_i	C_c
Sun	High	AT	13.5 (0.3) b	0.122 (0.005) a	0.163 (0.005) c	8.26 (0.48) b	1.78 (0.07) a	1.60 (0.04) ab	179.8 (3.2) a	92.2 (2.9) a
		ET	13.1 (0.3) b	0.123 (0.005) a	0.153 (0.007) bc	6.57 (0.39) ab	2.21 (0.09) a	1.90 (0.05) b	187.9 (2.9) a	92.2 (2.8) a
Shade	Low	AT	10.4 (0.1) a	0.150 (0.005) a	0.117 (0.004) ab	6.24 (0.50) a	1.93 (0.07) a	1.40 (0.04) a	255.4 (3.8) b	160.0 (4.1) c
		ET	10.0 (0.1) a	0.146 (0.005) a	0.116 (0.004) a	5.43 (0.51) a	2.23 (0.09) a	1.60 (0.05) a	253.8 (4.1) b	160.3 (3.5) bc
	High	AT	18.1 (0.3) c	0.255 (0.007) b	0.184 (0.003) c	5.85 (0.33) a	3.42 (0.12) b	1.40 (0.04) a	237.4 (2.2) b	137.4 (1.9) b
		ET	16.7 (0.2) c	0.246 (0.009) b	0.177 (0.003) c	5.02 (0.35) a	3.81 (0.15) b	1.70 (0.04) ab	238.1 (3.2) b	141.7 (2.8) bc
P value			0.001	0.001	0.001	0.001	0.001	0.005	0.001	0.001

3.4.2 Photosynthetic capacity and leaf photosynthesis rates

The photosynthetic parameters J_{max} and V_{cmax} were higher in sun compared to shade leaves (Table 3.1), as estimated from AC_i curves (Figure 3.2a). Within leaf types, no effect of the warming treatment was detected on either parameter. Among the sampled leaves, V_{cmax} was positively related to leaf N_a across leaf types and temperature treatments (P = 0.01, Figure 3.2b).

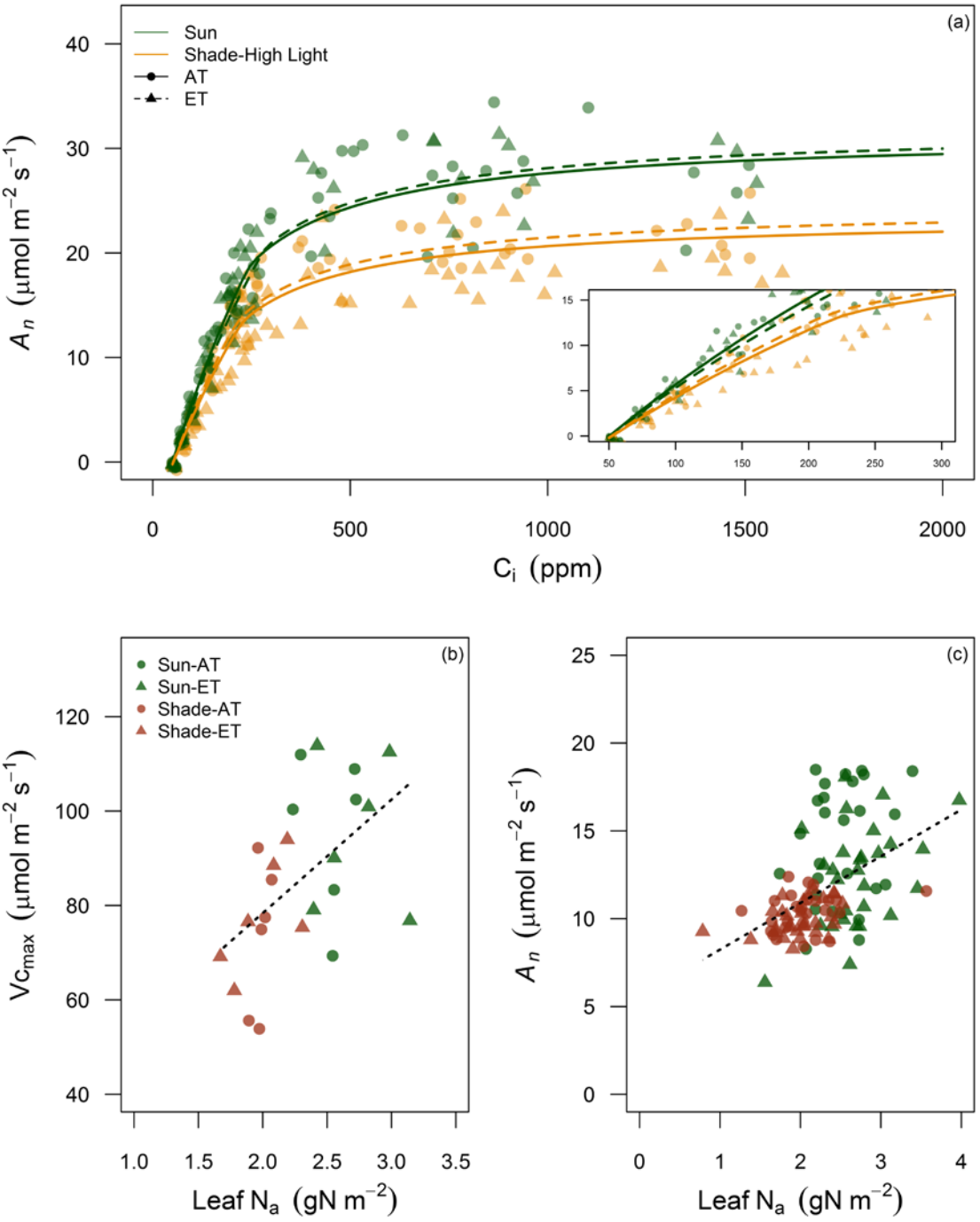

Figure 3.2. (a) ACi curves for sun and shade leaves at elevated (ET) and ambient (AT) temperature treatments. ACi curves were measured once on all trees, in February 2014, at 25°C and at saturating light (1800 μmols m^{-1} s^{-1}). (b) The relationship between V_{cmax} and mean leaf N_a for each chamber, including sun leaves and shade leaves at low light.

(c) The relationship between A_n and leaf N_a for sun and shade leaves measured under their ambient light and temperature conditions. For (b,c) the dashed line represents the significant linear model fit for all leaves, with a marginal and conditional R^2 of 0.28 and 0.35 for (b) and 0.24 and 0.33 for (c).

Mean A_n was significantly higher in sun compared to shade leaves (+23%), when measured at their local light environment (Table 3.2). Additionally, leaf N_a was positively related to A_n across gas exchange campaigns and leaf types measured under ambient light and temperature conditions ($P < 0.001$, Figure 3.2c). Following an increase in light intensity to match high-light conditions, A_n of shade leaves increased to values significantly greater than sun leaves at high light ($P < 0.001$, Table 3.2). No effect of the warming treatment was detected on A_n of sun leaves measured at high light or shade leaves at either low or high light. Photosynthesis within leaf types and treatments was similar through time and across the range of leaf temperatures measured (Figure 3.S3a).

3.4.3 Stomatal conductance and leaf water-use efficiency

On average, g_s was 18% higher in shade compared to sun leaves under their local light environment (Table 3.2). Photosynthesis was positively correlated with g_s in all leaves measured under high light conditions, however, g_s and A_n were not correlated in shade leaves under low light (Figure 3.3a). Following increased PPFD, g_s of shade leaves was significantly greater than both shade leaves at low light and sun leaves, pooled across all measurement dates (Figure 3.4a). No effect of the warming treatment was detected on g_s within or across leaf types. Stomatal conductance within leaf types and treatments was similar through time and across the range of leaf temperatures measured (Figure 3.S4b).

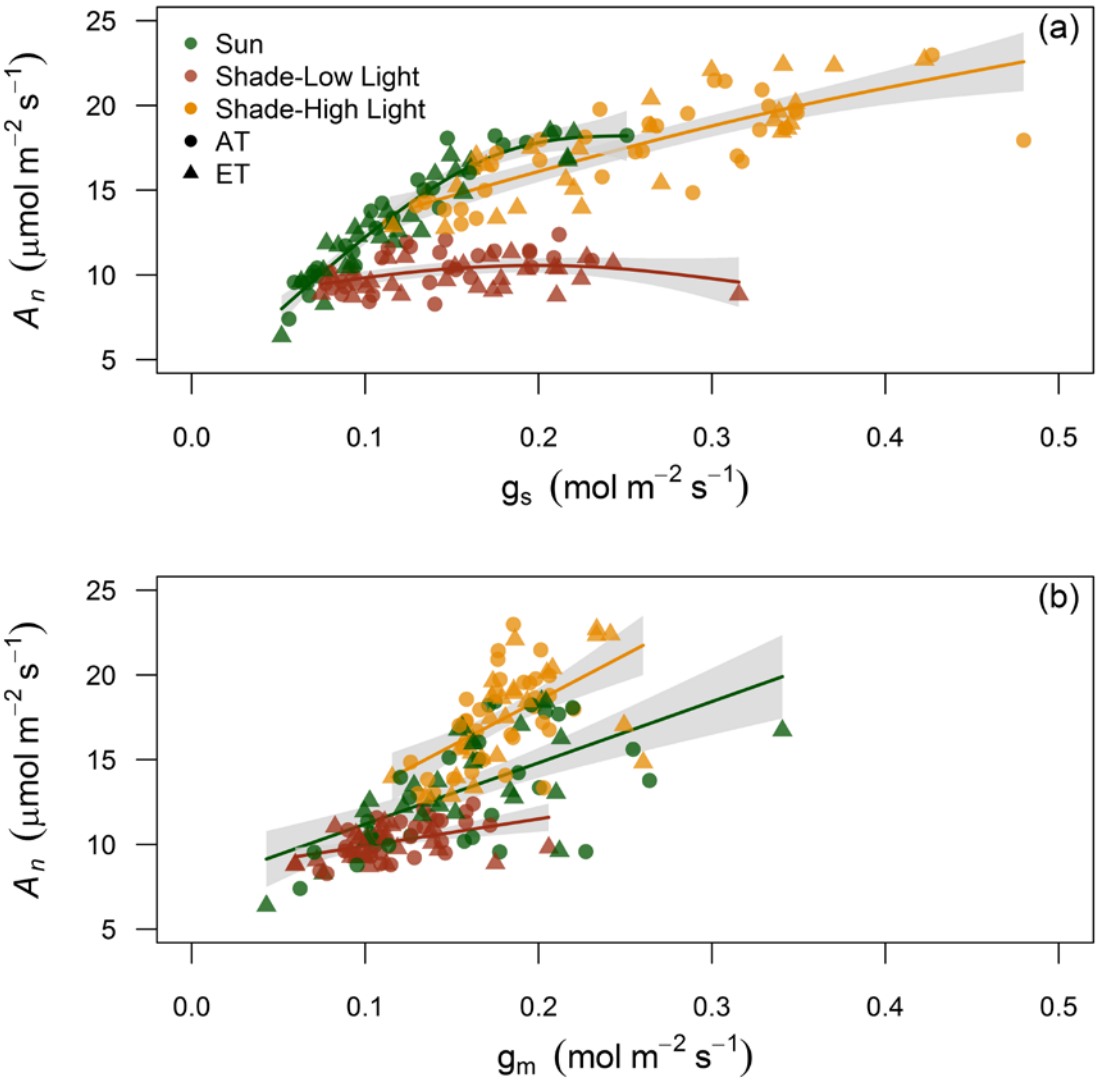

Figure 3.3. The response of A_n to g_s (a) and g_m (b) for sun leaves measured at high light and shade leaves measured at both low and high light under their respective elevated and ambient temperature treatments. Lines represent either smoothed regressions from a generalized additive model fit (a) or linear model fits (b). Grey areas are 95% confidence intervals for the mean.

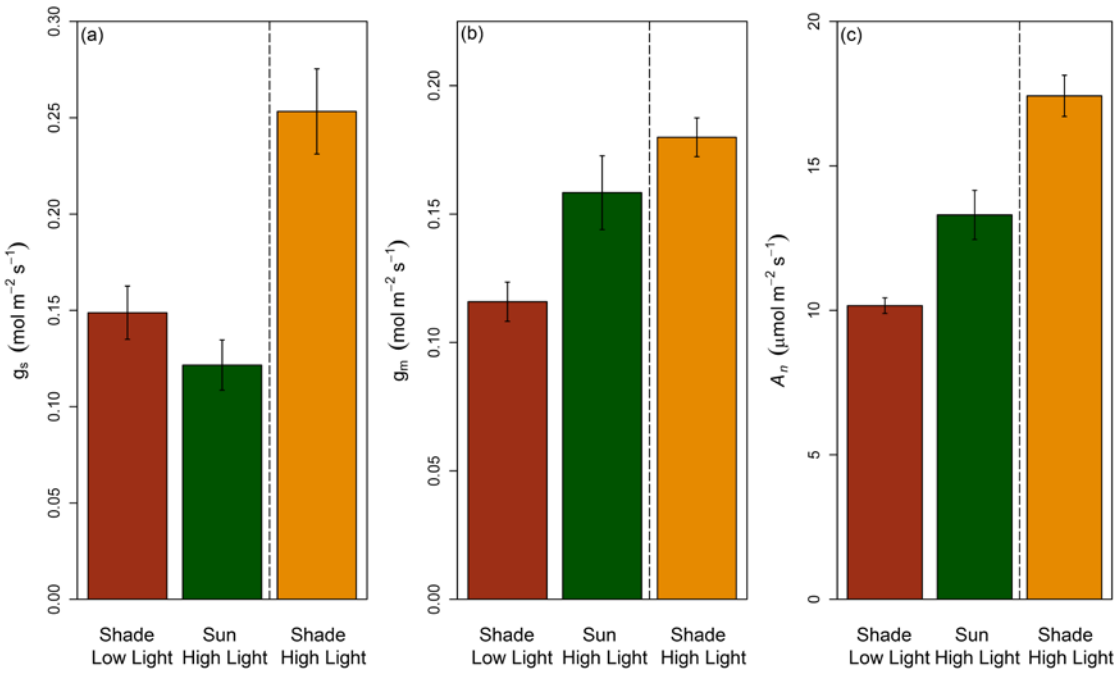

Figure 3.4. The mean ± 1 standard error of g_s (a), g_m (b) and A_n (c) of sun leaves and shade leaves at both low and high light pooled across six measurement dates.

Measured under ambient light and temperature, leaf ITE was significantly greater in sun leaves than in shade leaves at low light (+21%, P = 0.001). Following an increase in PPFD to high-light conditions, ITE of shade leaves did not differ from shade leaves at low light and was therefore significantly lower than sun leaves (P < 0.001). Instantaneous transpiration efficiency in sun leaves was reduced in the warming treatment, but no warming effect was detected in shade leaves measured at low or high light (Table 3.2). The mean estimated g_1 for sun leaves was 1.51±0.11 and for shade leaves with low and high light was 2.59±0.12 and 2.74±0.04. For all leaf types and light treatments there was a strong response of ITE to VPD and individual data points broadly corresponded to response curves from the optimal ITE model with a g_1 value for each leaf type and treatment (Figure 3.5a). Within leaf types and light treatments the response

of VPD to leaf temperature was similar across all measurement campaigns (Figure 3.S4a).

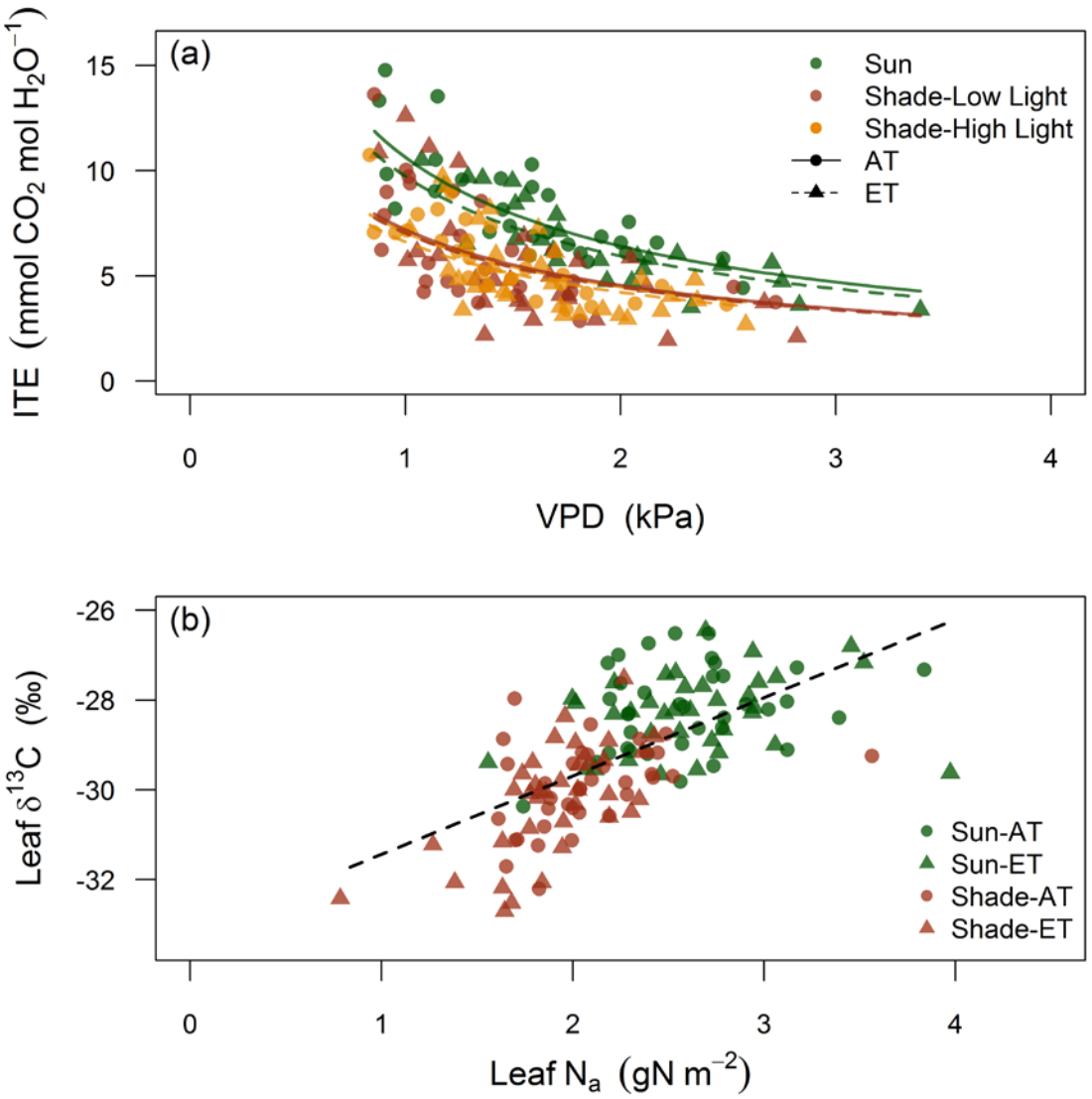

Figure 3.5. (a) Response of instantaneous transpiration efficiency (ITE) to VPD for sun leaves and shade leaves at both low and high light with elevated and ambient temperature treatments. (b) The relationship between leaf $\delta^{13}C$ and leaf N_a for sun leaves at high light and shade leaves at low light. For (a) VPD is the leaf to air pressure difference inside the gas exchange cuvette and lines represent predictions from the optimal ITE model with a g_1 value for each leaf type and treatment. For (b) the dashed

line represents the significant linear model fit for all leaves with a marginal and conditional R^2 of 0.41 and 0.45, respectively.

Bulk-leaf δ^{13}C, as an index of integrated water-use efficiency (Marshall et al. 2007), was significantly lower in shade leaves compared to sun leaves by ca. 2‰ (Table 3.1). No effects of the warming treatment on leaf δ^{13}C were detected. Leaf δ^{13}C and N_a were positively correlated for all leaves (P<0.001, Figure 3.5b), with less negative δ^{13}C (higher water-use efficiency) and higher N investment in sun leaves.

3.4.4 Leaf carbon isotope discrimination and mesophyll conductance

The observed carbon isotope discrimination (Δ_o) measured during photosynthesis was positively correlated with C_i:C_a for all leaf types (P < 0.001), with larger Δ_o detected for sun leaves and shade leaves at high light than shade leaves at low light (Figure 3.6). Carbon isotope discrimination associated with g_m accounted for the majority of Δ_o (69.7±0.4%) and varied little across measurement temperatures, leaf types, or warming treatments. The remainder Δ_o consists of the contributions of g_s, respiration and photorespiration to discrimination.

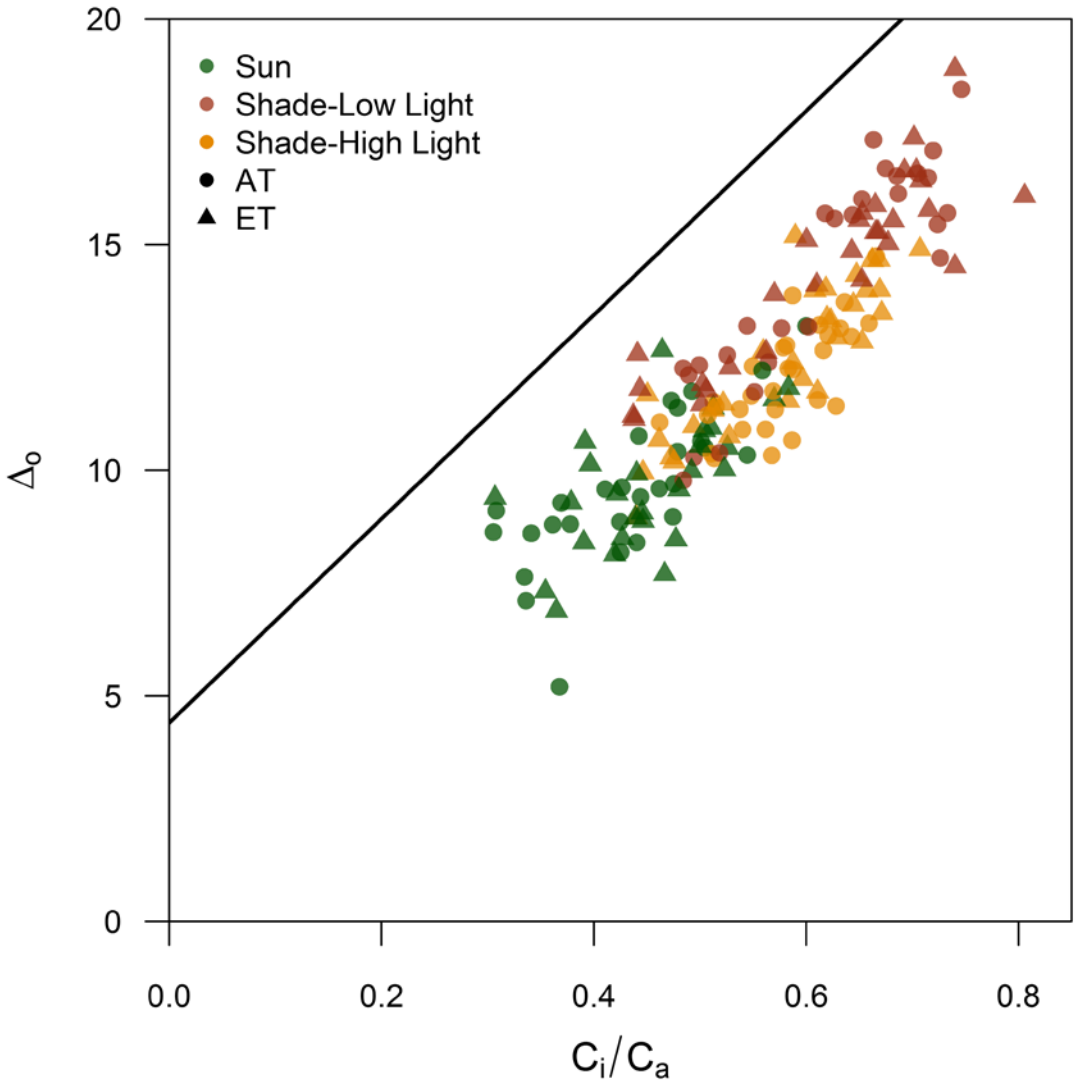

Figure 3.6. Relationship between the observed discrimination of $^{13}CO_2$ measured during photosynthesis (Δ_o) and measured C_i/C_a for sun leaves measured at high light and shade leaves measured at both low and high light. The solid line represents the theoretical line for C3 plants from Evans et al. (1986).

Mean g_m was higher in sun compared to shade leaves (+27%) under their local light environment ($P < 0.001$). Following a short-term increase in PPFD from low to high light, g_m of shade leaves increased to values significantly greater than sun leaves (Table 3.2). Proportional increases in g_m were matched by proportional increases in A_n from low to high light in shade leaves (Figure 3.4b,c). Photosynthesis scaled positively with increases in g_m for all leaves, with similar intercepts but different slopes between leaf type and light treatment ($P = 0.0186$). The large increases in g_m in shade leaves under high light likely resulted in the highest rates of A_n (Figure 3.3b). No differences in g_m were detected with the warming treatment within leaf types. Mesophyll conductance did not vary across measurements campaigns within leaf types and light treatments (Figure 3.S3b), but a weak negative relationship with increasing leaf temperature was detected with sun and shade leaves under their local light environment ($P = 0.001$ & 0.04, respectively). We also simulated AC_c curves to determine if treatment differences in J_{max} and V_{cmax} where instead the result of differences in g_m. Comparison of AC_c curves (Figure 3.S2) and AC_i curves revealed similar differences between sun and shade leaves.

3.4.5 Variation in intercellular and chloroplastic CO_2 concentrations

Higher rates of g_s in shade leaves under low and high light led to significant increases in C_i compared to sun leaves (Figure 3.7a). The chloroplast CO_2 partial pressure was comparable between shade leaves when measured at both low and high light conditions (Figure 3.7c). In sun leaves C_c was significantly lower than shade leaves, consistent with a lower C_i. The drawdown of CO_2 from intercellular spaces to the chloroplast, C_i-C_c, measures the coordination between g_m and A_n (Von Caemmerer and Evans 2014). This drawdown was similar between sun and shade leaves measured at their local light

environment and increased marginally in shade leaves at high light (Figure 3.7c). This was the result of the proportional relationship between g_m and A_n across all leaves. The CO_2 drawdown from C_a to C_i and C_i to C_c were both relatively stable across the range of temperatures measured and gas exchange campaigns (Figure 3.S4c and 3.S3c, respectively).

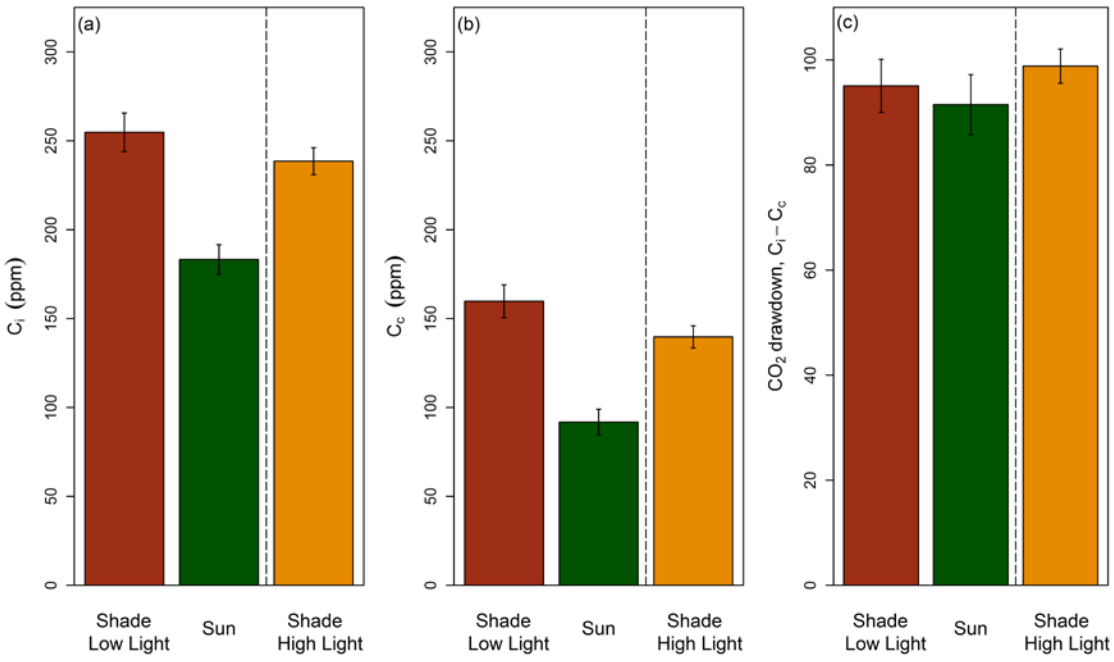

Figure 3.7. The mean ± 1 standard error of (a) intercellular CO_2 concentration (C_i), (b) CO_2 concentration in the chloroplasts (C_c) and (c) CO_2 drawdown from substomatal cavities to sites of carboxylation of sun leaves and shade leaves at both low and high light (C_i-C_c).

3.5 Discussion

Here we show that A_n in leaves within canopies of *Eucalyptus tereticornis* are limited by their local light environment, however, shade leaves increased rates of leaf C gain exceeding sun leaves when light availability increased. Although shade leaves in lower light environments exhibited relatively high g_s and C_i, it was rapid increases in g_m under periods of high light availability that allowed for this up-regulation of A_n. Although we know shade leaves experience transient periods of sun and shade (Pearcy 1990), a lack of empirical data within tree canopies currently impedes our ability to predict whole canopy C gain. These findings offer new insights into how aspects of leaf physiology may be optimized differently in sun and shade leaves and reveal how the total leaf CO_2 conductance pathway should be accounted for when testing optimizations of canopy C uptake in future studies. Additionally, with measurements recorded across a large natural range of air temperatures only minimal effects a +3 °C warming treatment were detected on leaf physiology.

3.5.1 Resource distribution and photosynthetic capacity

The allocation of N_a constrains A_n and is thus a key trait in determining the relative contribution of individual leaves to canopy C gain. Decreasing light availability should decrease the investment into photosynthetic enzyme within a canopy (Mooney and Gulmon 1979). As a result, acclimation of photosynthetic capacity to irradiance is typically reflected in the key photosynthetic biochemical parameters V_{cmax} and J_{max} (Farquhar et al. 1980). Our data agree with these conventional conclusions as the distribution of N_a, both measures of photosynthetic capacity and A_n were all reduced in

shade leaves. Leaf mass per area, however, was not different between sun and shade leaves. This could be due to leaf formation under comparative light conditions or unmeasured differences in total non-structural carbohydrates contents between leaf types. Alternatively, plasticity in leaf structure and anatomy of this species may have been necessary to achieve the observed dynamic physiological responses to light. As gradients in LMA within tree canopies are commonly observed, this finding warrants further study.

Photosynthesis is also limited by the ability to supply water to the upper canopy. Ultimately, the ability of tree hydraulic architecture to supply water to foliage across increasing pathlengths affects productivity and survival (Sellin et al. 2008). Using a two-leaf model, Peltoniemi et al. (2012) theorizes that optimal N distribution will be proportional to light distribution only if K_l is also optimally distributed. In this study, variation in leaf N distribution and A_n rates were not associated with subsequent changes in K_l between sun and shade leaves. Thus, no direct relationship between water supply and N distribution or A_n within the canopy were detected.

Unexpected higher rates of g_s in shade leaves compared to sun leaves led to decreased ITE in shade leaves throughout the experiment. As the VPD used to calculate ITE was recorded from controlled cuvette leaf temperatures, it is unknown if actual leaf temperatures varied within the canopy and how this could alter patterns in ITE. However, consistently higher leaf $\delta^{13}C$ in shade leaves suggests that the observed patterns in instantaneous ITE were likely prevalent long term. From a canopy perspective this pattern in water-use efficiency initially appears to be detrimental to C

gain as A_n in sun leaves was characterized by low rates of g_s and low C_i. Relative to the differences in A_n between leaf types, higher rates of g_s in shade leaves appear to exhibit inefficient water use. As whole canopy C gain integrates the efficiency of all leaves, this begs the question of why shade leaves maintained a lower ITE compared to sun leaves.

3.5.2 Physiological behaviour of sun and shade leaves

The pattern of inefficient water use in shade leaves is important as we hypothesized that g_s and A_n would be proportional across sun and shade leaves. In sun leaves, A_n and g_s were strongly correlated, exhibiting behaviour broadly consistent with optimal stomatal theory. However, lower rates of A_n in shade leaves were not coupled with decreases in g_s, leading to the observed decreases in ITE. This is significant as optimal stomatal regulation to balance C gain with water loss has been reported across a wide range of ecosystems and plant functional types; however, empirical data is often collected only on sun leaves (e.g. Prentice et al. 2014, Lin et al. 2015). As a result, the often used economic framework of balancing costs of using water versus N allocation to predict A_n (Wright et al. 2003) may break down when considering all leaves within a tree canopy.

It is possible that reducing stomatal response time, by sustaining higher g_s, is a strategy to take advantage of high light quickly in shade leaves (Tausz et al. 2005). Evidence from this study supports this hypothesis, as shade leaves increased A_n equivalent or even outperforming sun leaves under identical light intensity. Transpiration-induced cooling in shade leaves, by keeping stomata open, has also been suggested as an effective strategy to reduce sunfleck induced thermal load (Schymanski et al. 2013). This is because rapid increases in leaf temperature with sunflecks have been shown to inhibit C

gain (Leakey et al. 2003). However, this response likely occurs at very high air temperatures and may not explain the observed g_s in shade leaves across the large natural range of temperatures included in this study. How prevalent each of these strategies are within tree canopies is still unknown, as empirical studies assessing photosynthetic responses to sunflecks generally focus on seedlings (Küppers and Schneider 1993, Pepin and Livingston 1997, Leakey et al. 2002) and understory plants, often in deep shade (Chazdon and Pearcy 1991, Allen and Pearcy 2000, Brantley and Young 2009). Thus, our findings highlight a critical need for empirical measurements of shade leaves under dynamic light environments in order to accurately scale C gain from leaf to canopy (see De Pury and Farquhar 1997).

We found that A_n and g_m scaled positively across leaf types and, surprisingly, increased rapidly (within minutes) and proportionately when light intensity was increased in shade leaves. Research has suggested that aquaporins can facilitate increases in the CO_2 permeability of the cell membranes resulting in rapid modulation of g_m (Hanba et al. 2004, Heinen et al. 2009, Li et al. 2014). This provides a potential explanation for the observed rapid increases in g_m, but the impacts of aquaporins on g_m are yet to be tested in leaves of tree species. Our findings support a growing wealth of evidence that g_m is highly variable and can respond to environmental variables (Flexas et al. 2008). Here we provide empirical data showing g_m not only varies within a canopy but the up-regulation of g_m plays a critical role in the photosynthetic response of shade leaves to sunflecks.

If shade leaves "lie in wait" for sunflecks, then perhaps we should consider an alternate

leaf economic strategy to maximize C gain, beyond conventional trade-offs associated with canopy resource distribution. This is because the role of g_s in regulating photosynthetic induction impacts the capacity of a leaf to utilize sunflecks (Way and Pearcy 2012). If the valuation of sunflecks as a C resource is large enough, then costs of sub-optimal stomatal behaviour could be offset over the leaf lifespan or across the entire canopy when considering both sun and shade leaf types. For example, the potential C gain in leaves where sunflecks constitute a large proportion of total daily PFFD may be large enough to tolerate decreases in ITE. However, accounting for the heterogeneous nature of light within a canopy remains a current challenge for empirical and modelling studies. Thus, models which predict leaf photosynthesis from N distribution within a canopy will be incomplete unless inclusion of canopy light extinction and the integration of sunflecks on shade leaves are included (De Pury and Farquhar 1997).

3.5.3 Conclusions

Here we show that dynamic physiological responses of shade leaves to altered light environments has important implications for upscaling leaf level measurements to the canopy. Although resource allocation constrains leaf photosynthetic capacity it is the physiological behaviour of individual leaves which actually determine C gain. These findings suggest that current theories of leaf optimal behaviour should be extended to include dynamic light environments, which will have important implications for process-based models that predict canopy C gain from rates of leaf photosynthesis. Furthermore, the dynamic nature of g_m cannot be simply parameterized in tree growth models and possibly should be excluded until it can be represented properly. Additional empirical data, across multiple tree species, are needed to determine both the mechanisms and the

capacity of g_m to rapidly increase CO_2 drawdown. To improve our ability to predict whole canopy C gain, future research should prioritize the incorporation of both sun and shade leaf physiology, which may be optimized differently.

3.6 Supporting Information

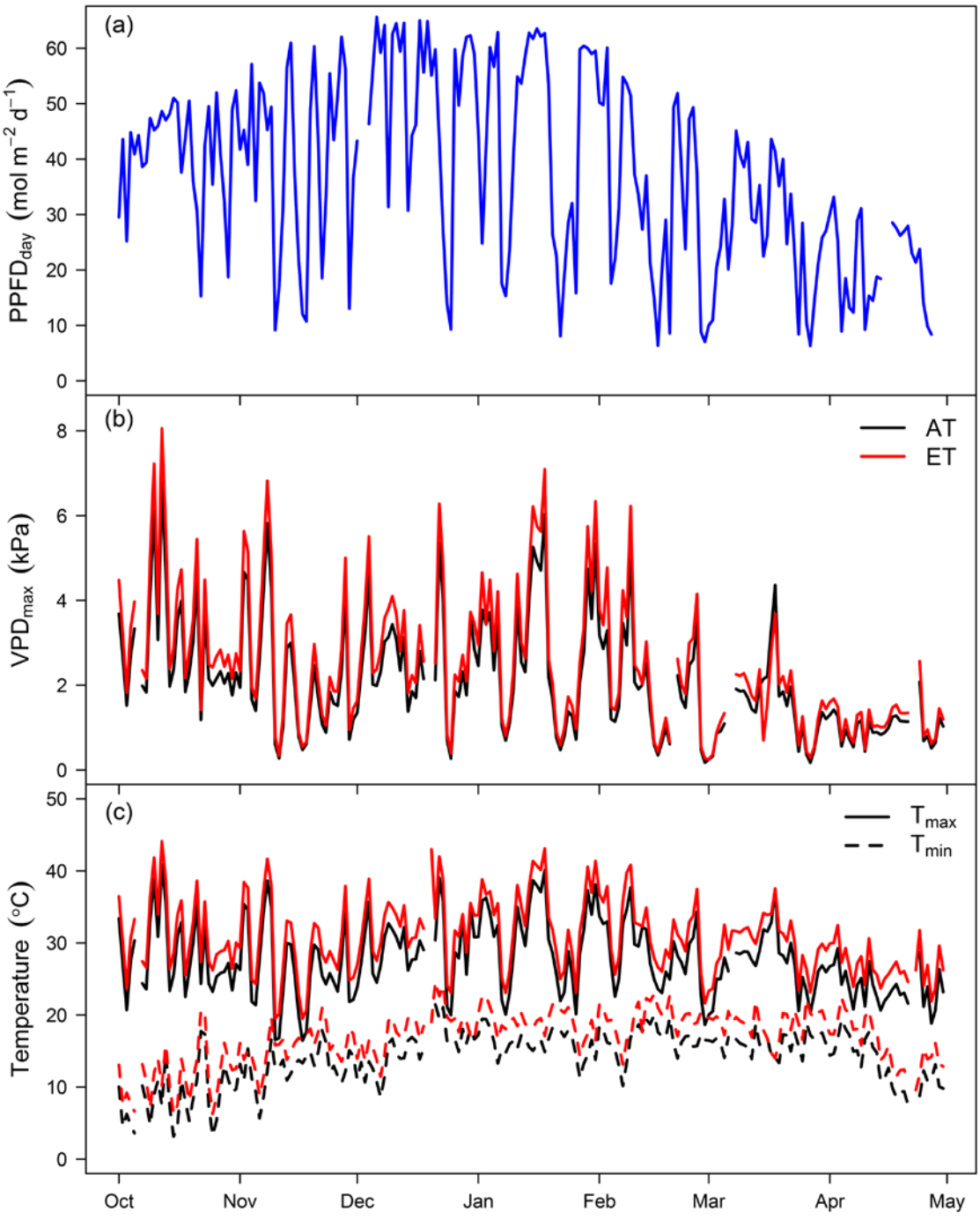

Figure 3.S1. Daily maximum and minimum temperature (a), daily maximum VPD (b) and total daily PPFD (c) for each chamber across the experiment duration.

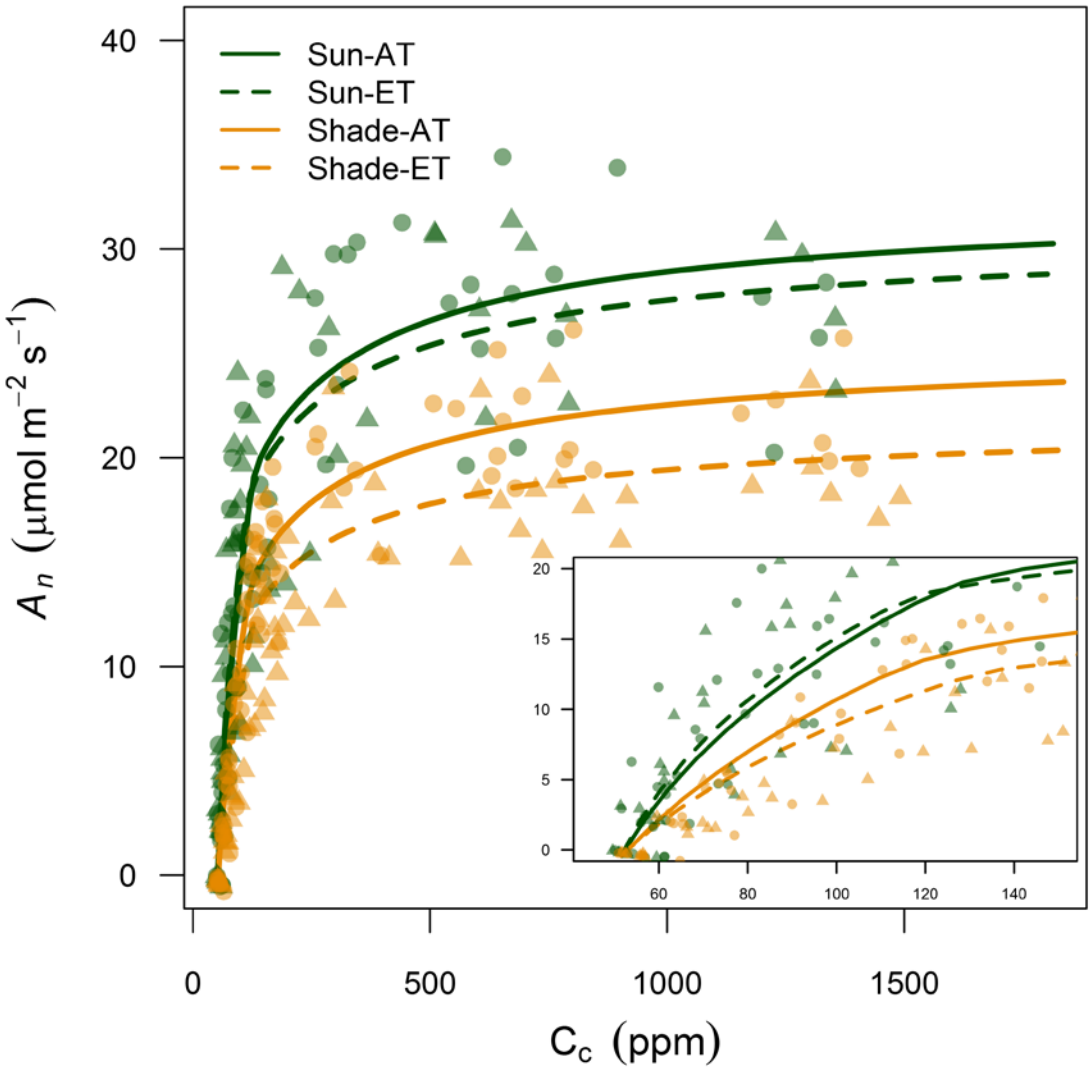

Figure 3.S2. Photosynthetic CO_2 response (AC_c) curves for sun and shade leaves at elevated and ambient temperature treatments. C_c values were predicted with g_m and curves represent chloroplastic photosynthetic parameters at 25°C and saturating light (1800 μmols m^{-1} s^{-1}).

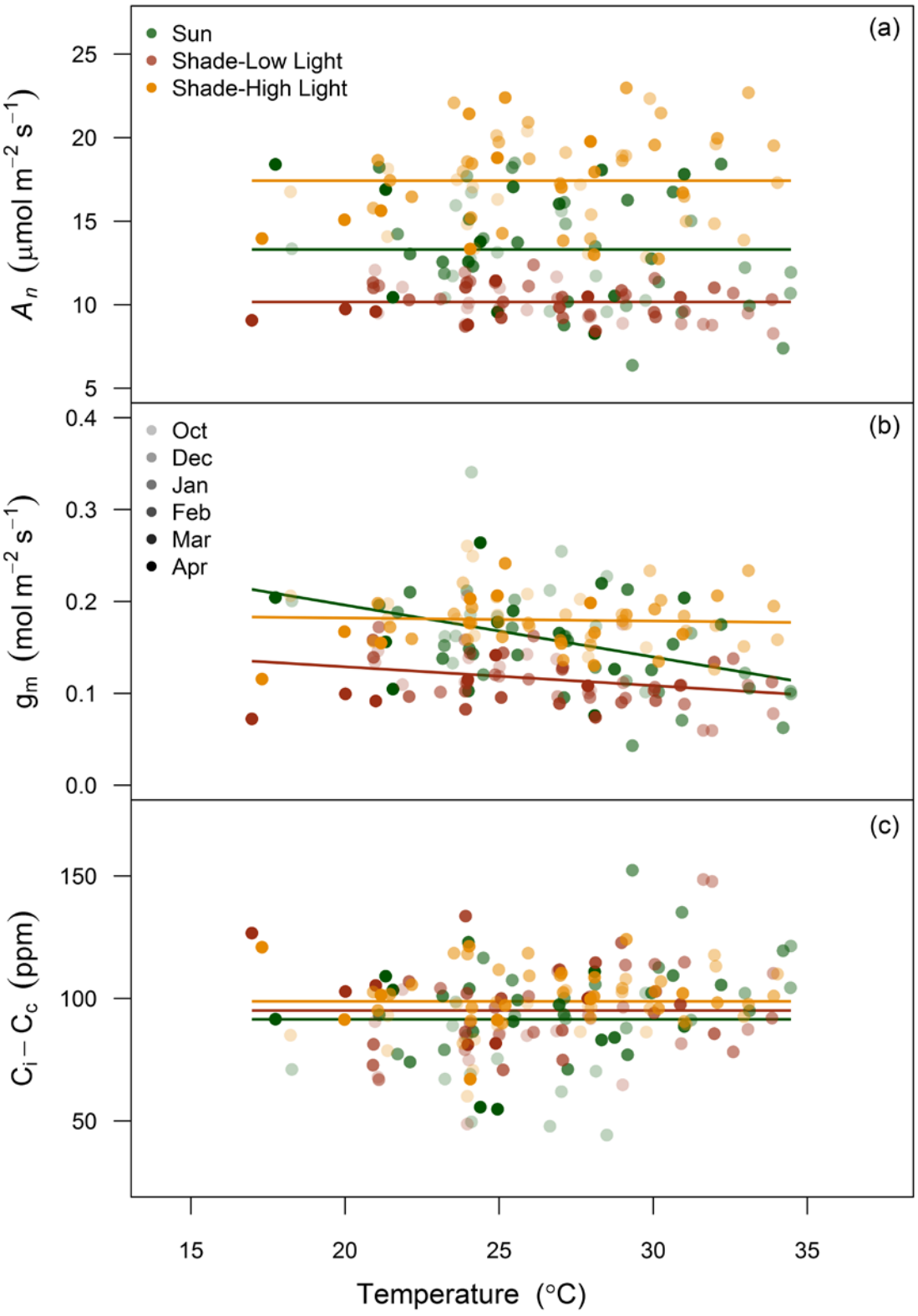
(a)
Sun
Shade-Low Light
Shade-High Light
A_n (μmol m^{-2} s^{-1})
25
20
15
10
5
(b)
Oct
Dec
Jan
Feb
Mar
Apr
g_m (mol m^{-2} s^{-1})
0.4
0.3
0.2
0.1
0.0
(c)
$C_i - C_c$ (ppm)
150
100
50
15
20
25
30
35
Temperature (°C)

Figure 3.S3. Response of A_n (a), g_m (b) and C_i-C_c to leaf temperature for sun leaves and shade leaves at low and high light. Shaded symbols represents each monthly measurement campaign. Solid lines, colored by leaf and light type, are fitted line for the relationship with each variable and leaf temperature across all measurement campaigns. All variables with no relationship are fitted with zero slope and the overall mean value for each treatment combination. Weak negative relationships with g_m and increasing leaf temperature were detected with sun and shade leaves under their local light environment (R^2 = 0.16 and 0.08, respectively).

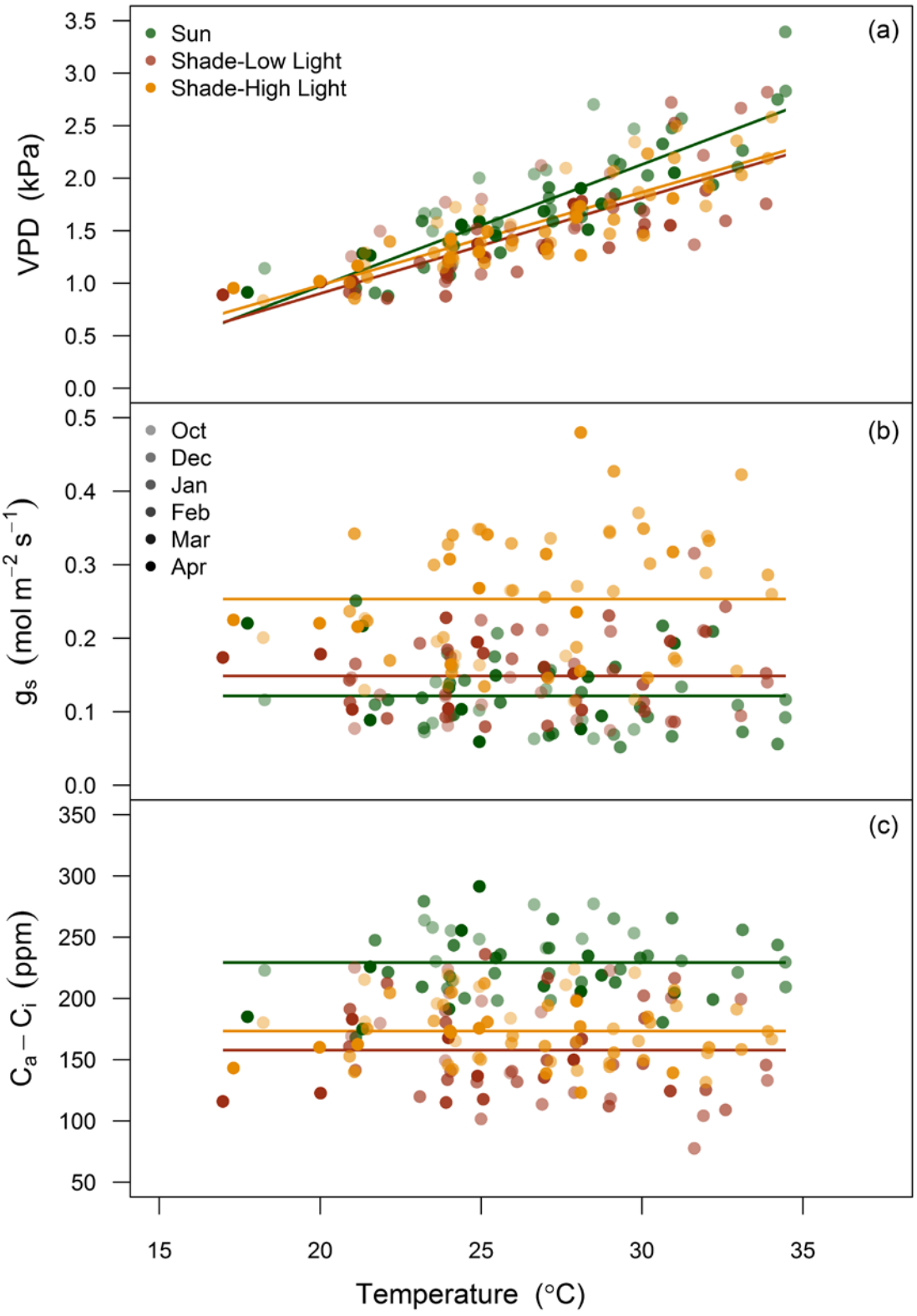
(a)
Sun
Shade-Low Light
Shade-High Light
VPD (kPa)
3.5
3.0
2.5
2.0
1.5
1.0
0.5
0.0
(b)
Oct
Dec
Jan
Feb
Mar
Apr
g_s (mol m^{-2} s^{-1})
0.5
0.4
0.3
0.2
0.1
0.0
(c)
$C_a - C_i$ (ppm)
350
300
250
200
150
100
50
15
20
25
30
35
Temperature (°C)

Figure 3.S4. Response of VPD (a), g_s (b) and C_a-C_i to leaf temperature for sun leaves and shade leaves at low and high light. Shaded symbols represents each monthly measurement campaign. Solid lines, colored by leaf and light type, are fitted line for the relationship with each variable and leaf temperature across all measurement campaigns. All variables with no relationship are fitted with zero slope and the overall mean value for each treatment combination. Leaf VPD inside the gas exchange cuvette was positively correlated with increasing leaf temperature for sun leaves and shade leaves at low and high light (R^2 = 0.73, 0.58 and 0.72, respectively).

Chapter 4

Elevated atmospheric CO_2 and drought does not alter total belowground carbon allocation in *Eucalyptus saligna*

4.1 Abstract

Accurately measuring carbon (C) allocation in large trees above and belowground remains a difficult task and is challenging to represent in models of forest C cycling. Understanding how global change impacts the distribution of tree photosynthate is an essential process in determining future terrestrial C balance. We utilized climate-controlled whole tree chambers (WTCs) to measure cumulative net aboveground CO_2 uptake of *Eucalyptus saligna* trees, which was expected to correlate to harvested tree C mass. We then investigated how elevated atmospheric CO_2 concentration and a 4-month drought period affected both tree biomass partitioning and the allocation of photosynthetic C to various above and belowground pools. We calculated total belowground C allocation (TBCA) for each WTC, which includes all belowground processes, as the residual between daily aboveground net CO_2 uptake and aboveground C mass accrual. It was hypothesized that that both drought and elevated CO_2 would increase biomass partitioning to roots, as well as TBCA. Cumulative aboveground net CO_2 uptake correlated positively to both whole tree C mass and mean leaf area over the entire 11 month measured chamber flux period. Surprisingly, biomass partitioning to roots and cumulative TBCA were unaffected by either elevated CO_2 or drought. As a

fraction of total aboveground net C flux, TBCA remained relatively stable (ca. 40%) across the final 11 months of the experiment for all trees. Carbon allocation to leaves increased under elevated CO_2, while the effects of a 4 month drought were negligible on biomass production or C allocation of aboveground tissues. The novel approaches used here provide evidence that belowground processes may not be as sensitive to global change as previously thought. These results reveal how quantifying the investment of photosynthetic C beyond biomass production is key to assessing functional tree growth responses, while also providing an empirical framework to test model representations of C allocation in trees.

4.2 Introduction

Carbon (C) allocation in trees encompasses investment into biomass production above and belowground as well as fluxes including tissue respiration and exudation (Litton et al. 2007). Trees must allocate C to maximize competitive fitness, reproduction and growth across their life cycle (Dickson 1989). Plants should maximize growth by allocating resources to support leaf growth to increase C acquisition (Monsi and Saeki 2005), however, fluctuations in water, nutrient and light availability cause plants to invest in roots for belowground resources or stem elongation for increased light harvesting (Friedlingstein et al. 1999). These potential changes in C investment are part of a dynamic system: as the tree grows or sink activities are altered, the fate of C assimilate can shift through time. Understanding allocation is vital, as partitioning

among plant organs and their feedback processes profoundly impacts plant growth (Friedlingstein et al. 1999, Lacointe 2000, Shipley and Meziane 2002).

Variation in C allocation responses to environmental change combined with a lack of understanding of the mechanisms driving C allocation impede accurate modelling of terrestrial C cycling (Friedlingstein et al. 1999, Landsberg 2003, Litton et al. 2007, Epron et al. 2012, McMurtrie and Dewar 2013). The representation of C allocation lags behind leaf photosynthesis (A_n) in process-based forest models (Friedlingstein et al. 1999, Franklin et al. 2012, Iversen and Norby 2014) and this deficiency is due to the difficulty in defining principles that are valid under a wide range of conditions (Franklin et al. 2012, Mäkelä 2012). Partitioning coefficients or fixed fractions of assimilation to individual components are often used in models of forest C cycling (Litton et al. 2007, Franklin et al. 2012). Unfortunately, using inappropriate or over-simplified allocation schemes can lead to models producing unintended responses or giving the expected answer for the wrong reason (De Kauwe et al. 2014, Fatichi et al. 2014). As a result, there is continued need to empirically measure patterns of tree C allocation under multi-factor global change manipulations to better understand shifts in future forest C balance.

The allocation of photosynthate above and belowground is an important factor in terrestrial C cycling, yet our knowledge of how global change drivers impact C allocation is incomplete (Litton et al. 2007, Warren et al. 2012). With rising atmospheric CO_2, forest C allocation has drawn particular interest due to its potential effect on C sequestration and the global C balance (Franklin et al. 2012). Across four forested free-

air CO_2 enrichment (FACE) experiments the total flux of C belowground (TBCA), which includes all belowground processes, was found to be enhanced under elevated CO_2 (eC_a) (Palmroth et al. 2006). In FACE experiments this enhancement has been attributed to factors such as increases in C allocation to root biomass production (Iversen 2010) and root exudation (Phillips et al. 2011). Alternatively, a meta-analysis by Poorter et al. (2000) concluded that on average, the distribution of biomass to roots, stems or leaves did not change in herbaceous and woody plants grown under eC_a.

Understanding forest responses to global change also depends on disentangling complex relationships between interacting factors (Rustad 2008). For example, drought stress in trees can have deleterious effects on leaf (Bradford and Hsiao 1982, Schulze et al. 1987, Broeckx et al. 2014), stem (Brando et al. 2008) and root production (Meier and Leuschner 2008, Anderegg 2012). It has also been shown that C allocation to root systems can increase in drought environments when the severity and duration of the drought periods are substantial (Poorter, Niklas, et al. 2012). The impacts of leaf water savings during CO_2 enrichment may also enhance tree biomass production under drought conditions (Atwell et al. 2007), but sustained enhancement is inhibited by the availability of a limited soil water supply to support larger overall canopies (Health and Kerstiens 1997). The effects of drought may limit C sequestration by the terrestrial biosphere (Iversen and Norby 2014), yet how limitations imposed by drought interact with the growth-stimulating effects of eC_a requires more attention (Duursma et al. 2011).

Despite its importance, data on TBCA remain sparse as reliable estimates of root biomass, exudation, turnover and respiration in field conditions are difficult to obtain (Cheng et al. 2005, Litton et al. 2007, Phillips et al. 2008, Strand et al. 2008, Poorter, Niklas, et al. 2012). In forest ecosystems, TBCA has been shown to be equal or greater than aboveground production (Law et al. 1999), yet the controls of this belowground flux are poorly understood (Raich and Nadelhoffer 1989, Giardina et al. 2005). In stand or ecosystem studies, TBCA is often estimated as a residual, by subtracting the changes in C pools of litter, soil and roots from total soil CO_2 efflux (Raich and Nadelhoffer 1989, Davidson et al. 2002, Giardina and Ryan 2002, Palmroth et al. 2006, Adair et al. 2009). A key assumption of this approach is that C pools are in steady-state conditions (Raich and Nadelhoffer 1989), which is not always true. Additionally, the reliance on soil respiration in this approach is problematic as studies are often forced to scale up short-term measurements (often monthly) to cumulative yearly fluxes, while also using a variety of measurement techniques. As allocation of C belowground remains one of the most difficult components of tree C budgets to calculate, new approaches are needed to in order accurately track and account for the investment of C belowground.

The whole-tree chambers (WTC), located at the Hawkesbury Forest Experiment, were designed to allow continuous measurement of net tree CO_2 fluxes, allowing canopy A_n and respiration to be calculated using a mass balance approach (Medhurst et al. 2006, Barton et al. 2010). Here, we grew a single *Eucalyptus saligna* Sm. tree inside each of these 12 large, outdoor and sunlit WTCs for a period of 2 years. Each WTC can resolve net aboveground C uptake (canopy A_n minus respiration of aboveground woody

components), at high temporal resolution, while also controlling temperature and air humidity to track prevailing environmental conditions. Generally, measuring total canopy A_n is difficult as variation in photosynthetic capacity exists within the canopy in response to the environment, requiring leaf measurements and models to upscale to the canopy (Ryan et al. 2010). Combining continuous aboveground net CO_2 flux measurements with an evergreen *Eucalyptus* species, which grows throughout the year, enables tree C allocation to be tracked over long periods of time.

Previous findings in this experiment have shown that *Eucalyptus saligna* trees grown under eC_a treatments were smaller than ambient trees and that larger trees under ambient CO_2 had a smaller reduction in canopy transpiration in drought conditions, via deeper rooting access to water resources (Duursma et al. 2011). The smaller final tree sizes in eC_a trees were attributed to an early setback in growth, which may or may not have resulted from effects of the eC_a treatment. The specific objectives of this study were to determine the response of biomass partitioning among foliage, aboveground woody components and roots of a native Australian tree species to changes in CO_2 and altered water availability. Utilizing the unique WTC design we aimed to test how cumulative net aboveground C gain correlates to whole tree C mass increment, as a function of tree size. We then applied a mass balance approach to track the allocation of C above and belowground throughout the course of an 11 month period under the combined treatments of eC_a and drought.

Our hypotheses were:

(1) As C uptake and growth should be coordinated over long time periods, we expected both total leaf area and harvested tree C mass to correlate with cumulative total aboveground net canopy C uptake.

(2) At the end of the 2-year experiment we expected partitioning of C to harvested roots to increase under eC_a. We also expected increases in partitioning to roots under drought treatments to alleviate water limitation.

(3) As increases in partitioning to root biomass were hypothesized, we expected TBCA to increase through time as cumulative tree C flux became affected by eC_a and drought.

4.3 Methods

4.3.1 Terminology

Carbon allocation terminology commonly employed in ecosystem literature is inconsistent (Litton et al. 2007). Here, important distinctions are made between patterns in live tree biomass and the distribution of photosynthate to all tree components. Clarification of these two terms is essential in accurately quantifying and representing C allocation in this work and in future studies.

Mass partitioning: the relative distribution of biomass between different tree tissue components such as leaves, branches, bole and roots.

Carbon allocation: the fraction of canopy photosynthesis distributed to different components such as tissue biomass pools, respiratory C fluxes, non-structural carbohydrate storage pools or root C exudation.

4.3.2 Whole tree chamber experiment

From April 2007 *Eucalyptus saligna* seedlings were grown in 12 whole-tree chambers (WTCs) at the Hawkesbury Forest Experiment in Richmond, Australia. One seedling per WTC (9 m high) was grown for 2 years and chamber conditions tracked outside air temperature and humidity. Each WTC was fitted with a root enclosure barrier that extended to the soil hard layer (1 m depth), separating WTC tree roots from neighboring trees. Roots were allowed to grow freely in the chamber soil volume and below 1 m. Neutron probe soil water measurements were utilized to show that trees in this experiment were able extract water deeper than the soil hard layer (Duursma et al. 2011). Soils at the WTC facility are an alluvial formation of low-fertility sandy loam, with clay deposits at a depth of about 1 m. Full descriptions of the chamber design and operation are provided in Barton et al. (2010). This multi-factor experimental design included CO_2 × drought treatments with three WTC replicates in each of four treatments. Six chambers were kept at ambient CO_2 of 380 ppm (aC_a) and six were maintained at elevated CO_2 of +240 ppm above ambient (eC_a). Through October 2008 all trees were kept well-watered, with 10 mm of water every 3 days. Half of the chambers in each CO_2 treatment were then subjected to a drought treatment by completely withholding water

(dry) and the remaining six chambers were kept well-watered as an irrigated control (wet). The drought treatment lasted through mid-February 2009 when heavy rainfall ended the drought effect, despite the presence of a root enclosure (Duursma et al. 2011).

4.3.3 Aboveground chamber CO_2 flux

Floors installed 45 cm above the soil surface, enclosing the main bole, permitted the chambers to function as cuvettes, excluding water and CO_2 fluxes from the soil surface and allowed for aboveground whole tree fluxes of CO_2 (and H_2O) to be monitored once trees were ca. 3.5 m in height. This allowed high resolution CO_2 flux data at 14 min intervals to be collected during the final eleven months of the experiment (from April 2008 to March 2009). The raw data were averaged over an hourly time-step and missing CO_2 flux data were gap filled with SOLO (self-organizing linear output map) (see Abramowitz 2005). This self-fitting model predicted the flux as a function of photosynthetically active radiation, air temperature, vapor pressure deficit and day of year. In total, 27% of the observations were gap filled. This gap filling included a 5-6 week gap in late winter 2008 when WTC height was extended, as well as shorter periods in which chamber access doors were open during regular use. For each WTC, cumulative 24 hour net aboveground C uptake ($F_{c,d}$, g C d^{-1}) represented daily total canopy A_n of each tree minus respiration of stems and branches. Then $F_{c,d}$ was summed over the flux monitoring period ($F_{c,T}$) to compare to tree C mass, leaf area and C allocation above and belowground.

4.3.4 Harvested tree carbon mass

A final destructive harvest was completed in March 2009. The canopy of each tree was divided into five equal vertical layers, extending from the floor to the top and harvested. Dry biomass of leaves, branches and boles were measured for each layer and summed for each WTC. Root mass was obtained by excavating and sieving all soil inside each root exclusion barrier to the hard layer. Five root cores (10 cm diameter), sampled before the harvest, where collected from 0-70 cm in each chamber. Biomass from cores was added back to the standing crop total instead of scaling-up fine root biomass from cores to total chamber area. Fine root biomass (<2 mm diameter) was first estimated by scaling-up dry root biomass collected from cores to total chamber area, but highly variable root biomass across cores resulted in unreliable estimates. As a result, root biomass from cores was added back to the standing crop total instead of scaling-up fine root biomass. Consequently, the fine root biomass pool is likely underestimated.

Carbon mass was assumed to be 48% of dry biomass for all non-leaf tissue components and this conversion was performed for all harvest and survey data (see below). This value represents the mean value of wood C of angiosperms from the Dyrad global wood C database, including measurements of stems, twigs, branches, bark, coarse roots and fine roots (Thomas and Martin 2012a, 2012b). Leaf and litter C mass was calculated by multiplying biomass by the WTC specific mean leaf C content (%). Leaf C content was determined from a sub-sample of final harvest dried and milled leaves analyzed using a Leco TruSpec Micro elemental analyzer (LECO corporation, MI, USA). Carbon mass

fractions of leaves, boles+branches (stems) and roots were then calculated by dividing their respective total C mass by whole tree C mass at the end of the experiment.

Prior to the initiation of the experiment potted *Eucalyptus saligna* seedlings were harvested to develop relationships between above and belowground biomass (n=17, mean height of 217±17 cm). These seedlings were grown in 25 l pots inside each WTC until the experiment started, using the same soil as each WTC, while chamber [CO_2] treatment conditions were maintained.

4.3.5 Tree allometry surveys

Tree height was measured every 14 days and diameters were recorded monthly at regular height intervals (30 cm) along the main bole and split stems. Bole diameters at 65 cm height were used as the starting reference diameter for each survey. Diameter and length for every branch, including forked branches, were surveyed seven times between April 2008 and March 2009. The first branch survey coincided with the installation of chamber floors and initiation of whole tree flux measurements. Branch diameter measurements were recorded at 5 cm from their individual insertion points. Leaf litter was collected from the chambers every two weeks, oven-dried and weighed.

4.3.6 Bole carbon mass

During the final harvest, diameter measurements were recorded as described above and 1 cm wide cross sections were removed from the bole at equally spaced positions along the bole midpoint between the diameter measurement points. Wood density for each section was calculated by dividing the dry mass by the fresh volume separately for bark

and wood. The mean total bole density for each tree (ρ_{bo}, g cm^{-3}) was then calculated as the total density of bark and wood, weighted by the total diameter of each section. We assumed that ρ_{bo} did not change through time.

For boles, individual volume units were constructed as concentric cylinders between each diameter measurement from base to tree top for each monthly survey. The tree top section was calculated as a cone with a tip radius of .001 cm. The volume below the starting reference diameter (65 cm) was calculated separately in order to interpolate taper into this section. Using the height of the tree and the standard diameter, the diameters at 30cm and base were estimated by extending the length of the pre-existing cone (from tree top to 65 cm). This resulted in two additional volume units. All volume units were summed, including forked stems, to calculate total bole volume. Bole mass was calculated as total volume multiplied by WTC tree-specific ρ_{bo}.

4.3.7 Branch carbon mass

Measured dry mass, length and basal area of all harvested branches was used to determine the branch wood density (ρ_{br}) as well as a geometric shape factor (ϕ, see Mäkelä 1997) for each WTC tree by rearranging the equation:

(1)

$$M_{br} = L_{br} A_{br} \rho_{br} \phi_{br}$$

where M_{br} is summed dry mass of all harvested branches, L_{br} is summed branch length (cm), A_{br} is summed branch basal area (cm^2), ρ_{br} represents the combined density of

wood and bark (g cm^{-3}) and ϕ corrects branch volume estimates to an intermediate shape between a cone and a cylinder (Mäkelä 1997). The ratio of measured M_{br} to $L_{br}A_{br}$ was used to generate a WTC-specific $\phi_{br}\rho_{br}$.

For each survey period, M_{br} was estimated by solving the above equation with L_{br} and A_{br} for individual branches with $\phi_{br}\rho_{br}$ specific to each WTC. We assumed that $\phi_{br}\rho_{br}$ did not change through time. Total dry branch mass at each survey point was the total mass of all individual branches.

4.3.8 Leaf area and carbon mass

Total tree leaf area and dry mass were measured for each of the five canopy layers at the final tree harvest in March 2009. Specific leaf area (SLA, $cm^2\ g^{-1}$) was calculated by dividing total projected one sided leaf area by dry leaf mass for each canopy layer. Mean SLA for each WTC tree was obtained by weighting SLA of each of the 5 layers by their foliage mass fraction. Estimates of standing leaf area were also obtained in April 2008 from leaf counts for each tree, multiplied by tree-specific mean leaf size (based on a sub-sample).

Canopy leaf area was modeled on daily time steps, between April 2008 and March 2009, using the leaf count census and harvest leaf area estimates, along with height growth and litter fall rates. This was the method applied by Barton et al. (2012). Briefly, leaf growth was assumed to coincide with height growth, so that no leaf growth occurred when height growth had ceased. This method assumes that total cumulative leaf area (i.e.

standing leaf area plus that produced by litter fall) followed and allometric relationship with tree height such that:

(2)

$$A_{L,T} = a\ H^b$$

where $A_{L,T}$ is the total 'potential' leaf area (m^2), a and b are tree specific coefficients and H is tree height (m). Then standing leaf area at time *t* are obtained from tree height at time *t* and cumulative litterfall:

(3)

$$A_L = a\ H(t)^b - \int_{t=0}^{t} L\,(t)dt$$

where L(t) is the litterfall ($m^2\ t^{-1}$) rate at time *t*. Litter was assumed to be produced by all canopy layers. The daily leaf area contribution of litterfall is the difference between $A_{L,T}$ and A_L. The mean SLA for each harvested tree was multiplied by daily estimates leaf and litterfall area to calculate biomass. SLA derived from the harvested trees was assumed to be constant over the entire flux measurement period.

4.3.9 Tissue C allocation

Tissue specific C allocation represents the fraction of net canopy C uptake distributed to a given tissue, which determines the change in biomass of that tissue through time such that:

(4)

$$\frac{dM_c}{dt} = a_c NPP - \lambda_c M_c$$

where M_c is the standing C mass of a component (g C), a_c is the allocation to that component (0-1) and λ_c is the component specific turnover (d^{-1}).

Here, total C allocation to leaves and aboveground wood (branches + bole) could be estimated from the sums of tissue C mass, net aboveground C flux and tissue turnover for each day of the experiment such that:

(5)

$$M_{c,T} = \int a_c F_{c,d} dt - \int \lambda M_c dt$$

where $M_{c,T}$ is the total dry C mass of either leaves or wood and $F_{c,d}$ is the daily net aboveground C uptake (g C d^{-1}). From equation 5, we estimated allocation by solving for a_c (as all other components were measured). For example, C allocation to leaves (a_l) was determined by combining measurements of harvested dry C mass of leaves ($M_{l,T}$) with $F_{c,T}$ and total litterfall ($L_{l,T}$), giving:

(6)

$$M_{l,T} = a_l F_{c,T} - L_{l,t}$$

and then solving for leaf C allocation:

(7)

$$a_l = (M_{l,t} - L_{l,t})/F_{c,t}$$

Allocation to aboveground wood C was estimated in the same manner with turnover measured as total dry C mass of branch litter collected across the experiment. For roots, only total belowground C allocation (TBCA) could be calculated (explained below) since root turnover was not measured.

4.3.10 Total belowground carbon allocation

As the installation of chamber floors into each WTC separated the aboveground CO_2 uptake from the soil CO_2 efflux, TBCA at any time point *t* was calculated as:

(8)

$$TBCA_t = \int_0^t F_{c,d}\, dt - C_{ab}$$

where C_{ab} is the aboveground standing crop C mass (g C) of stems, branches, leaves and total leaf litterfall. As the final standing crop of root biomass was known, TBCA could be further broken down into the total C mass of roots ($C_{r,T}$) and the residual belowground C flux ($F_{c,r}$). The residual belowground C flux includes root and microbial respiration, root turnover, root exudation and any unaccounted for root C mass. The use of aboveground allometry to interpolate C_{ab} through time combined with measured daily

$F_{c,d}$ allowed TBCA to be estimated on daily time steps over the final eleven months of the experiment while cumulative $F_{c,r}$ was calculated at the final harvest.

4.3.11 Mass balance relationships between $F_{c,d}$ and carbon allocation.

The cumulative sum of $F_{c,d}$ for each WTC, at any given time point, represented the running total of net C uptake since the chamber floors were installed. Daily allocation of C to boles and branches was estimated by linear interpolation between 14-day survey measurements and the final harvest, starting at the first branch survey (April 2008). These daily estimates of leaf and litter C were added to bole and branch C mass to estimate C_{ab} on any given day. The contribution of each aboveground component to the cumulative sum of $F_{c,d}$ was then tracked from April 2008 to March 2009. The initial estimated C mass of each aboveground component and $F_{c,d}$ on the day when chamber floors were installed was subtracted from all respective daily values so mass balance could be tracked with a 0 starting value. This allowed cumulative estimates of TBCA to be generated across the final 11 months of the experiment. Additionally, the significant log-linear relationship between above and belowground mass of both harvested trees and potted seedlings (R^2 = 0.98, Figure 4.S1) was used to estimate $C_{r,T}$ from C_{ab} on the last day of the 11 month period. The major carbon allocation pathways and subsequent above- and belowground C pools measured in each WTC are further depicted in Figure 4.1.

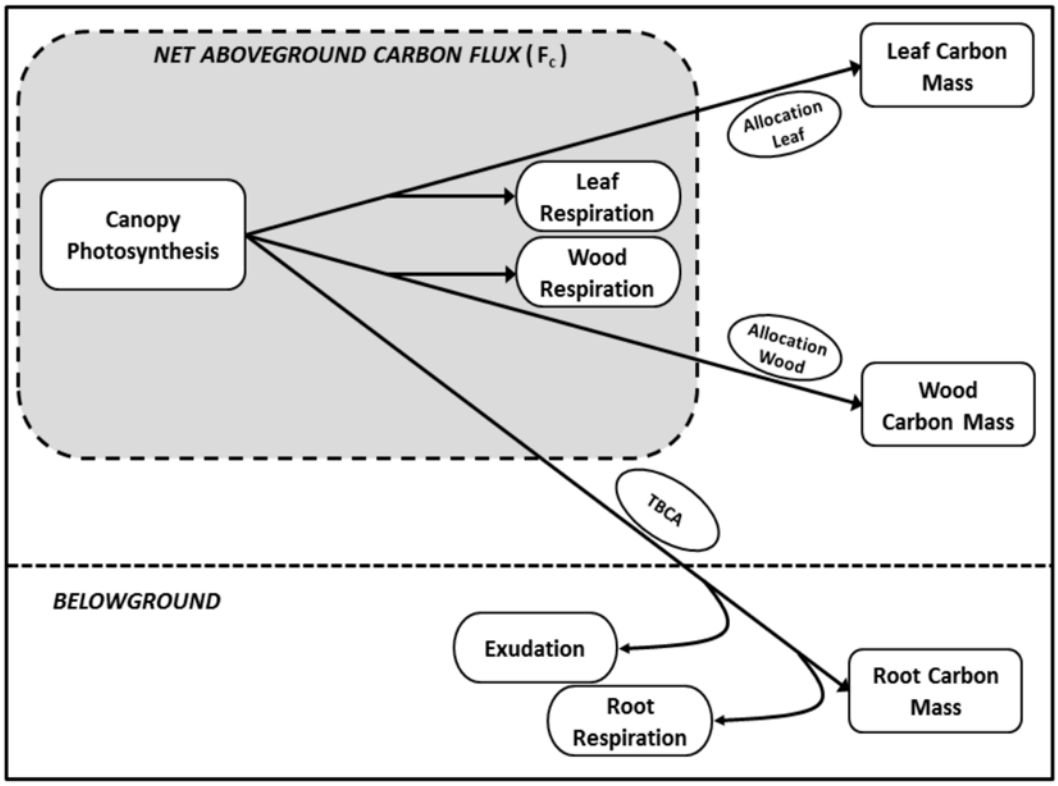

Figure 4.1. Conceptual diagram depicting the major components of C flow among plant components including; uptake via photosynthesis, allocation to component tissues, tissue respiration and root exudation. Mass pools of leaves, wood and roots include tissue turnover. Net aboveground C uptake (F_c), shown in the shaded box, represents the flux of C measured within each WTC. With the WTC experimental design, total belowground C allocation (TBCA) is measured as the residual between $F_{c,T}$ and total aboveground C mass.

4.3.12 Data analysis

Differences in experimental variables in response to the interactive effects of CO_2 and drought treatments at the final harvest were analysed as a completely randomized experimental design with factorial treatment combinations using two-way ANOVA in R (R Development Core Team 2011). Tukey's post-hoc tests were performed in conjunction with ANOVA to determine which specific paired comparisons among climate change treatments were different. Significance level was set at an alpha of 0.05 and findings between 0.05 and 0.10 were considered marginally significant.

4.4 Results

4.4.1 Total aboveground carbon flux, whole tree C mass and leaf area

Both whole tree C and C_{ab} from the final harvest were reduced in eC_a treatments by 32 % (both $P < 0.03$). Over the entire 11 month measured chamber flux period the summed aboveground C uptake ($F_{c,T}$) was significantly reduced by 30.5 % in eC_a treatments ($P = 0.043$), while no effects of the drought treatment were detected (Table 4.1). $F_{c,T}$ was positively correlated with estimates of both whole tree C ($R^2 = 0.74$, Figure 4.2a) and C_{ab} ($R^2 = 0.69$, Figure 4.2b) over the same time period. Whole tree C mass increment estimated during the chamber flux period represented ca. 75 % of total harvested tree C mass. As the majority of biomass production occurred during this period, the allometric estimates of whole tree C were used for comparison to $F_{c,T}$.

Table 4.1. Final harvest C mass of above and belowground tissues, cumulative aboveground tree C uptake ($F_{c,T}$) and specific leaf area (SLA). Each value represents the mean (± 1 standard error) for each treatment combination. Units for C mass and $F_{c,T}$ are g C, while SLA is $cm^2\ g^{-1}$. For each variable, different letters represent significant differences between treatments from the overall model which includes CO_2 * drought interactions. P values represent overall differences of CO_2 or drought main effects and the CO_2 * drought interaction.

Treatment	**Bole**	**Branch**	**Leaf**	**Litter**	**Root**	**$F_{c,T}$**	**SLA**
aCO_2-dry	5231.8 (687.0) b	2799.2 (628.3) a	2642.8 (370.7) a	1129.8 (336.0) a	3052.9 (500.2) a	19394.2 (2169.5) a	83.2 (3.3) a
aCO_2-wet	7785.1 (267.1) ab	3154.6 (687.1) a	3254.2 (393.5) a	1043.1 (47.3) a	3677.4 (316.8) a	23556.5 (1689.0) a	87.9 (2.8) a
eCO_2-dry	4080.5 (682.5) a	1926.0 (369.4) a	2232.1 (235.4) a	889.4 (82.6) a	2518.7 (481.6) a	14620.7 (3456.2) a	70.6 (3.6) a
eCO_2-wet	4026.3 (783.3) a	1856.8 (474.5) a	2358.3 (473.6) a	919.0 (244.3) a	2213.9 (705.8) a	15197.9 (3253.5) a	81.8 (6.1) a
CO_2 effect (P)	0.005	0.086	0.122	0.417	0.091	0.044	0.053
Drought effect (P)	0.085	0.803	0.358	0.897	0.766	0.413	0.089
CO_2 * Drought (P)	0.075	0.712	0.539	0.792	0.397	0.532	0.454

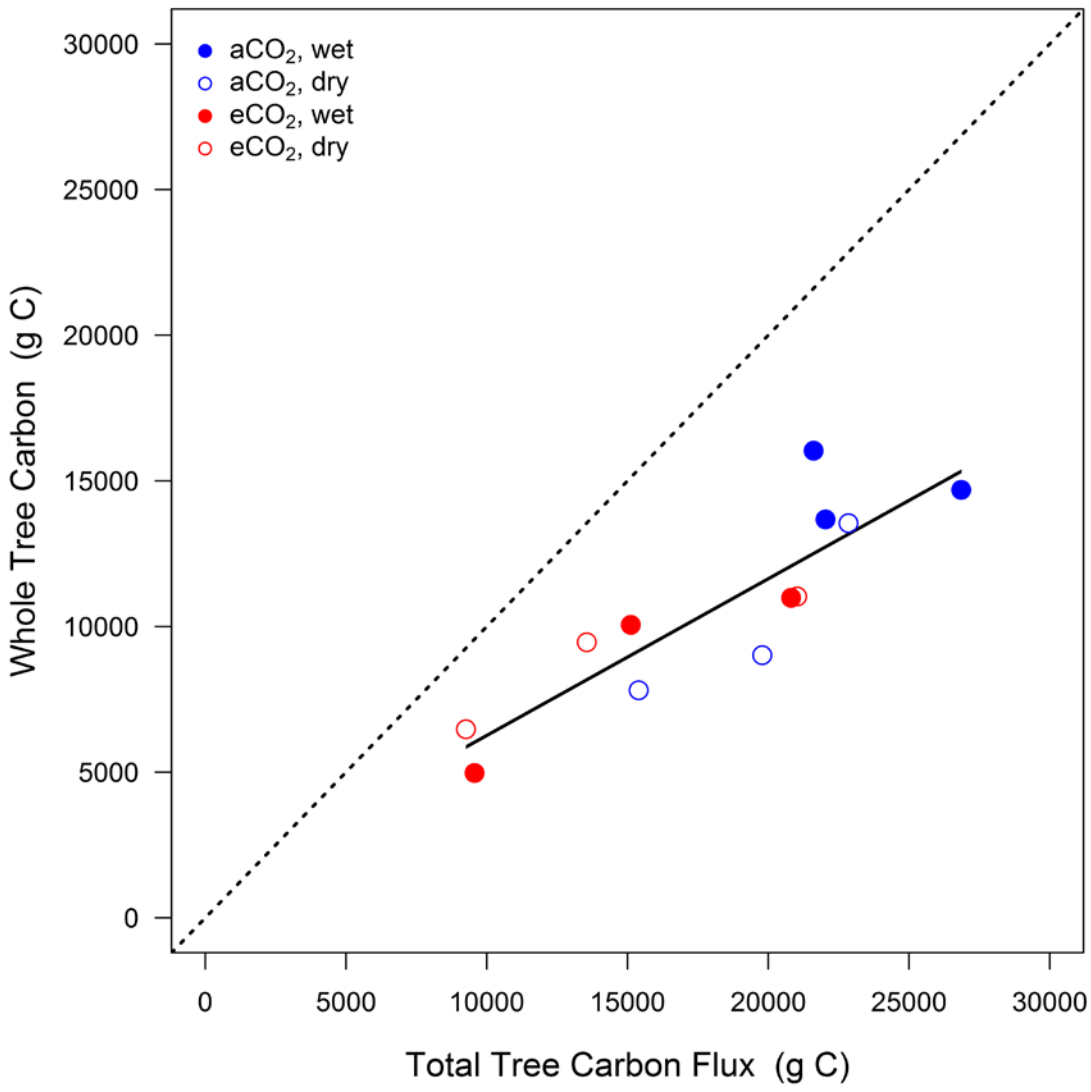

Figure 4.2. Whole tree C mass as a function of cumulative aboveground C flux for each WTC tree. Values of cumulative aboveground net C flux were measured over the final eleven months of the experiment. Whole tree C mass represents the sum of bole, branch, leaf and root C mass from allometric estimates over the same time period. The dotted line is the 1:1 relationship and the solid line represents the significant overall linear model fit from the equation $y = 0.56x + 878.2$ ($R^2 = 0.86$).

Leaf area at the final harvest was significantly reduced by 31.3 % under eC_a ($p < 0.001$) and this pattern was observed across the final eleven months of the experiment (Figure 4.3). Specific leaf area was reduced by 10.9 % in eC_a treatments ($P = 0.053$), and by 8.9 % in drought treatments ($P = 0.089$, Table 4.1). Overall, $F_{c,T}$ was positively correlated with mean leaf area ($P < 0.001$, Figure 4.4). Intercepts and slopes between separate linear regressions of $F_{c,T}$ and mean leaf area for aC_a and eC_a treatments were not different, however, there was negligible overlap of data between treatments. Thus, we were unable to determine if reductions in $F_{c,T}$ in eC_a treatments were a function of lower mean leaf area or shifts in A_n and tissue respiration rates.

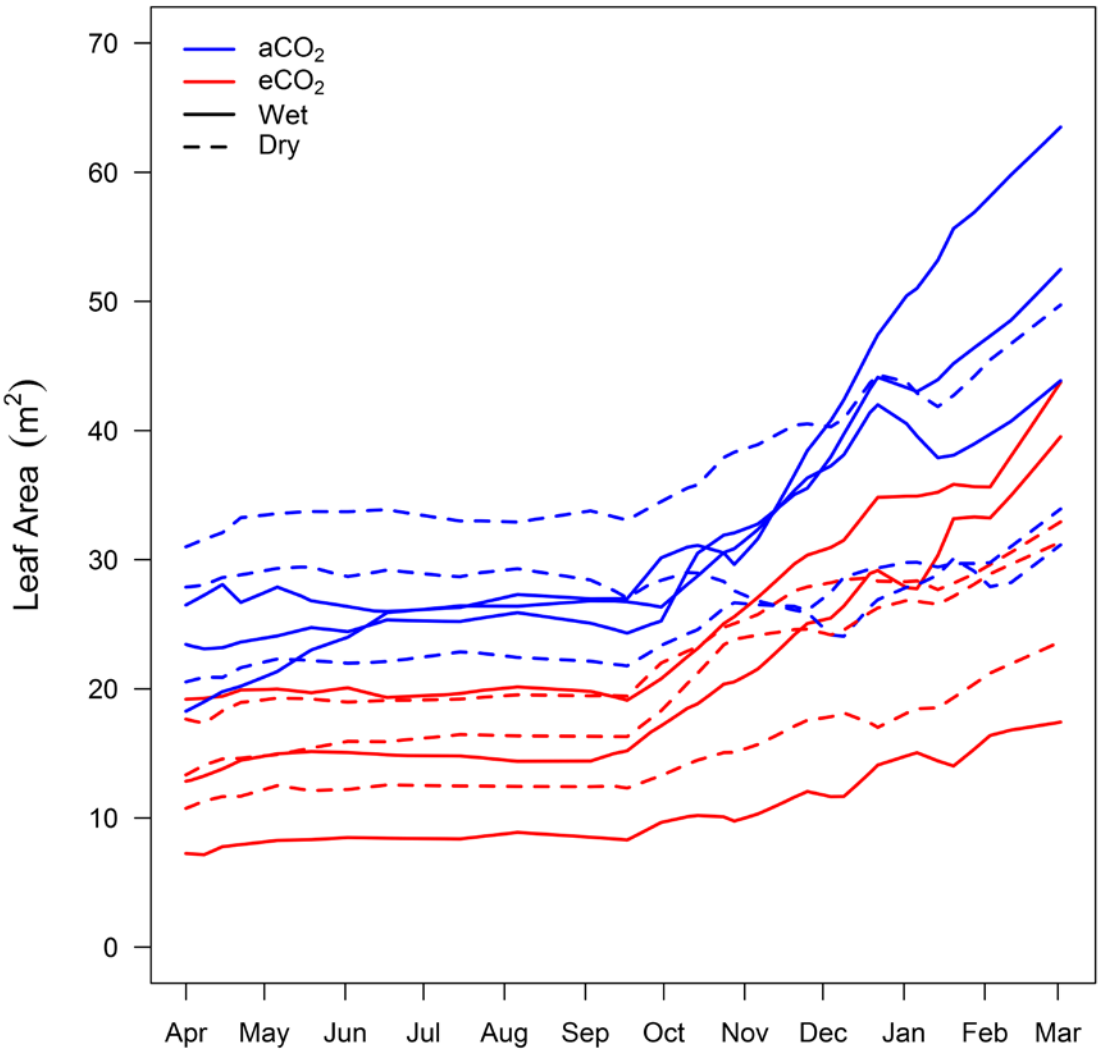

Figure 4.3. Estimated canopy leaf area for each WTC tree over the final eleven months of the experiment (April 2008 to March 2009). Estimates are based on height growth, litterfall rates and two leaf area estimates following Barton et al. (2012). Color and line type distinguish the treatment combination for each WTC.

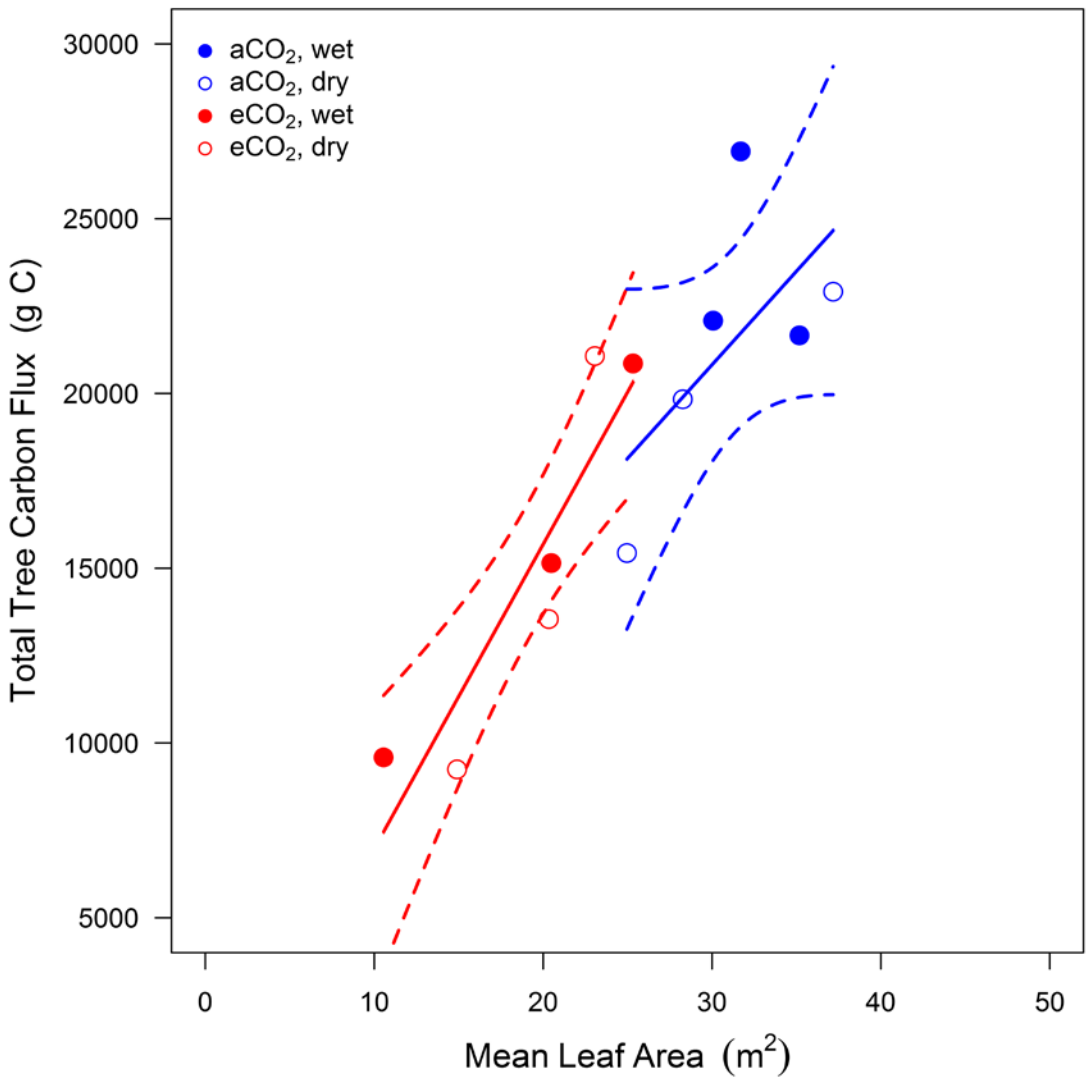

Figure 4.4. Treatment means of cumulative aboveground C flux as a function of mean daily canopy leaf area over the final eleven months of the experiment. The solid line represents the significant overall linear model fit ($R^2 = 0.77$) from the equation: y = 611.9x + 2791.2. Separate 95% confidence intervals are shown for linear regression between $F_{c,T}$ and mean leaf area for aC_a and eC_a treatments.

4.4.2 Harvested tissue carbon mass and biomass partitioning

At the end of this two year experiment, harvested C mass of tissue components was affected in eC_a but not drought treatments (Table 4.1). Aboveground wood C mass was reduced by 37 % in eC_a treatments (P = 0.015), driven mostly by eC_a effects on bole wood. Neither standing crop leaf C mass or total litterfall C mass over the study period differed between CO_2 treatments. Total root C mass was reduced by 29% in eC_a treatments (P = 0.091).

Leaf mass fraction (LMF) increased by 15.0 % in eC_a treatments (P = 0.011) but was not affected by the drought treatment. Leaf mass fraction was negatively correlated with whole tree C mass (P= 0.007, Figure 4.5a). Stem mass fraction (SMF) was marginally reduced by 6.0 % under eC_a (P = 0.077), with no effect of the drought treatment detected. Stem mass fraction had a weak positive correlation with whole tree C mass (P = 0.08, Figure 4.5c). Root mass fraction (RMF) was not affected by either treatment and was not correlated to whole tree C mass (Figure 4.5e).

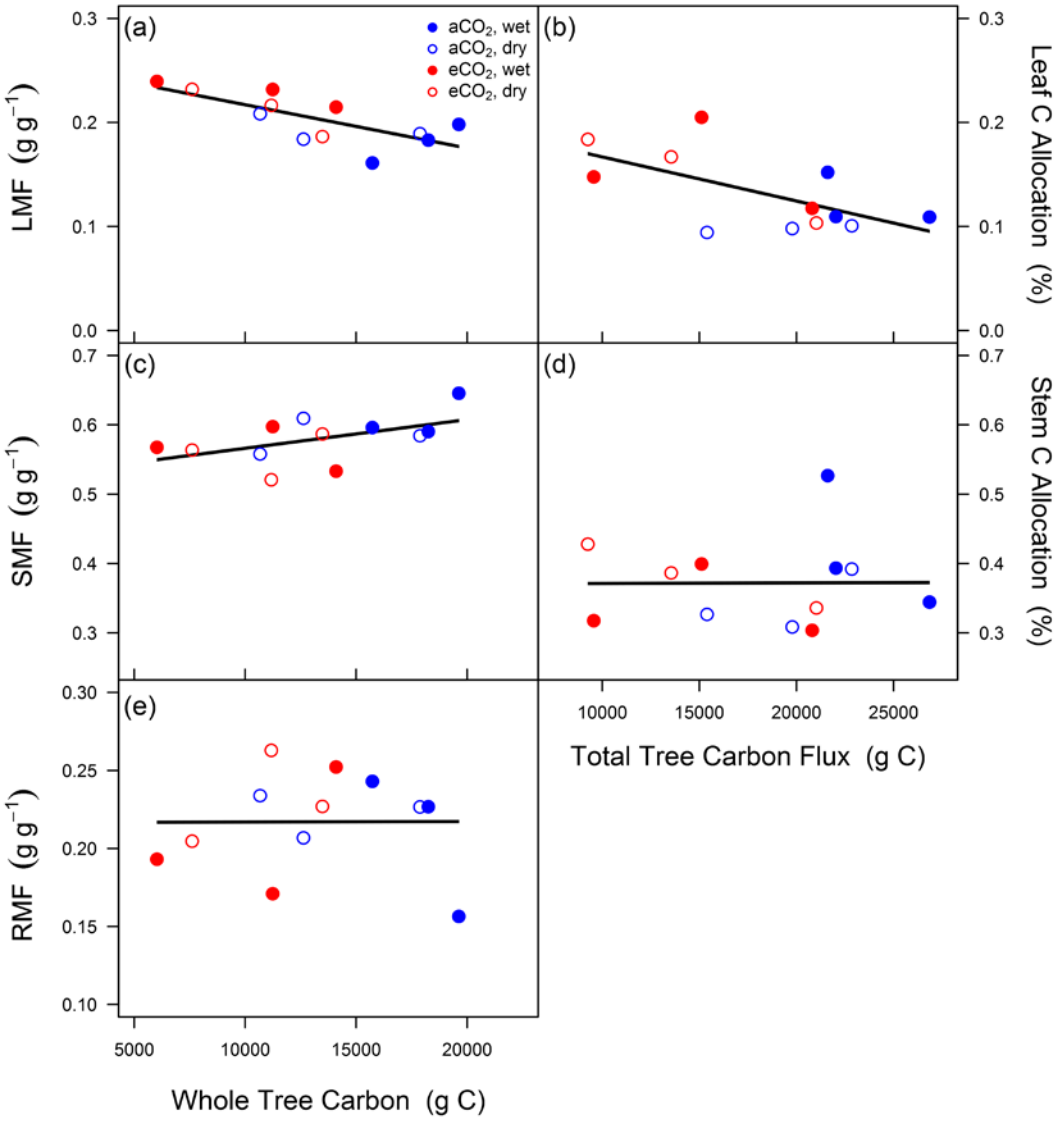

Figure 4.5. Treatment means of C mass fractions of leaves (a), stems (branches+boles) (c) and roots (e) as a function of tree size, via whole tree C mass. Treatment means of C allocation to leaves (b) and stems (d) as a function of cumulative aboveground net C flux. Root C allocation could not be estimated as root turnover was not known. Values for C mass fractions are calculated from final harvest biomass totals. Values for C allocation are estimated from cumulative total aboveground net C flux over the final eleven months of the experiment. Solid lines represent overall linear model fit for leaf,

stem and root mass fractions (R^2 = 0.53, 0.26 and 0.01, respectively), as well as leaf and stem C allocation (R^2 = 0.39, 0.01, respectively).

4.4.3 Aboveground carbon allocation

Treatment effects on tissue C allocation were determined from C mass estimates obtained from allometry over the final eleven months of the experiment and $F_{c,T}$ over the same time period. Total C allocation to leaves increased by 28% in eC_a treatments (P = 0.052), with no effect of the drought treatment detected. Leaf C allocation was negatively correlated with $F_{c,T}$ (P = 0.031, Figure 4.5b). Alternatively, C allocation to aboveground wood was not affected by either treatment and was not correlated to whole tree C (Figure 4.5d).

4.4.4 Belowground carbon allocation

Across all treatment combinations, the total C mass of boles, branches, leaves and roots produced through the course of the measured flux measurement period was on average 61.0±0.02 % of $F_{c,T}$ (Figure 4.6). As mass balance must be achieved, TBCA and the residual belowground C flux ($F_{c,r}$) were estimated from Figure 4.6 as residuals between $F_{c,T}$ and whole tree mass excluding and including estimates of roots over the flux measurement period, respectively. Total belowground C allocation was on average 49.9±0.02 % of $F_{c,T}$ and ranged from 46.1 to 54.9 % across treatment combinations. Across a large range in tree size among the treatment combinations and replicate WTCs, similar patterns were detected for each tree (Figure 4.S2). Neither cumulative TBCA nor $F_{c,r}$ were affected by CO_2 or drought treatments (Figure 4.7). The time course of cumulative daily TBCA and $F_{c,T}$ were positively correlated over the final 11 months of

the experiment ($R^2 = 0.78$, $P < 0.001$) and the proportion of C allocated belowground was relatively stable through time and between treatments (Figure 4.8).

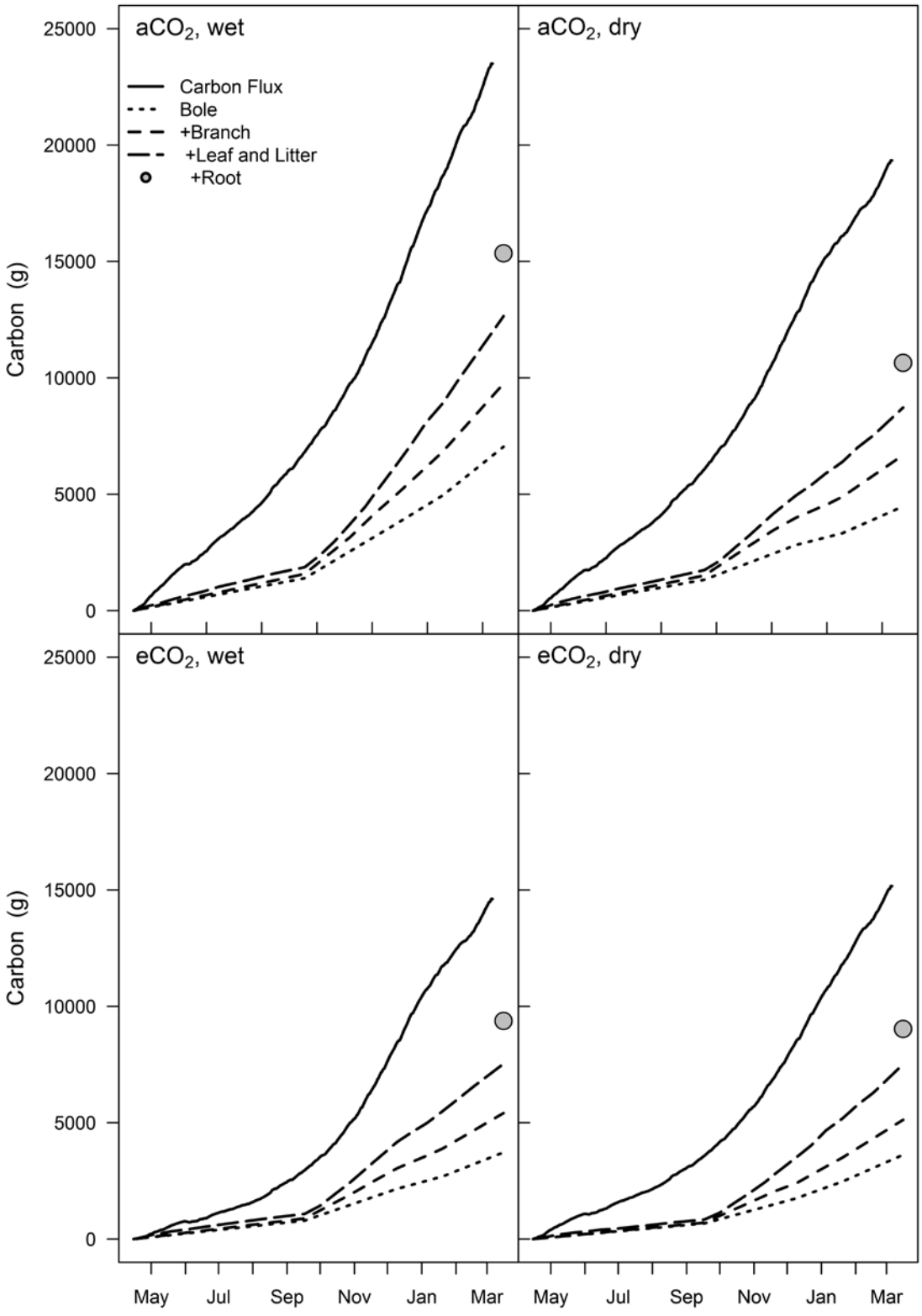
aCO2, wet
aCO2, dry
eCO2, wet
eCO2, dry
Carbon Flux
Bole
+Branch
+Leaf and Litter
+Root
Carbon (g)
0
5000
10000
15000
20000
25000
May
Jul
Sep
Nov
Jan
Mar

Figure 4.6. Cumulative aboveground net C flux and additive C allocation to individual tree components from 15 April 2008 to 16 March 2009. Each panel represents mean values for each treatment combination (n=3). Both aboveground net C flux and tissue C allocation where set to 0 on 15 April 2008 in order to track the allocation of C in daily time steps. Root C mass, predicted from the logarithmic relationship between above and belowground mass partitioning of pre-planting seedlings and harvested trees, is shown on the last date.

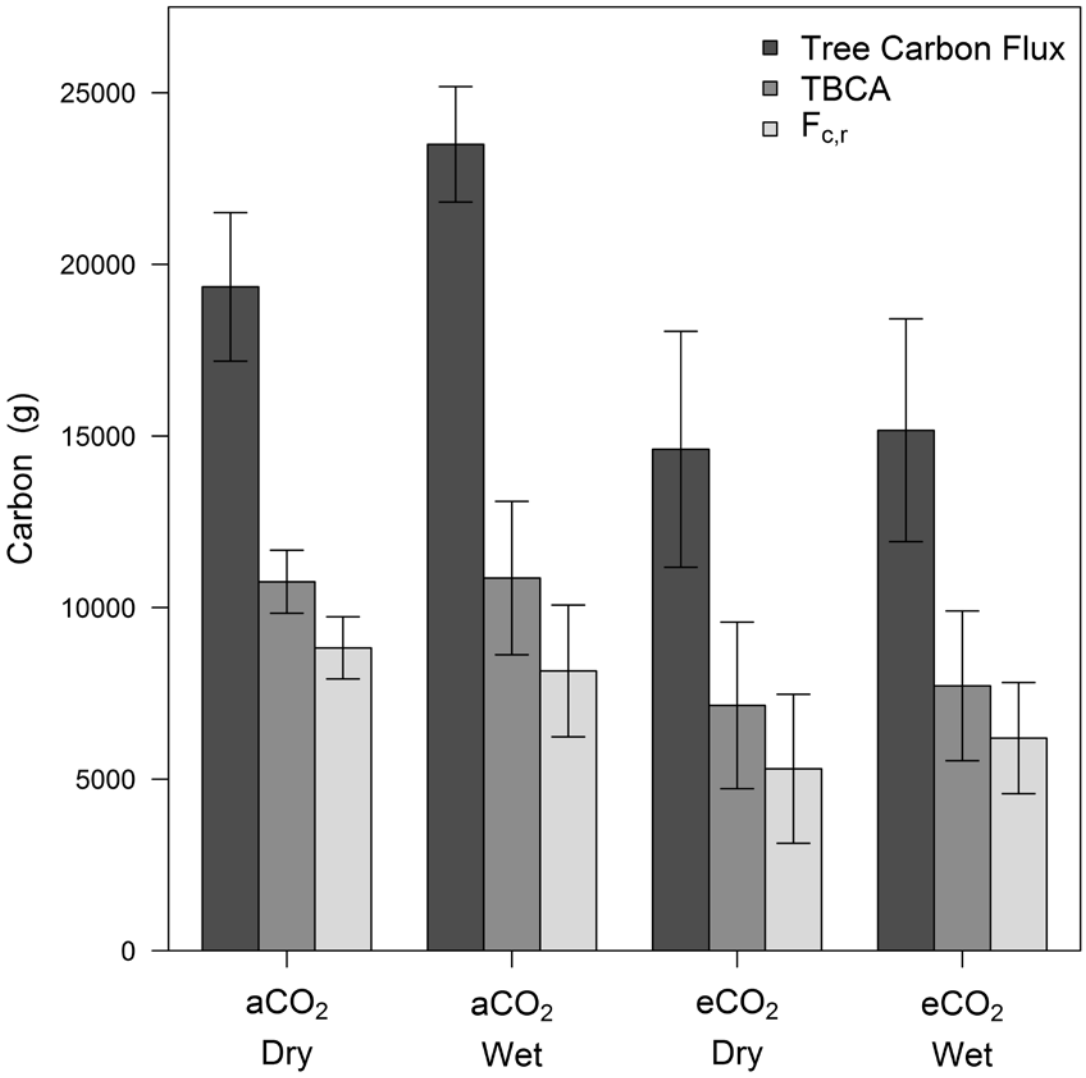

Figure 4.7. Treatment means ± 1 standard error of cumulative aboveground net C flux, TBCA, and the residual belowground C flux ($F_{c,r}$). Values of cumulative aboveground net C flux were measured over the final eleven months of the experiment. Values for TBCA are the residual between the cumulative C flux and total C mass aboveground estimated from allometric surveys over the same time period. Values for $F_{c,r}$ were calculated as the residual between TBCA and root C mass predicted on the last date of the eleven month period.

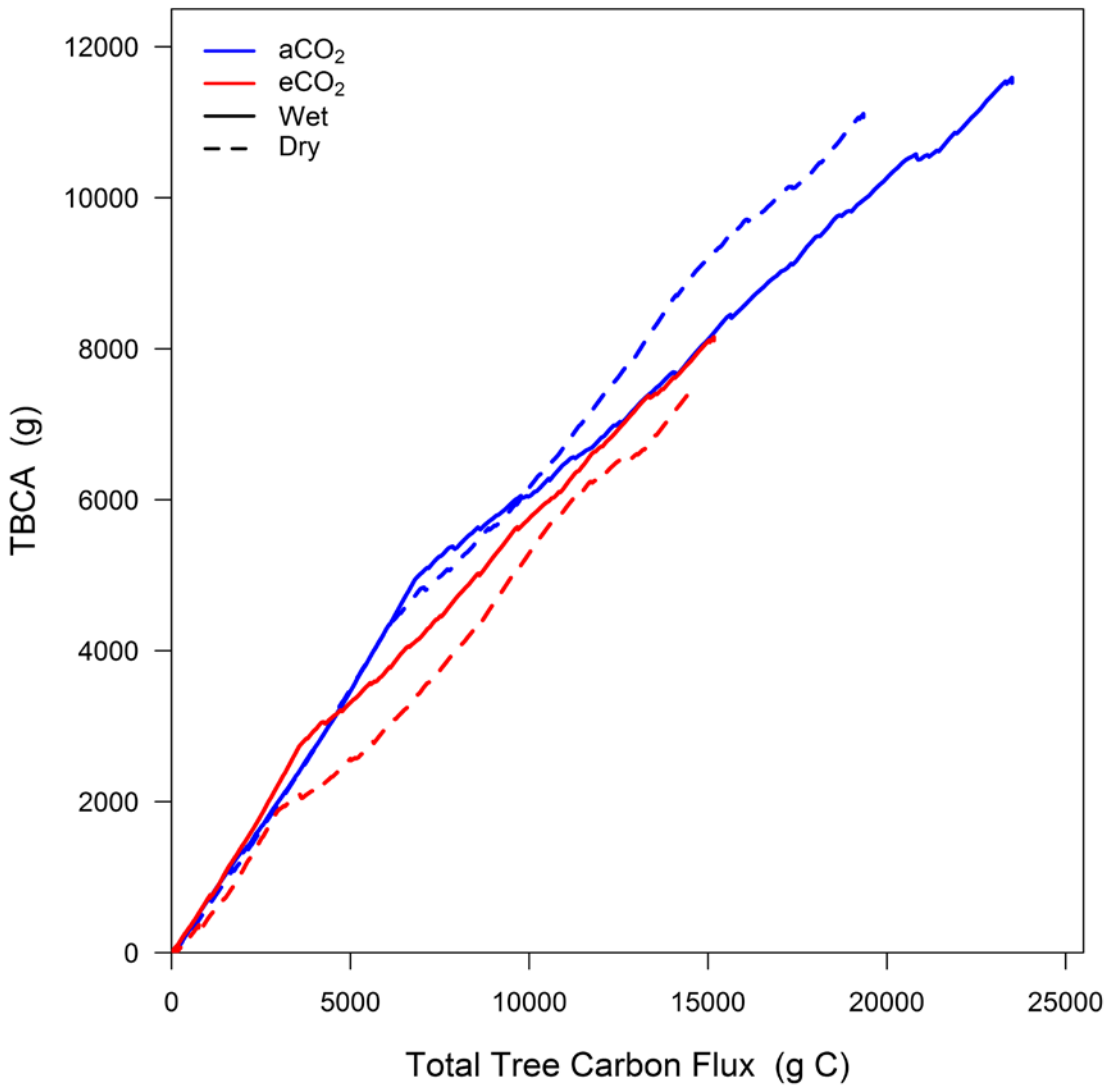

Figure 4.8. Total belowground C allocation as a function of cumulative aboveground net C flux across the final eleven months of the experiment. Carbon mass aboveground was estimated from allometric surveys, interpolated on a daily time scale and then subtracted from the aboveground net C flux to quantify TBCA. Individual lines represent treatment means, with color and line type distinguishing treatment combinations.

4.5 Discussion

A whole-tree chamber experiment provided a unique opportunity to study the C balance of *Eucalyptus* trees. We found that biomass partitioning and C allocation of component tissues were differentially affected by eC_a. Despite previous findings of negative impacts of drought on leaf and canopy physiology in this study (see Crous et al. 2011, 2012, Duursma et al. 2011), minimal effects of a four month drought were detected on total tree C flux, biomass partitioning and tissue C allocation. Using a novel methodological framework, we show that TBCA may be less sensitive to climate change factors than previously assumed. As reliable estimates of TBCA are notoriously hard to obtain, we provide essential empirical data that can be compared to model predictions where C allocation is represented.

4.5.1 Relationships between tree C flux, leaf area and tree C mass

A novel aspect of this study was the ability to measure whole tree C fluxes directly and compare these fluxes to observed patterns in leaf area and growth. Tree C uptake and growth were strongly coordinated across this two year experiment. The net C uptake of plants should be a function of the canopy leaf area and light interception (Wilson 1965, Monsi and Saeki 2005) and correlate to canopy assimilation and tree productivity (Waring 1983, McCarthy et al. 2006, Lindroth et al. 2008). Estimates of tree canopy C flux, however, are limited by simple upscaling of single leaf measurements (Amthor 1994), oversimplification of big leaf models (De Pury and Farquhar 1997) or parameterization of more complex models with assumptions of canopy behavior (Leuning et al. 1995). We found that leaf area was consistently reduced in eC_a

treatments, likely leading to reductions in both tree C uptake and whole tree C mass of near identical magnitudes (ca. 30 %).

A shortage of empirically measured whole tree C fluxes also makes inferring relationships with biomass or C allocation difficult. Biomass and C fluxes have been found to be poorly related in forest ecosystems due to difficulty in accounting for C retention of different tissues (Litton et al. 2007). This partial accounting of C likely inhibits the ability of many studies to precisely test the coordination between canopy A_n and growth. The advantage of the WTC approach is the ability to compare cumulative whole tree C fluxes to absolute biomass production over long time periods. Here, we show empirically measured aboveground tree C uptake (F_c) was strongly correlated to tree biomass production across a 2.5 fold size range in *Eucalyptus* trees.

4.5.2 Responses of biomass partitioning and C allocation to climate change

We first used final harvest biomass to determine patterns of biomass partitioning to leaves, stems and roots. We then combined cumulative tree C fluxes with tissue biomass production and turnover to measure C allocation to stems, leaves and TBCA, via mass balance. This approach allowed us to evaluate the impacts of climate change treatments on tree growth through potential shifts in tissue biomass production or C allocation. This is because there are many possible fates for C assimilates beyond just the production of plant biomass (Körner et al. 2005). Changes in C allocation encompass effects of tissue turnover, the storage and use of carbohydrates and root exudation to stimulate microbial activity, with each representing significant tree or ecosystem responses to environmental

change. Thus, patterns in biomass partitioning and C allocation may not be consistent with respect to the tissue in question, which contributes to the current uncertainty in modelling tree growth responses to interacting climate change factors.

We found that stem C mass was reduced in eC_a treatments. Opposite responses of stem growth under eC_a have been found across different forested FACE experiments, including no effect in a mixed deciduous forest at WEB-FACE (Körner et al. 2005) and a positive enhancement in a loblolly pine forest at duke FACE (DeLucia et al. 2005). It is possible that observed patterns in stem C mass were related to allometric trajectories as a function of plant size (Tjoelker et al. 1998, Müller et al. 2000) more than direct effects of eC_a on stem biomass production. Stem mass fractions (SMF) were found to increase with total plant size and were marginally reduced in eC_a treatments. Carbon allocation to stems was unaffected in eC_a treatments, however, inferring that patterns in SMF were a consequence of size-dependent relationships between larger aC_a trees compared to smaller eC_a trees. Trees in this experiment followed commonly observed developmental patterns in biomass partitioning, with increases in SMF and decreases in LMF as tree became larger (Poorter et al. 2015). Thus, it is likely that eC_a treatments negatively affected other tree processes which first decreased overall tree size.

Contrary to expectation, we found that both LMF and C allocation to leaves increased in eC_a treatments independent of tree size effects. As leaf production and turnover were not subsequently affected in the smaller eC_a trees, it is likely that changes in other physiological processes were necessary to explain observed increases leaf C allocation.

Previously reported increases in leaf respiration under eC_a treatments (Crous et al. 2011, 2012) are intrinsically included in the measurement of $F_{c,d}$, thus observed increases in leaf C allocation in terms of leaf biomass production are independent of shifts in respiration. Decreases in SLA were detected in WTC trees under eC_a treatments, which is often found across eC_a enrichment studies (Yin 2002, Ainsworth and Long 2005, Wang et al. 2012). Concentrations of leaf non-structural carbohydrates (TNC) often increase under eC_a (Roden and Ball 1996, Picon et al. 1997, Poorter et al. 1997, Loewe et al. 2000, Walter et al. 2005) and are often associated with subsequent decreases in SLA in trees (Barron-Gafford et al. 2005, Körner et al. 2005). Here, increased C allocation to leaves may have resulted in the observed increase in leaf TNC under eC_a (see Crous et al. 2011) to fulfill increased canopy respiratory demands or meet sink demands of other tissues. Taken together, results for aboveground tissues highlight the importance of separating impacts on measured biomass from those of total C allocation associated with growth when evaluating tree responses to climate change.

4.5.3 TBCA response to climate change in a single-tree ecosystem

Despite increased attention to the effects of climate change on belowground processes, the difficulty in measuring TBCA currently hinders our ability to make well-founded empirical conclusions. One of our specific objectives was to use a novel method to calculate TBCA to test the hypothesis that TBCA was enhanced in eC_a treatments and then to evaluate potential shifts in TBCA across shorter times scales. For example, changes in TBCA to eC_a or drought could occur as sustained or pulsed responses through time. Enhancement of TBCA has been reported across forested FACE experiments (Palmroth et al. 2006) but the single-tree ecosystem design of the WTC

allowed us to evaluate the effects of climate change factors without the inherent environmental complexity of a forest community. The unique design of the WTC allowed us to track TBCA as a cumulative total and across daily time steps, both of which can be used to validate and constrain models where C allocation is represented.

With high resolution flux data and reliable estimates of aboveground dry mass production we show that TBCA was not affected by eC_a or drought treatments over the final eleven months of the experiment. Contrary to expectation, we detected minimal effects of eC_a or drought treatments on root biomass partitioning, although it was not possible to differentiate fine and coarse root production and turnover. Although these findings disagree with TBCA results from forested FACE experiments (see Palmroth et al. 2006), comparisons between single-tree studies with evidence from forest ecosystem experiments should be made with caution. Nevertheless, we show that TBCA in *Eucalyptus* trees may be less sensitive to climate change factors than expected over a ~1 year period.

A lack of cumulative change in TBCA, however, does not imply that belowground processes were unaffected by either treatment. For example, trees under drought stress may increase C allocation to root systems to alleviate water stress (Poorter and Nagel 2000), but this increase could be offset by reduced root exudation (Iversen and Norby 2014), reduced C demand via decreases in root respiration rates (Burton et al. 1998) or increased root mortality and turnover (Marshall 1986, Meier and Leuschner 2008). Quantification of root exudation, respiration and turnover should remain a priority in

future studies to further elucidate temporal patterns in TBCA. Alternatively, the lack of belowground competition for soil mineral resources in this single tree ecosystem might have delayed enhancement of TBCA to eC_a treatments, such as increased root production and exudation.

With an estimation of daily aboveground C mass gain and measured cumulative whole tree C uptake we were able to uniquely track dynamic short term effects of eC_a or drought on TBCA. Across daily time steps, we observed a relatively stable fraction of total tree C flux distributed to TBCA over a period of eleven months. The ability to calculate TBCA as a simple residual between measured aboveground processes gives us reliable estimates of the absolute amount of C distributed belowground each day, which appears to be insensitive to sustained exposure to eC_a and a four month drought. Similar to Palmroth et al. (2006) we cannot quantify allocation to specific belowground pools, but our approach with the WTC design does not have to make assumptions about C residence time in any tissue or soil component. As a result, the lack of a cumulative response of TBCA raises questions about the consistency of belowground responses to climate change factors often reported. Our results confirm the need for more reliable estimates of TBCA in future studies, which are crucial for predicting forest responses to climate change.

4.5.4 Conclusions

Here we use novel aspects of the WTC experimental facility to show that whole tree C flux and tree growth were highly correlated, while patterns in biomass partitioning alone were insufficient to explain eC_a effects on tree growth. With individual *Eucalyptus*

saligna trees we show different responses of above and belowground C allocation to eC_a treatments, which may have important implications for how C allocation should be represented in process-based forest models. As empirical measurements of belowground processes are still difficult to obtain, models may have to assume that responses of aboveground tissues to global change represent those of belowground tissues (Giardina et al. 2005). As a result, continued empirical measurements to define C allocation patterns constrained by functional relationships with biomass production are needed to reduce uncertainty and improve model predictions (De Kauwe et al. 2014). Continuing to apply novel approaches to better evaluate TBCA and empirically measure whole tree C fluxes, such as the WTC experiment, are the way forward in addressing questions regarding the fate of assimilated C under global climate change.

4.6 Supporting Information

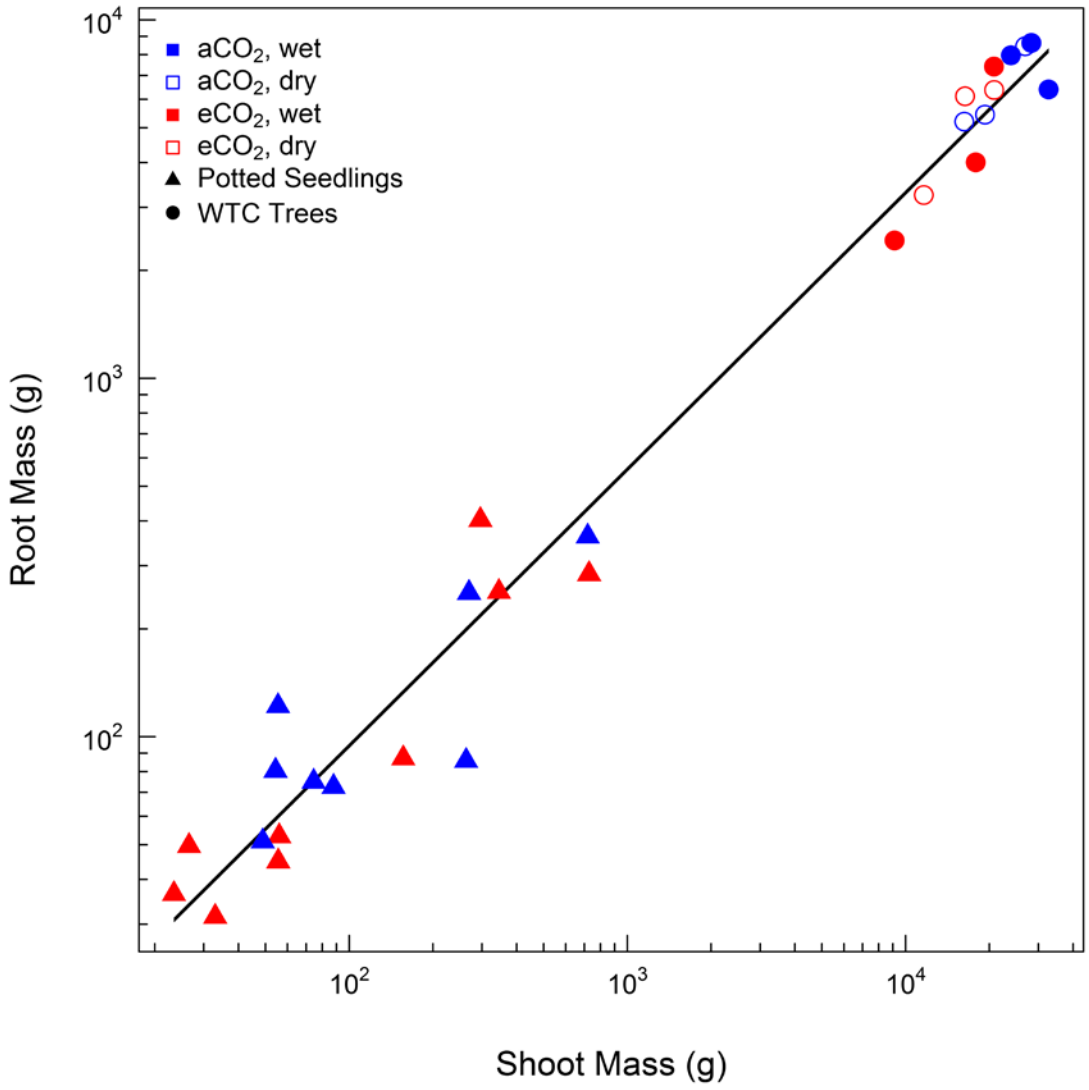

Figure 4.S1. Root mass as a function of shoot mass in *Eucalyptus saligna* for potted seedlings harvested before planting of WTC trees (n=17) and WTC trees harvested after 2 years (n=12). Potted seedlings were grown in 25 l pots inside each WTC, while chamber [CO_2] treatments conditions were maintained. The solid line represents the significant log-log model fit (R^2 = 0.98) from the equation: log(x) = 0.77(log(y)) + 0.43.

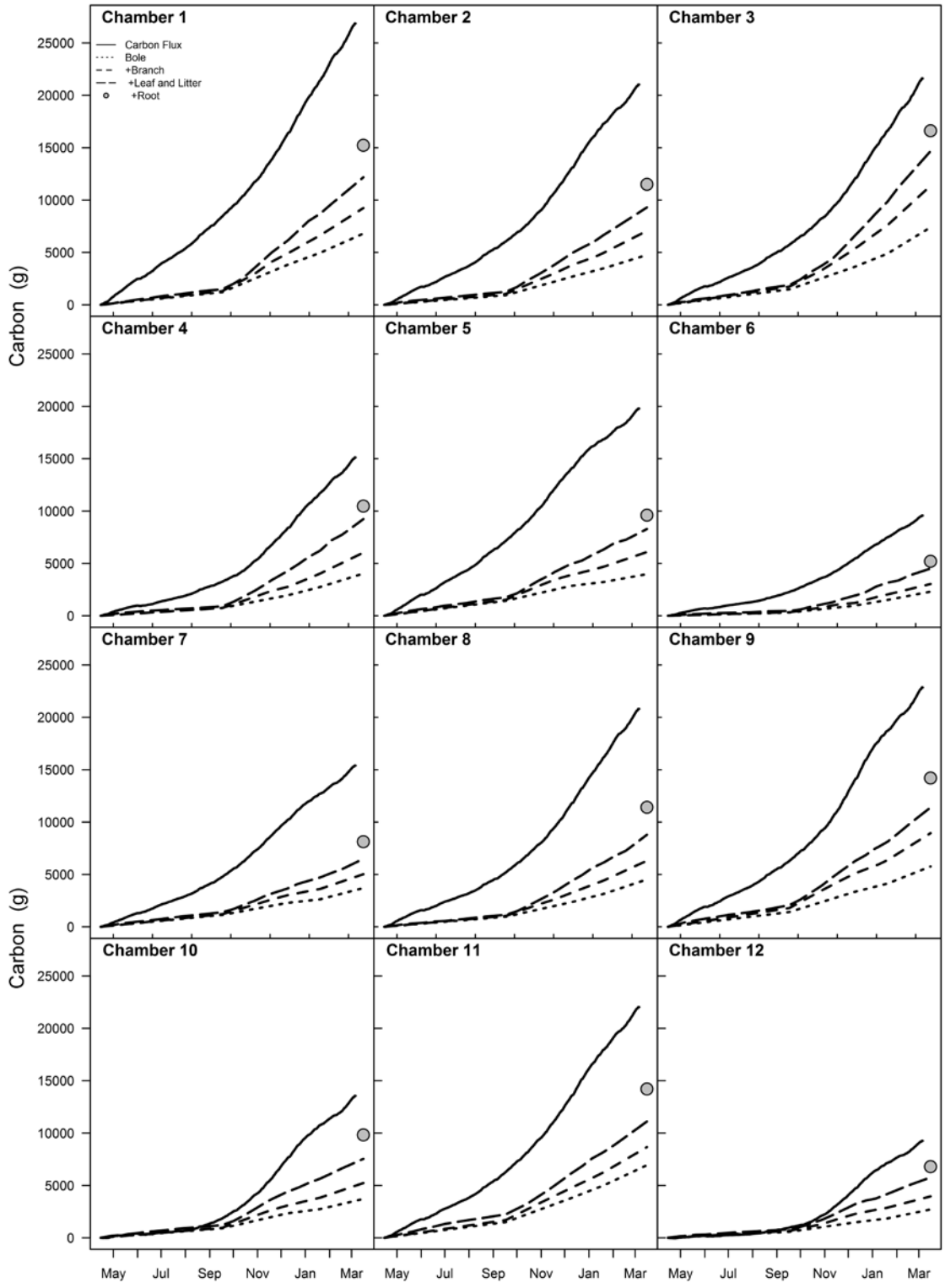
Chamber 1
Chamber 2
Chamber 3
Chamber 4
Chamber 5
Chamber 6
Chamber 7
Chamber 8
Chamber 9
Chamber 10
Chamber 11
Chamber 12
Carbon Flux
Bole
+Branch
+Leaf and Litter
+Root
Carbon (g)
0
5000
10000
15000
20000
25000
May
Jul
Sep
Nov
Jan
Mar

Figure 4.S2. Cumulative aboveground net C flux and additive C allocation to individual tree components from 15 April 2008 to 16 March 2009. Panels represent each individual WTC. Both aboveground net C flux and tissue C allocation where set to 0 on 2008-4-15 in order to track the allocation of C in daily time steps. Total root C mass, predicted from the log relationship between above and belowground mass partitioning of pre-planting seedlings and harvested trees, is shown on the last date.

Chapter 5

Synthesis and Conclusions

5.1 Synthesis

It has long been recognized that resources limit plant growth in different environments, at different life stages and individual plant processes are limited by different resources (Bazzaz et al. 2000). Consequently, a quantitative understanding of how plants gain and allocate resources is necessary to predict their success in any environment (Mooney 1972). In this thesis, resources allocated for growth in *Eucalyptus* tree species are classified into two distinct groups. The first group consists of environmental plant resources, such as N and H_2O, that are captured, distributed and utilized to drive rates of leaf photosynthesis (A_n) and thus tree C gain. These C assimilates comprise the second group, which are the essential internal resource required for tissue growth, storage and to fuel respiration. These two resource groups are inextricably linked and interact to define plant growth across spatial and temporal scales. For example, the C expended in acquiring N makes up a significant fraction of the total energy a plant consumes, while leaf N investment constrains photosynthetic capacity (Chapin et al. 1987). In trees, rates of A_n will then depend on the photosynthetic light response of individual leaves and the energetic trade-offs of gas exchange related to transpiration and water supply (Givnish 1988).

The research presented in this thesis was designed to investigate resource allocation in trees at individual tissue and whole plant scales in *Eucalyptus*. I sought to address theories of plant functional balance by testing biomass partitioning in seedlings and trees subjected to various environmental manipulations. As observed biomass production may not necessarily reveal shifts in plant functional responses to environmental change, I evaluated the sensitivity of the allocation of photosynthate above and belowground across different temporal scales. Using mass balance approaches I then tested the coordination between growth and A_n, using leaf gas exchange parameters in seedlings and measurements of net canopy C gain in trees. To help bridge the knowledge gap between leaf and canopy C gain I investigated the distribution of N and supply of H_2O as a function of light availability within canopies and the effect this has on individual leaf physiology. By utilizing novel experimental approaches, evidence from this work improves our understanding of functional processes that determine the net C uptake of trees and then how this assimilated C is used to fuel growth. The contribution of this body of work provides fundamental evidence underlying resource allocation in ecologically and commercially important *Eucalyptus* tree species.

5.1.1 Where does the carbon go?

This thesis question arises from large uncertainties that remain regarding fundamental processes which affect terrestrial C cycling. The question "Where does the carbon go?" arises from the need to track the fate of C from canopy A_n to determine the contribution of forests ecosystems to C cycling (Litton et al. 2007). Currently, empirical data on C allocation are critical to the further development of forest models and subsequent

predictions of global C balance under climate change (Franklin et al. 2012). Growth responses during early phases of tree establishment (seedlings or young trees) to changes in soil resource availability or climate change factors will likely depend on shifts in the plant C budget to balance growth, respiration and storage. Consequently, understanding environmentally driven shifts in C allocation in young *Eucalyptus* trees will be crucial to manage their fitness in native ecosystems and their productivity in terms of timber production and quality in forestry systems.

First, I examined patterns in biomass partitioning of *E. tereticornis* seedlings with belowground resource limitation (Chapter 1) and with *E. saligna* trees exposed to eC_a and drought treatments (Chapter 2). Across these studies, partitioning of biomass largely followed allometric trajectories related to plant size, nearly independent of treatment manipulation. Partitioning to roots, leaves and stems in *E. tereticornis* seedlings was conserved across a ten-fold variation in seedling biomass with and without soil volume restriction. During this early growth stage, these results can be used to infer that growth inhibition from reduced belowground sink strength did not elicit a functional partitioning response. With much larger 2 year old *E. saligna* trees, grown in WTCs, differences in partitioning to stem biomass were detected between aC_a and eC_a treatments. These patterns were also attributed to size dependent relationships associated with ontogeny (see Poorter et al. 2015), rather than a direct functional response to eC_a.

Combined results from these two experiments argue against traditional views of plant functional balance in the context of observed biomass production. These theories posit

that plants will “optimally forage” for the most limiting resource, thus shifts in biomass partitioning should occur. However, adaptive plant responses may not include changes in biomass production at any given “snapshot” in time. This makes tracking C allocation to processes other than observed biomass just as important in assessing overall responses to manipulations of resource availability. Here, empirical and modelling evidence from Chapters 2 & 4 reveal that detection in shifts of tissue C allocation were necessary to interpret whole tree response to environmental manipulations. For *E. tereticornis* seedlings, modelling results infer that increases in C allocation to pools other than biomass, such as TNC or respiration, were required to fully explain the effects of soil volume restriction on seedling growth. For *E. saligna* trees, increased leaf C demand under eC_a treatments resulted in higher C allocation to leaves without altering observed leaf biomass production. Overall, the ability to distinguish biomass production from C allocation across tissues reveals that alternate explanations are likely need to interpret the degree in which trees exhibit functional balance.

Alternatively, shifts in tissue morphology, metabolism or turnover to alter resource uptake of loss (Reich et al. 2002), increased root exudation to alleviate resource limitation (Phillips et al. 2011) or increased C allocation to storage (Sala et al. 2012 , Dietze et al. 2014) may be used to balance trade-offs between tissue sink strength, resource availability and source C supply. Partial evidence for these ‘non-biomass’ responses were evident in *E. tereticornis* seedlings in research presented in Chapter 2. Increases in specific root length were detected in some, but not all, of seedlings with soil volume restriction. Modelling results also revealed that increases in tissue respiration

rates were a possible mechanism to account for the oversupply of C not allocated to biomass. Increases in leaf carbohydrate storage were correlated with reduced belowground sink strength in these seedlings, and it is possible that C storage increased in other tissues. Although not measured, root exudation may have increased in response to adverse poor quality soil conditions with *E. tereticornis* seedlings in containers or in *E. saligna* trees under eC_a to meet resource demand.

The ability to compare biomass partitioning with aspects of C allocation across multiple experiments highlights how partial accounting of C may lead to erroneous conclusions regarding adaptive plant responses to changing environments. Overall, these results reveal why studies using only biomass partitioning to assess functional balance or allometric based theories have mixed results. Additionally, shifts in above but not belowground C allocation in *E. saligna* trees disagrees with the common observation of enhancement of belowground processes in other trees species under eC_a (see Palmroth et al. 2006, Iversen and Norby 2014). Shipley et al. (2002) states that it is more appropriate to state that plants shift biomass allocation to reduce imbalances between leaf source activity and tissue resource acquisition. Collectively, results from this research tend to agree with this conclusion, with the caveat that the concept of allocation must be extended to include fates of C other than measured biomass. Consequently, I agree with Poorter, Niklas, et al. (2012) that understanding C allocation above and belowground requires a better understanding of the interactions between tissue source and sink activity at any time point. In order to fully understand the impact environmental change

has on forest productivity approaches to quantify patterns in C allocation must be prioritized in future studies.

5.1.2 When do photosynthesis and growth not add up?

This thesis question addresses the debate over how strongly plant growth is controlled by either source or sink activity, which may disrupt the coordination between A_n and growth at different temporal scales. Assimilated C is first allocated to provide sufficient sugars for the immediate demands of the plant during the day, and sufficient starch to meet 'anticipated' demands during the following night (Smith and Stitt 2007). The C demands for each tissue, referred to as tissue C sinks, determine the C budget for the entire plant and regulate C allocation. Despite competition among highly integrated C sinks, woody plants also maintain storage carbohydrate pools as C reserves (Kozlowski 1992). Understanding the coordination between plant growth and A_n thus requires mass balance approaches to quantify the fractions of C supply allocated to growth, storage and respiration of different organs. Reductions in tissue sink strength have been shown to signal the down regulation of A_n, which can led to increased starch synthesis for storage (Sage 1994, Kitao et al. 2007). This had led to support for the argument that increased shifts to C storage will compete with C available for plant growth (Chapin et al. 1990), which may then disrupt the coordination between A_n and growth at short time scales.

To address this thesis question the belowground sink strength of *E. tereticornis* seedlings was manipulated, through container size treatments, to test the effects of putative sink limitation on A_n and leaf TNC production (Chapter 1). Empirical results and modelling approaches were combined to test the coordination of A_n and growth of seedlings with

and without soil volume limitation over 120 days. First, apparent reductions in belowground sink strength negatively impacted leaf N content and photosynthetic capacity, while leaf starch increased. These results support other findings where manipulation of tissue C sinks leads to carbohydrate accumulation and photosynthetic down regulation (Hoch et al. 2002, Iglesias et al. 2002, Equiza et al. 2006, Urban and Alphonsout 2007, Haouari et al. 2013). Second, large reductions of harvested biomass in seedlings with soil volume limitation initially suggested that observed reductions in A_n and growth were tightly linked. As previously shown in thesis Question 1, however, partial accounting of C allocation could lead to premature conclusions regarding this linkage. Importantly, using measured reductions in A_n with a mass balance seedling growth model largely over-predicted biomass production from observed results. These findings reveal that not only can A_n and growth not add up when belowground sink strength changes, but other mechanisms beyond A_n and carbohydrate accumulation must now be explored to explain growth responses.

At long enough time scales, however, A_n and respiratory losses together determine net C balance and must be coordinated with plant growth. Consequently, we need to evaluate if trade-offs between storage and growth actually matter for long term C balance of trees (Palacio et al. 2014). The difficulty in measuring total canopy C uptake and the allocation of this assimilate to different tissue sinks currently impedes the ability to quantify whole tree C balance through time. Combining allometric approaches to estimate growth with seasonal variation in carbohydrates of stem wood and roots, Genet et al. (2010) found contrasting results with the C balance between storage and growth

across a chronosequence of stand age. Utilizing the novel WTC experimental design, I sought to address this knowledge gap by applying a simple mass balance approach with *E. saligna* trees (Chapter 4). Empirical measurements of net cumulative C uptake were correlated with whole tree C mass, which integrates the total allocation of C to growth and storage over an 11 month period. This simplified method allows for the coordination of A_n and growth to be tested with minimal issues in accounting for C retention in tissues through time. During this time period, total tree C mass was strongly correlated to net canopy photosynthetic C gain across a 2.5 fold range in tree size. Even though the C balance between growth and storage was likely disrupted by eC_a in these trees, it did not affect the overall coordination between C supply and growth over ~1 yr. Overall, results from Chapters 2 & 4 highlight how utilization of C mass balance improves our ability to explore mechanisms in which source and sink activity feedback to tree growth. Although I show that answers to the debate regarding the coordination of allocation of C to storage and growth requires a deeper understanding C allocation, it appears that whole canopy assimilation and tree growth are tightly coordinated over long periods.

5.1.3 Are whole canopies optimized for carbon gain?

Scaling from single leaf photosynthetic performance to net canopy assimilation is difficult because of concomitant variations in environment and foliage physiology and structure (Niinemets and Anten 2009). The ability to estimate whole canopy C gain involves knowledge of the non-linear responses of A_n to light between shaded and sunlit leaves (De Pury and Farquhar 1997, Linderson et al. 2012), which requires the ability to differentiate light energy utilization, environmental resource distribution, physiological behavior and CO_2 fluxes within tree canopies (Dai et al. 2004, Niinemets 2012,

Peltoniemi et al. 2012). Theory suggests that interactions between traits which influence A_n and transpiration should determine optimal patterns of behavior for whole plant C gain (Givnish 1988). Theories of optimal resource allocation and leaf physiological behavior have been developed (Cowan and Farquhar 1977, Medlyn et al. 2011, Peltoniemi et al. 2012) and subsequently tested (Wright et al. 2003, Héroult et al. 2013, Prentice et al. 2014, Lin et al. 2015) across different ecosystems and plant functional types. This thesis question arises because optimal leaf physiology is commonly assessed for seedlings or 'full sun' leaves, thus our understanding of how resource allocation and individual leaf physiology interact to maximize net canopy C uptake is surprisingly limited. Seeking answers to ecological questions such as "Where does the carbon go?" and "When do photosynthesis and growth not add up?" first requires an understanding of "Where is the carbon fixed?".

Theories of leaf economic strategies are often used to describe the patterns in which resources are distributed in order for plants to optimize A_n (Wright et al. 2003). In this economic framework, I first evaluated how N and water supply were distributed in relation to photosynthetic capacity within *E. tereticornis* tree canopies (Chapter 3). Leaf N and photosynthetic capacity were found to be highest in full sun leaves, which agree with conventional theory that resources for A_n should be preferentially invested relative to light availability. Overall, higher measured rates of A_n in full sun leaves compared to shade leaves implies that N resources were invested to maximize source activity in upper canopy full sun leaves. The distribution of leaf hydraulic conductance, however, was not correlated with canopy N gradients or A_n between sun and shade leaves. It was therefore

necessary to further investigate relationships between leaf physiology, carbon uptake and water-use efficiency (WUE) across leaf types.

It has been previously hypothesized that stomatal conductance (g_s) should be distributed within a canopy to utilize supplies of light, N and water to maximize A_n (Peltoniemi et al. 2012). Under ambient light conditions g_s was consistently higher in shade leaves despite lower rates of A_n. The resultant inefficient water use in shade leaves suggests that stomatal behavior may be optimized differently within tree canopies. Pearcy and Way (2012) theorize that shade leaves may have mechanisms to enhance sunfleck use, including changes in induction through enzyme regulation or stomatal opening. Our data agree with Tausz et al. (2005) that sustaining higher g_s may be a strategy to efficiently utilize sunflecks through reduced stomatal response time. This strategy, however, does not guarantee increased leaf C uptake as mesophyll conductance (g_m) may still limit A_n. Under high light conditions g_m and A_n responded rapidly in shade leaves, leading to leaf C gain of greater magnitude than sun leaves. Rarely have relationships between A_n and both g_s and g_m been quantified within tree canopies, thus I reveal a possible new mechanism of how leaf physiological behavior responds to light. These findings show that resources may also be distributed within a canopy to utilize sunflecks and that both CO_2 resistance pathways must be accounted for when evaluating leaf behavior to determine canopy C gain.

5.2 Conclusions

5.2.1 General conclusions

The diversity and non-linearity of plant ecophysiological processes poses challenges in predicting and analyzing structure and function of ecological systems (Field 1983). These processes include complex strategies in ways plant uptake, distribute and utilize resources for growth in fluctuating environments. I examined how these resources, in the context of external environmental resources and new C assimilate, are allocated to fuel growth in both current and future climate conditions. This thesis work demonstrates that quantifying the underlying processes defining tree growth requires knowledge of the feedbacks between leaf source activity and tissue sink strength, which are both constrained by resource availability. When addressing the fates of assimilated C across multiple experiments it was determined that biomass partitioning patterns did not support theories of "optimal foraging" when faced with eC_a, drought, or belowground resource limitation. If trees strive to maintain functional balance, this collective research indicates that quantifying shifts in C allocation beyond biomass production are the key to unraveling adaptive responses. Additionally, I show how measuring shifts in C allocation are now necessary to gain new perspectives regarding sink and source controls of growth and A_n. This thesis research advocates for continued use of C mass balance approaches which include empirically measured or accurately modeled whole plant net C uptake. As this research presents new strategies to determine whether or not tree canopies are optimized for C gain, further investigation of resource allocation and leaf physiological behavior within canopies should be prioritized to advance predictions

of tree C gain. It will be the ability to quantify cumulative plant C gain through time combined with continued exploration of the fate of assimilated C that will allow future research to elucidate plant responses to environmental change beyond “snapshots” in time.

5.2.2 Eucalyptus forests

A goal of this thesis was to contribute to the knowledge of the physiological ecology of *Eucalyptus* tree species to aid in understanding the susceptibility of threatened native forest ecosystems and the productivity of commercially important tree species to future climate change. First, findings related to the response of shade leaf physiology to dynamic light environments contributes to the overall understanding of canopy C gain in *Eucalyptus* trees. This utilization of sunflecks may play a critical role in productivity of *Eucalyptus* open-forests, specifically dry sclerophyll forests, in Australian ecosystems. Canopy cover in these open forest types likely allow for frequent sunflecks of high intensity at varying lengths. Additionally, many *Eucalyptus* species are characterized by steep leaf angles which can alter light penetrating the canopy, leaf physiology, radiation loads and C gain (Cowan 1981, King 1997, James and Bell 2000, Falster and Westoby 2003). Integration of these research findings with the functional role of leaf orientation may explain how *Eucalyptus* trees maintain positive C and energy balance in resource poor ecosystems and may be applicable to improve commercial stand productivity through thinning or pruning.

Second, aspects of leaf physiology and C allocation in these *Eucalyptus* trees species were less sensitive to manipulations of warming, eC_a and drought than hypothesized.

Eucalyptus trees are often characterized as being highly adaptable in order to cope with Australia's prevailing climate and soils. It is possible that this adaptability plays a role in the observed stability of ecophysiological processes across the duration of these experiments (months to years). Consequently, warming treatments and simulated droughts may not have been of large enough magnitude to elicit functional plant response within experimental time frames. However, these results should by no means be used to conclude that Australian forest ecosystems are overly resilient to future climate regimes. Future climate scenarios predict increased frequency of extreme daily temperatures, heat waves, and limited water resources due to higher temperature and decreased rainfall in Australia (IPCC 2014). Importantly, this research emphasizes that further empirical data quantifying C allocation to specific tissue, flux and ecosystem pools are critical in uncovering the drivers of tree responses to climate. Continued investigation of the cumulative impacts of eC_a, warming and drought on *Eucalyptus* tree growth and fitness, such as the WTC experiments, will develop our ability to predict 'tipping points' for Australian forest ecosystems under future climate change.

References

Abramowitz G (2005) Towards a benchmark for land surface models. Geophysical Research Letters 32(22): L22702.

Adair EC, Reich PB, Hobbie SE, Knops JMH (2009) Interactive effects of time, CO_2, N, and diversity on total belowground carbon allocation and ecosystem carbon storage in a grassland community. Ecosystems 12:1037–1052.

Ainsworth EA, Long SP (2005) What have we learned from 15 years of free-air CO_2 enrichment (FACE)? A meta-analytic review of the responses of photosynthesis, canopy properties and plant production to rising CO_2. New Phytologist 165:351–372.

Ainsworth EA, Rogers A (2007) The response of photosynthesis and stomatal conductance to rising [CO_2]: mechanisms and environmental interactions. Plant, Cell & Environment 30:258–270.

Allen MT, Pearcy RW (2000) Stomatal behavior and photosynthetic performance under dynamic light regimes in a seasonally dry tropical rain forest. Oecologia 122:470–478.

Amthor JS (1994) Scaling CO_2-photosynthesis relationships from the leaf to the canopy. Photosynthesis Research 39:321–350.

Anderegg WRL (2012) Complex aspen forest carbon and root dynamics during drought. Climatic Change 111:983–991.

Arp WJ (1991) Effects of source-sink relations on photosynthetic acclimation to elevated CO_2. Plant, Cell & Environment 14:869–875.

Atwell BJ, Henery ML, Rogers GS, Seneweera SP, Treadwell M, Conroy JP (2007) Canopy development and hydraulic function in *Eucalyptus tereticornis* grown in drought in CO_2-enriched atmospheres. Functional Plant Biology 34:1137–1149.

Baldocchi DD, Wilson KB, Gu L (2002) How the environment, canopy structure and canopy physiological functioning influence carbon, water and energy fluxes of a temperate broad-leaved deciduous forest—an assessment with the biophysical model CANOAK. Tree Physiology 22:1065–1077.

Barron-Gafford G, Martens D, Grieve K, Biel K, Kudeyarov V, McLain JET, Lipson D, Murthy R (2005) Growth of Eastern Cottonwoods (*Populus deltoides*) in elevated [CO_2] stimulates stand-level respiration and rhizodeposition of carbohydrates, accelerates soil nutrient depletion, yet stimulates above-and belowground biomass production. Global Change Biology 11:1220–1233.

Barton CVM, Duursma RA, Medlyn BE, Ellsworth DS, Eamus D, Tissue DT, Adams MA, Conroy J, Crous KY, Liberloo M, Others (2012) Effects of elevated atmospheric [CO_2] on instantaneous transpiration efficiency at leaf and canopy scales in *Eucalyptus saligna*. Global Change Biology 18:585–595.

Barton CVM, Ellsworth DS, Medlyn BE, Duursma RA, Tissue DT, Adams MA, Eamus D, Conroy JP, McMurtrie RE, Parsby J, Others (2010) Whole-tree chambers for elevated atmospheric CO_2 experimentation and tree scale flux measurements in south-eastern Australia: The Hawkesbury Forest Experiment. Agricultural and Forest Meteorology 150:941–951.

Bates D, Maechler M, Bolker B, Walker S (2015) Fitting linear mixed-effects models using lme4. Journal of Statistical Software 67:1–48.

Bazzaz FA, Ackerly DD, Reekie EG (2000) Reproductive allocation in plants. In : Seeds: the ecology of regeneration in plant communities. Elsevier Academic Press, Cambridge, Massachusetts, pp 1-29.

Biran I, Eliassaf A (1980a) The effect of container size and aeration conditions on growth of roots and canopy of woody plants. Scientia Horticulturae 12:385–394.

Biran I, Eliassaf A (1980b) The effect of container shape on the development of roots and canopy of woody plants. Scientia Horticulturae 12:183–193.

Bloom AJ, Chapin FS, Mooney HA (1985) Resource limitation in plants–an economic analogy. Annual Review of Ecology and Systematics 16:363–392.

Boardman NK (1977) Comparative photosynthesis of sun and shade plants. Annual Review of Plant Physiology 28:355–377.

Boland DJ, Brooker MIH, Chippendale GM, Hall N, Hyland BPM, Johnston RD, Kleinig DA, McDonald MW, Turner JD (2006) Forest trees of Australia. CSIRO publishing, Collingwood, Victoria, pp 768.

Booth TH (2013) Eucalypt plantations and climate change. Forest Ecology and Management 301:28–34.

Bradford KJ, Hsiao TC (1982) Physiological responses to moderate water stress. In: Physiological plant ecology II. Springer-Verlag Berlin Heidelberg, New York, pp 263–324.

Brando PM, Nepstad DC, Davidson EA, Trumbore SE, Ray D, Camargo P (2008) Drought effects on litterfall, wood production and belowground carbon cycling in an Amazon forest: results of a throughfall reduction experiment. Philosophical Transactions of the Royal Society B: Biological Sciences 363:1839–1848.

Brantley ST, Young DR (2009) Contribution of sunflecks is minimal in expanding shrub thickets compared to temperate forest. Ecology 90:1021–1029.

Broeckx LS, Verlinden MS, Berhongaray G, Zona D, Fichot R, Ceulemans R (2014) The effect of a dry spring on seasonal carbon allocation and vegetation dynamics in a poplar bioenergy plantation. GCB Bioenergy 6:473–487.

Burgess SSO, Pittermann J, Dawson TE (2006) Hydraulic efficiency and safety of branch xylem increases with height in *Sequoia sempervirens* (D. Don) crowns. Plant, Cell & Environment 29:229–239.

Burton AJ, Pregitzer KS, Zogg GP, Zak DR (1998) Drought reduces root respiration in sugar maple forests. Ecological Applications 8:771–778.

Byrne M, Prober S, McLean E, Steane D, Stock W, Potts B, Vaillancourt R (2013) Adaptation to climate in widespread eucalypt species. Gold Coast: National Climate Change Adaptation Research Facility, pp 1-96.

Cannell MGR, Jackson JE (1985) Attributes of trees as crop plants. Institute of Terrestrial Ecology.

Chapin FS, Bloom AJ, Field CB, Waring RH (1987) Plant responses to multiple environmental factors. Bioscience 37:49–57.

Chapin FS, Schulze E-D, Mooney HA (1990) The ecology and economics of storage in plants. Annual Review of Ecology and Systematics 21:423–447.

Chazdon RL, Pearcy RW (1991) The importance of sunflecks for forest understory plants. Bioscience 41(11):760–766.

Cheng W, Fu S, Susfalk RB, Mitchell RJ (2005) Measuring tree root respiration using ^{13}C natural abundance: rooting medium matters. New Phytologist 167:297–307.

Cowan IR (1981) Coping with water stress. In: The biology of Australian Plants. University of West Australia Press, Nedlands, pp 1–32.

Cowan IR, Farquhar GD (1977) Stomatal function in relation to leaf metabolism and environment. Symposia of the Society for Experimental Biology 31:471–505.

Crous KY, Quentin AG, Lin Y-S, Medlyn BE, Williams DG, Barton CVM, Ellsworth DS (2013) Photosynthesis of temperate *Eucalyptus globulus* trees outside their native range has limited adjustment to elevated CO_2 and climate warming. Global Change Biology 19:3790–3807.

Crous KY, Walters MB, Ellsworth DS (2008) Elevated CO_2 concentration affects leaf photosynthesis–nitrogen relationships in *Pinus taeda* over nine years in FACE. Tree Physiology 28: 607–614.

Crous KY, Zaragoza-Castells J, Ellsworth DS, Duursma RA, Loew M, Tissue DT, Atkin OK (2012) Light inhibition of leaf respiration in field-grown *Eucalyptus saligna* in whole-tree chambers under elevated atmospheric CO_2 and summer drought. Plant, Cell & Environment 35:966–981.

Crous KY, Zaragoza-Castells J, Loew M, Ellsworth DS, Tissue DT, Tjoelker MG, Barton CVM, Gimeno TE, Atkin OK (2011) Seasonal acclimation of leaf respiration in *Eucalyptus saligna* trees: impacts of elevated atmospheric CO_2 and summer drought. Global Change Biology 17:1560–1576.

Dai Y, Dickinson RE, Wang Y-P (2004) A two-big-leaf model for canopy temperature, photosynthesis, and stomatal conductance. Journal of Climate 17:2281–2299.

Davidson RL (1969) Effect of root/leaf temperature differentials on root/shoot ratios in some pasture grasses and clover. Annals of Botany 33:561–569.

Davidson EA, Savage K, Bolstad P, Clark DA, Curtis PS, Ellsworth DS, Hanson PJ, Law BE, Luo Y, Pregitzer KS, Others (2002) Belowground carbon allocation in forests estimated from litterfall and IRGA-based soil respiration measurements. Agricultural and Forest Meteorology 113:39–51.

De Kauwe MG, Medlyn BE, Zaehle S, Walker AP, Dietze MC, Wang Y-P, Luo Y, Jain AK, El-Masri B, Hickler T, Others (2014) Where does the carbon go? A model–data intercomparison of vegetation carbon allocation and turnover processes at two temperate forest free-air CO_2 enrichment sites. New Phytologist 203:883–899.

De Pury DGG, Farquhar GD (1997) Simple scaling of photosynthesis from leaves to canopies without the errors of big-leaf models. Plant, Cell and Environment 20:537–557.

DeLucia E, Drake JE, Thomas RB, Gonzalez-Meler M (2007) Forest carbon use efficiency: Is respiration a constant fraction of gross primary production? Global Change Biology 13:1157–1167.

DeLucia EH, Moore DJ, Norby RJ (2005) Contrasting responses of forest ecosystems to rising atmospheric CO_2: implications for the global C cycle. Global Biogeochemical Cycles 19(3): GB3006.

Dickson RE (1989) Carbon and nitrogen allocation in trees. In: Annales des sciences forestières. Elsevier, pp 631s–647s.

Dietze MC, Sala A, Carbone MS, Czimczik CI, Mantooth JA, Richardson AD, Vargas R (2014) Nonstructural carbon in woody plants. Annual Review of Plant Biology 65:667–687.

Drake JE, Aspinwall MJ, Pfautsch S, Rymer PD, Reich PB, Smith RA, Crous KY, Tissue DT, Ghannoum O, Tjoelker MG (2014) The capacity to cope with climate warming declines from temperate to tropical latitudes in two widely distributed *Eucalyptus* species. Global Change Biology 21:459–472.

Drake BG, Gonzàlez-Meler MA, Long SP (1997) More efficient plants: a consequence of rising atmospheric CO_2? Annual Review of Plant Biology 48:609–639.

Duan W, Fan PG, Wang LJ, Li WD, Yan ST, Li SH (2008) Photosynthetic response to low sink demand after fruit removal in relation to photoinhibition and photoprotection in peach trees. Tree Physiology 28:123–132.

Duursma RA (2014) YplantQMC: plant architectural analysis with Yplant and QuasiMC. http://www.remkoduursma.com/yplantqmc, https://www.bitbucket.org/remkoduursma/yplantqmc/.

Duursma RA (2015) Plantecophys - An R package for analysing and modelling leaf gas exchange data. PLoS ONE 10(11): e0143346.

Duursma RA, Barton CVM, Eamus D, Medlyn BE, Ellsworth DS, Forster MA, Tissue DT, Linder S, McMurtrie RE (2011) Rooting depth explains [CO_2] x drought interaction in *Eucalyptus saligna*. Tree Physiology 31:922–931.

Duursma RA, Barton CVM, Lin Y-S, Medlyn BE, Eamus D, Tissue DT, Ellsworth DS, McMurtrie RE (2014) The peaked response of transpiration rate to vapour pressure deficit in field conditions can be explained by the temperature optimum of photosynthesis. Agricultural and Forest Meteorology 189:2–10.

Duursma RA, Falster DS, Valladares F, Sterck FJ, Pearcy RW, Lusk CH, Sendall KM, Nordenstahl M, Houter NC, Atwell BJ, Others (2012) Light interception efficiency explained by two simple variables: a test using a diversity of small-to medium-sized woody plants. New Phytologist 193:397–408.

Duursma RA, Payton P, Bange MP, Broughton KJ, Smith RA, Medlyn BE, Tissue DT (2013) Near-optimal response of instantaneous transpiration efficiency to vapour pressure deficit, temperature and [CO_2] in cotton (*Gossypium hirsutum* L.). Agricultural and Forest Meteorology 168:168–176.

Ebell LF (1969) Variation in total soluble sugars of conifer tissues with method of analysis. Phytochemistry 8:227–233.

Ellsworth DS, Reich PB (1993) Canopy structure and vertical patterns of photosynthesis and related leaf traits in a deciduous forest. Oecologia 96:169–178.

Epron D, Nouvellon Y, Ryan MG (2012) Introduction to the invited issue on carbon allocation of trees and forests. Tree Physiology 32:639–643.

Equiza MA, Day ME, Jagels R, Li X (2006) Photosynthetic downregulation in the conifer *Metasequoia glyptostroboides* growing under continuous light: the significance of carbohydrate sinks and paleoecophysiological implications. Botany 84:1453–1461.

Evans JR (1995) Carbon fixation profiles do reflect light absorption profiles in leaves. Functional Plant Biology 22:865–873.

Evans J, Poorter H (2001) Photosynthetic acclimation of plants to growth irradiance: the relative importance of specific leaf area and nitrogen partitioning in maximizing carbon gain. Plant, Cell & Environment 24:755–767.

Evans JR, Von Caemmerer S (2013) Temperature response of carbon isotope discrimination and mesophyll conductance in tobacco. Plant, Cell & Environment 36:745–756.

Evans JR, Sharkey TD, Berry JA, Farquhar GD (1986) Carbon isotope discrimination measured concurrently with gas exchange to investigate CO_2 diffusion in leaves of higher plants. Functional Plant Biology 13:281–292.

Eyles A, Pinkard EA, Davies NW, Corkrey R, Churchill K, O'Grady AP, Sands P, Mohammed C (2013) Whole-plant versus leaf-level regulation of photosynthetic responses after partial defoliation in *Eucalyptus globulus* saplings. Journal of Experimental Botany 64:1625–1636.

Falik O, Reides P, Gersani M, Novoplansky A (2005) Root navigation by self inhibition. Plant, Cell & Environment 28:562–569.

Falster DS, Westoby M (2003) Leaf size and angle vary widely across species: What consequences for light interception? New Phytologist 158:509–525.

Farquhar GD, Cernusak LA (2012) Ternary effects on the gas exchange of isotopologues of carbon dioxide. Plant, Cell & Environment 35:1221–1231.

Farquhar GD, Sharkey TD (1982) Stomatal conductance and photosynthesis. Annual Review of Plant Physiology 33:317–345.

Farquhar GD, Caemmerer S von von, Berry JA (1980) A biochemical model of photosynthetic CO_2 assimilation in leaves of C3 species. Planta 149:78–90.

Fatichi S, Leuzinger S, Körner C (2014) Moving beyond photosynthesis: from carbon source to sink-driven vegetation modeling. New Phytologist 201:1086–1095.

Field C (1983) Allocating leaf nitrogen for the maximization of carbon gain: leaf age as a control on the allocation program. Oecologia 56:341–347.

Field CH, Mooney HA (1986) Photosynthesis–nitrogen relationship in wild plants. In: On the economy of plant form and function: Proceedings of the sixth maria moors cabot symposium. Cambridge University Press, Cambridge, UK, pp 25-55.

Flexas J, Diaz-Espejo A, Galmes J, Kaldenhoff R, Medrano H, Ribas-Carbó M (2007) Rapid variations of mesophyll conductance in response to changes in CO_2 concentration around leaves. Plant, Cell & Environment 30:1284–1298.

Flexas J, Ribas-Carbó M, Diaz-Espejo A, Galmes J, Medrano H (2008) Mesophyll conductance to CO_2: current knowledge and future prospects. Plant, Cell & Environment 31:602–621.

Fourcaud T, Zhang X, Stokes A, Lambers H, Körner C (2008) Plant growth modelling and applications: the increasing importance of plant architecture in growth models. Annals of Botany 101:1053–1063.

Franklin O, Johansson J, Dewar RC, Dieckmann U, McMurtrie RE, Brännström Å, Dybzinski R (2012) Modeling carbon allocation in trees: a search for principles. Tree Physiology 32:648–666.

Friedlingstein P, Joel G, Field CB, Fung IY (1999) Toward an allocation scheme for global terrestrial carbon models. Global Change Biology 5:755–770.

Genet H, Bréda N, Dufrêne E (2010) Age-related variation in carbon allocation at tree and stand scales in beech (*Fagus sylvatica* L.) and sessile oak (*Quercus petraea* (Matt.) Liebl.) using a chronosequence approach. Tree Physiology 30:177–192.

Giardina CP, Ryan MG (2002) Total belowground carbon allocation in a fast-growing *Eucalyptus* plantation estimated using a carbon balance approach. Ecosystems 5:487–499.

Giardina CP, Coleman MD, Hancock JE, King JS, Lilleskov EA, Loya WM, Pregitzer KS, Ryan MG, Trettin CC (2005) The response of belowground carbon allocation in forests to global change. In: Tree species effects on soils: Implications for global change. Springer, pp 119–154.

Givnish TJ (1988) Adaptation to sun and shade: a whole-plant perspective. Functional Plant Biology 15:63–92.

Gough CM, Vogel CS, Schmid HP, Su H-B, Curtis PS (2008) Multi-year convergence of biometric and meteorological estimates of forest carbon storage. Agricultural and Forest Meteorology 148:158–170.

Gould SJ (1966) Allometry and size in ontogeny and phylogeny. Biological Reviews 41:587–640.

Grace J (1997) Toward Models of Resource Allocation by Plants. In: Plant Resource Allocation. Academic Press, pp 279–291.

Griffiths H, Helliker BR (2013) Mesophyll conductance: internal insights of leaf carbon exchange. Plant, Cell & Environment 36:733–735.

Gunderson CA, Wullschleger SD (1994) Photosynthetic acclimation in trees to rising atmospheric CO_2: a broader perspective. Photosynthesis Research 39:369–388.

Hanba YT, Shibasaka M, Hayashi Y, Hayakawa T, Kasamo K, Terashima I, Katsuhara M (2004) Overexpression of the barley aquaporin HvPIP2; 1 increases internal CO_2 conductance and CO_2 assimilation in the leaves of transgenic rice plants. Plant, and Cell Physiology 45:521–529.

Handa IT, Körner C, Hättenschwiler S (2005) A test of the treeline carbon limitation hypothesis by in situ CO_2 enrichment and defoliation. Ecology 86:1288–1300.

Hanson B, Sugden A, Alberts B (2011) Making data maximally available. Science 331:649.

Haouari A, Van Labeke M-C, Steppe K, Mariem FB, Braham M, Chaieb M (2013) Fruit thinning affects photosynthetic activity, carbohydrate levels, and shoot and fruit development of olive trees grown under semiarid conditions. Functional Plant Biology 40:1179–1186.

Hassiotou F, Ludwig M, Renton M, Veneklaas EJ, Evans JR (2009) Influence of leaf dry mass per area, CO_2, and irradiance on mesophyll conductance in sclerophylls. Journal of Experimental Botany 60:2303–2314.

Health J, Kerstiens G (1997) Effects of elevated CO_2 on leaf gas exchange in beech and oak at two levels of nutrient supply: consequences for sensitivity to drought in beech. Plant, Cell and Environment 20:57–67.

Heinen RB, Ye Q, Chaumont F (2009) Role of aquaporins in leaf physiology. Journal of Experimental Botany 60:2971–2985.

Héroult A, Lin Y-S, Bourne A, Medlyn BE, Ellsworth DS (2013) Optimal stomatal conductance in relation to photosynthesis in climatically contrasting *Eucalyptus* species under drought. Plant, Cell & Environment 36:262–274.

Hoch G, Popp M, Körner C (2002) Altitudinal increase of mobile carbon pools in *Pinus cembra* suggests sink limitation of growth at the Swiss treeline. Oikos 98:361–374.

Hubbard RM, Ryan MG, Stiller V, Sperry JS (2001) Stomatal conductance and photosynthesis vary linearly with plant hydraulic conductance in ponderosa pine. Plant, Cell & Environment 24:113–121.

Hughes L (2003) Climate change and Australia: trends, projections and impacts. Austral Ecology 28:423–443.

Hughes L (2011) Cumberland Plain Woodland in the Sydney Basin Bioregion – proposed critically endangered ecological community listing. http://www.environment.nsw.gov.au/determinations/cumberlandplainpd.htm (1 November 2015, date last accessed).

Iglesias DJ, Lliso I, Tadeo FR, Talon M (2002) Regulation of photosynthesis through source: sink imbalance in citrus is mediated by carbohydrate content in leaves. Physiologia Plantarum 116:563–572.

IPCC (2014) Climate Change 2014: Synthesis Report. Contribution of working groups I, II and III to the fifth assessment report of the intergovernmental panel on climate change. IPCC, Geneva, Switzerland, pp 151.

IUFRO (2015) International Union of Forestry Research Organizations. http://www.euciufro2015.com/en/ (12 August 2015, date last accessed).

Iversen CM (2010) Digging deeper: fine-root responses to rising atmospheric CO_2 concentration in forested ecosystems. New Phytologist 186:346–357.

Iversen C, Norby R (2014) Terrestrial plant productivity and carbon allocation in a changing climate. In: Global environmental change. Springer, pp 297–316.

James SA, Bell DT (2000) Leaf orientation, light interception and stomatal conductance of *Eucalyptus globulus* ssp. globulus leaves. Tree Physiology 20:815–823.

Jifon JL, Syvertsen JP (2003) Moderate shade can increase net gas exchange and reduce photoinhibition in citrus leaves. Tree Physiology 23:119–127.

Kallarackal J, Somen CK (1997) An ecophysiological evaluation of the suitability of *Eucalyptus grandis* for planting in the tropics. Forest Ecology and Management 95:53–61.

King DA (1997) The functional significance of leaf angle in *Eucalyptus*. Australian Journal of Botany 45:619–639.

Kirschbaum MUF (2011) Does enhanced photosynthesis enhance growth? Lessons learned from CO_2 enrichment studies. Plant Physiology 155:117–124.

Kitao M, Lei TT, Koike T, Kayama M, Tobita H, Maruyama Y (2007) Interaction of drought and elevated CO_2 concentration on photosynthetic down-regulation and susceptibility to photoinhibition in Japanese white birch seedlings grown with limited N availability. Tree Physiology 27:727–735.

Klein T, Hoch G (2015) Tree carbon allocation dynamics determined using a carbon mass balance approach. New Phytologist 205:147–159.

Kozlowski TT (1992) Carbohydrate sources and sinks in woody plants. The Botanical Review 58:107–222.

Körner C (2006) Plant CO_2 responses: an issue of definition, time and resource supply. New Phytologist 172:393–411.

Körner C (2013) Growth controls photosynthesis–mostly. Nova Acta Leopoldina 114:273–283.

Körner C, Asshoff R, Bignucolo O, Hättenschwiler S, Keel SG, Peláez-Riedl S, Pepin S, Siegwolf RTW, Zotz G (2005) Carbon flux and growth in mature deciduous forest trees exposed to elevated CO_2. Science 309:1360–1362.

Küppers M, Schneider H (1993) Leaf gas exchange of beech (*Fagus sylvatica* L.) seedlings in lightflecks: effects of fleck length and leaf temperature in leaves grown in deep and partial shade. Trees 7:160–168.

Lacointe A (2000) Carbon allocation among tree organs: a review of basic processes and representation in functional-structural tree models. Annals of Forest Science 57:521–533.

Lambers H, Chapin FS, Pons TL (2008) Plant physiological ecology, 2nd ed. Springer, New York, pp 605.

Landsberg J (2003) Modelling forest ecosystems: state of the art, challenges, and future directions. Canadian Journal of Forest Research 33:385–397.

Law BE, Ryan MG, Anthoni PM (1999) Seasonal and annual respiration of a ponderosa pine ecosystem. Global Change Biology 5:169–182.

Layne DR, Flore JA (1995) End-product inhibition of photosynthesis in *Prunus cerasus* L. in response to whole-plant source-sink manipulation. Journal of the American Society for Horticultural Science 120:583–599.

Le Roux X, Lacointe A, Escobar-Gutiérrez A, Le Dizès S (2001) Carbon-based models of individual tree growth: a critical appraisal. Annals of Forest Science 58:469–506.

Leakey ADB, Press MC, Scholes JD (2003) High-temperature inhibition of photosynthesis is greater under sunflecks than uniform irradiance in a tropical rain forest tree seedling. Plant, Cell & Environment 26:1681–1690.

Leakey ADB, Press MC, Scholes JD, Watling JR (2002) Relative enhancement of photosynthesis and growth at elevated CO_2 is greater under sunflecks than uniform irradiance in a tropical rain forest tree seedling. Plant, Cell & Environment 25:1701–1714.

Leuning R (1997) Scaling to a common temperature improves the correlation between the photosynthesis parameters J_{max} and V_{cmax}. Journal of Experimental Botany 48: 345–347.

Leuning R, Kelliher FM, Pury DGG de, Schulze E-D (1995) Leaf nitrogen, photosynthesis, conductance and transpiration: scaling from leaves to canopies. Plant, Cell & Environment 18:1183–1200.

Li WD, Li SH, Yang SH, Yang JM, Zheng XB, Li XD, Yao HM (2005) Photosynthesis in response to sink-source manipulations during different phenological stages of fruit development in peach trees: regulation by stomatal aperture and leaf temperature. Journal of Horticultural Science & Biotechnology 80:481–487.

Li G, Santoni V, Maurel C (2014) Plant aquaporins: roles in plant physiology. Biochimica et Biophysica Acta (BBA)-General Subjects 1840(5):1574–1582.

Lin Y-S, Medlyn BE, Duursma RA, Prentice IC, Wang H, Baig S, Eamus D, Dios VR de, Mitchell P, Ellsworth DS, et al. (2015) Optimal stomatal behaviour around the world. Nature Climate Change 5:459–464.

Linderson M-L, Mikkelsen TN, Ibrom A, Lindroth A, Ro-Poulsen H, Pilegaard K (2012) Up-scaling of water use efficiency from leaf to canopy as based on leaf gas exchange relationships and the modeled in-canopy light distribution. Agricultural and Forest Meteorology 152:201–211.

Lindroth A, Lagergren F, Aurela M, Bjarnadottir B, Christensen T, Dellwik E, Grelle A, Ibrom A, Johansson T, Lankreijer H, et al. (2008) Leaf area index is the principal scaling parameter for both gross photosynthesis and ecosystem respiration of Northern deciduous and coniferous forests. Tellus B 60:129–142.

Litton CM, Raich JW, Ryan MG (2007) Carbon allocation in forest ecosystems. Global Change Biology 13:2089–2109.

Lleonart J, Salat J, Torres GJ (2000) Removing allometric effects of body size in morphological analysis. Journal of Theoretical Biology 205:85–93.

Lloyd J, Syvertsen JP, Kriedemann PE, Farquhar GD (1992) Low conductances for CO_2 diffusion from stomata to the sites of carboxylation in leaves of woody species. Plant, Cell & Environment 15:873–899.

Loewe A, Einig W, Shi L, Dizengremel P, Hampp R (2000) Mycorrhiza formation and elevated CO_2 both increase the capacity for sucrose synthesis in source leaves of spruce and aspen. New Phytologist 145(3):565–574.

Lohier T, Jabot F, Meziane D, Shipley B, Reich PB, Deffuant G (2014) Explaining ontogenetic shifts in root–shoot scaling with transient dynamics. Annals of Botany 114:513–524.

Maina GG, Brown JS, Gersani M (2002) Intra-plant versus inter-plant root competition in beans: avoidance, resource matching or tragedy of the commons. Plant Ecology 160:235–247.

Marchiori PER, Machado EC, Ribeiro RV (2014) Photosynthetic limitations imposed by self-shading in field-grown sugarcane varieties. Field Crops Research 155: 30–37.

Markkola A, Kuikka K, Rautio P, Härmä E, Roitto M, Tuomi J (2004) Defoliation increases carbon limitation in ectomycorrhizal symbiosis of *Betula pubescens*. Oecologia 140:234–240.

Marshall JD (1986) Drought and shade interact to cause fine-root mortality in Douglas-fir seedlings. Plant and Soil 91:51–60.

Marshall JD, Brooks JR, Lajtha K (2007) Sources of variation in the stable isotopic composition of plants. In: Stable Isotopes in Ecology and Environmental Science. Blackwell Publishing Ltd, Oxford, UK, pp 22–60.

Mäkelä A (1997) A carbon balance model of growth and self-pruning in trees based on structural relationships. Forest Science 43:7–24.

Mäkelä A (2012) On guiding principles for carbon allocation in eco-physiological growth models. Tree Physiology 32:644–647.

McCarthy HR, Oren R, Finzi AC, Johnsen KH (2006) Canopy leaf area constrains [CO_2]-induced enhancement of productivity and partitioning among aboveground carbon pools. Proceedings of the National Academy of Sciences 103:19356–19361.

McCleary BV, Gibson TS, Mugford DC (1997) Measurement of total starch in cereal products by amyloglucosidase-α-amylase method: Collaborative study. Journal of AOAC International 80:571–579.

McConnaughay KDM, Bazzaz FA (1991) Is physical space a soil resource? Ecology 72(1):94–103.

McConnaughay KDM, Coleman JS (1999) Biomass allocation in plants: ontogeny or optimality? A test along three resource gradients. Ecology 80:2581–2593.

McDowell NG, Beerling DJ, Breshears DD, Fisher RA, Raffa KF, Stitt M (2011) The interdependence of mechanisms underlying climate-driven vegetation mortality. Trends in Ecology & Evolution 26:523–532.

McMurtrie RE, Dewar RC (2013) New insights into carbon allocation by trees from the hypothesis that annual wood production is maximized. New Phytologist 199:981–990.

Medhurst J, Parsby J, Linder S, Wallin G, Ceschia E, Slaney M (2006) A whole-tree chamber system for examining tree-level physiological responses of field-grown trees to environmental variation and climate change. Plant, Cell & Environment 29:1853–1869.

Medlyn BE (1996) The optimal allocation of nitrogen within the C3 photosynthetic system at elevated CO_2. Functional Plant Biology 23: 593–603.

Medlyn BE, Badeck F-W, De Pury DGG, Barton CVM, Broadmeadow M, Ceulemans R, De Angelis P, Forstreuter M, Jach ME, Kellomäki S et al. (1999) Effects of elevated [CO_2] on photosynthesis in European forest species: a meta-analysis of model parameters. Plant, Cell & Environment 22: 1475–1495.

Medlyn BE, Dreyer E, Ellsworth D, Forstreuter M, Harley PC, Kirschbaum MUF, Le Roux X, Montpied P, Strassemeyer J, Walcroft A, et al. (2002) Temperature response of parameters of a biochemically based model of photosynthesis. II. A review of experimental data. Plant, Cell & Environment 25:1167–1179.

Medlyn BE, Duursma RA, Eamus D, Ellsworth DS, Prentice IC, Barton CVM, Crous KY, Angelis P de, Freeman M, Wingate L (2011) Reconciling the optimal and empirical approaches to modelling stomatal conductance. Global Change Biology 17:2134–2144.

Meier IC, Leuschner C (2008) Belowground drought response of European beech: fine root biomass and carbon partitioning in 14 mature stands across a precipitation gradient. Global Change Biology 14:2081–2095.

Mitchell PJ, O'Grady AP, Tissue DT, White DA, Ottenschlaeger ML, Pinkard EA (2013) Drought response strategies define the relative contributions of hydraulic dysfunction and carbohydrate depletion during tree mortality. New Phytologist 197:862–872.

Monsi M, Saeki T (2005) On the factor light in plant communities and its importance for matter production. Annals of Botany 95:549–567.

Mooney HA (1972) The carbon balance of plants. Annual Review of Ecology and Systematics 3:315–346.

Mooney HA, Gulmon SL (1979) Environmental and evolutionary constraints on the photosynthetic characteristics of higher plants. In: Topics in plant population biology, Columbia University Press, New York, pp 316-337.

Müller I, Schmid B, Weiner J (2000) The effect of nutrient availability on biomass allocation patterns in 27 species of herbaceous plants. Perspectives in Plant Ecology, Evolution and Systematics 3:115–127.

Nakagawa S, Schielzeth H (2013) A general and simple method for obtaining R^2 from generalized linear mixed-effects models. Methods in Ecology and Evolution 4:133–142.

Nebauer SG, Renau-Morata B, Guardiola JL, Molina R-V (2011) Photosynthesis down-regulation precedes carbohydrate accumulation under sink limitation in Citrus. Tree Physiology 31:169–177.

NeSmith DS, Duval JR (1998) The effect of container size. HortTechnology 8:495–498.

Niinemets Ü (2007) Photosynthesis and resource distribution through plant canopies. Plant, Cell & Environment 30:1052–1071.

Niinemets Ü (2010) A review of light interception in plant stands from leaf to canopy in different plant functional types and in species with varying shade tolerance. Ecological Research 25:693–714.

Niinemets Ü (2012) Optimization of foliage photosynthetic capacity in tree canopies: towards identifying missing constraints. Tree Physiology 32:505–509.

Niinemets Ü, Anten NPR (2009) Packing the photosynthetic machinery: from leaf to canopy. In: Photosynthesis in silico. Springer, pp 363–399.

Niinemets Ü, Valladares F (2004) Photosynthetic acclimation to simultaneous and interacting environmental stresses along natural light gradients: optimality and constraints. Plant Biology 6:254–268.

Norby RJ, DeLucia EH, Gielen B, Calfapietra C, Giardina CP, King JS, Ledford J, McCarthy HR, Moore DJP, Ceulemans R, et al. (2005) Forest response to elevated CO_2 is conserved across a broad range of productivity. Proceedings of the National Academy of Sciences of the United States of America 102:18052–18056.

Ovaska J, Sari R, Rintamäki E, Vapaavuori E (1993) Combined effects of partial defoliation and nutrient availability on cloned *Betula pendula* saplings II. Changes in net photosynthesis and related biochemical properties. Journal of Experimental Botany 44:1395–1402.

Ovaska J, Walls M, Vapaavuori E (1993) Combined effects of partial defoliation and nutrient availability on cloned *Betula pendula* saplings I. Changes in growth, partitioning and nitrogen uptake. Journal of Experimental Botany 44:1385–1393.

Palacio S, Hernández R, Maestro-Martínez M, Camarero JJ (2012) Fast replenishment of initial carbon stores after defoliation by the pine processionary moth and its relationship to the re-growth ability of trees. Trees 26:1627–1640.

Palacio S, Hoch G, Sala A, Körner C, Millard P (2014) Does carbon storage limit tree growth? New Phytologist 201:1096–1100.

Palmroth S, Oren R, McCarthy HR, Johnsen KH, Finzi AC, Butnor JR, Ryan MG, Schlesinger WH (2006) Aboveground sink strength in forests controls the allocation of carbon below ground and its $[CO_2]$-induced enhancement. Proceedings of the National Academy of Sciences 103:19362–19367.

Passioura JB (2002) Soil conditions and plant growth. Plant, Cell & Environment 25:311–318.

Paul MJ, Foyer CH (2001) Sink regulation of photosynthesis. Journal of Experimental Botany 52:1383–1400.

Pearcy RW (1990) Sunflecks and photosynthesis in plant canopies. Annual Review of Plant Biology 41:421–453.

Pearcy RW, Way DA (2012) Two decades of sunfleck research: looking back to move forward. Tree Physiology 32:1059–1061.

Peltoniemi MS, Duursma RA, Medlyn BE (2012) Co-optimal distribution of leaf nitrogen and hydraulic conductance in plant canopies. Tree Physiology 32:510–519.

Peng RD (2011) Reproducible research in computational science. Science 334:1226-1227.

Pepin S, Livingston NJ (1997) Rates of stomatal opening in conifer seedlings in relation to air temperature and daily carbon gain. Plant, Cell & Environment 20:1462–1472.

Phillips RP, Erlitz Y, Bier R, Bernhardt ES (2008) New approach for capturing soluble root exudates in forest soils. Functional Ecology 22:990–999.

Phillips RP, Finzi AC, Bernhardt ES (2011) Enhanced root exudation induces microbial feedbacks to N cycling in a pine forest under long-term CO_2 fumigation. Ecology Letters 14:187–194.

Picon C, Ferhi A, Guehl J-M (1997) Concentration and $\delta^{13}C$ of leaf carbohydrates in relation to gas exchange in *Quercus robur* under elevated CO_2 and drought. Journal of Experimental Botany 48:1547–1556.

Piel C, Frak E, Le Roux X, Genty B (2002) Effect of local irradiance on CO_2 transfer conductance of mesophyll in walnut. Journal of Experimental Botany 53:2423–2430.

Pinheiro J, Bates D, DebRoy S, Sarkar D, R Core Team (2015) nlme: Linear and nonlinear mixed effects models. R package version 3.1-122. http://cran.r-project.org/package=nlme.

Pinkard EA, Beadle CL, Davidson NJ, Battaglia M (1998) Photosynthetic responses of *Eucalyptus nitens* (Deane and Maiden) Maiden to green pruning. Trees 12:119–129.

Pinkard EA, Eyles A, O'Grady AP (2011) Are gas exchange responses to resource limitation and defoliation linked to source: sink relationships? Plant, Cell & Environment 34: 1652–1665.

Poorter H, Nagel O (2000) The role of biomass allocation in the growth response of plants to different levels of light, CO_2, nutrients and water: a quantitative review. Functional Plant Biology 27:595-607.

Poorter H, Bühler J, Dusschoten D van, Climent J, Postma JA (2012) Pot size matters: a meta-analysis of the effects of rooting volume on plant growth. Functional Plant Biology 39:839–850.

Poorter H, Jagodzinski AM, Ruiz-Peinado R, Kuyah S, Luo Y, Oleksyn J, Usoltsev VA, Buckley TN, Reich PB, Sack L (2015) How does biomass distribution change with size and differ among species? An analysis for 1200 plant species from five continents. New Phytologist 208:736–749.

Poorter H, Niinemets Ü, Poorter L, Wright IJ, Villar R (2009) Causes and consequences of variation in leaf mass per area (LMA): a meta-analysis. New Phytologist 182:565–588.

Poorter H, Niklas KJ, Reich PB, Oleksyn J, Poot P, Mommer L (2012) Biomass allocation to leaves, stems and roots: meta-analyses of interspecific variation and environmental control. New Phytologist 193:30–50.

Poorter H, Van Berkel Y, Baxter R, Den Hertog J, Dijkstra P, Gifford RM, Griffin KL, Roumet C, Roy J, Wong SC (1997) The effect of elevated CO_2 on the chemical composition and construction costs of leaves of 27 C3 species. Plant, Cell & Environment 20:472–482.

Prentice IC, Dong N, Gleason SM, Maire V, Wright IJ (2014) Balancing the costs of carbon gain and water transport: testing a new theoretical framework for plant functional ecology. Ecology Letters 17:82–91.

Pryor LD, Johnson LAS (1981) *Eucalyptus*, the universal Australian. In: Ecological biogeography of Australia. Springer, pp 499–536.

R Development Core Team R (2011) R: a language and environment for statistical computing team RDC (ed). 1:409. http://www.r-project.org.

Raich JW, Nadelhoffer KJ (1989) Belowground carbon allocation in forest ecosystems: global trends. Ecology 70:1346–1354.

Reich PB, Weisel Y, Eshel A, Kafkafi U (2002) Root-shoot relations: optimality in acclimation and adaptation or the 'Emperor's New Clothes'. In: Plant roots: the hidden half. Marcel Dekker, New York, pp 205–220.

Robbins NS, Pharr DM (1988) Effect of restricted root growth on carbohydrate metabolism and whole plant growth of *Cucumis sativus* L. Plant Physiology 87:409–413.

Rocha AV, Goulden ML, Dunn AL, Wofsy SC (2006) On linking interannual tree ring variability with observations of whole-forest CO_2 flux. Global Change Biology 12:1378–1389.

Roden JS, Ball MC (1996) The effect of elevated [co_2] on growth and photosynthesis of two *Eucalyptus* species exposed to high temperatures and water deficits. Plant Physiology 111:909–919.

Ronchi CP, DaMatta FM, Batista KD, Moraes GABK, Loureiro ME, Ducatti C (2006) Growth and photosynthetic down-regulation in *Coffea arabica* in response to restricted root volume. Functional Plant Biology 33:1013–1023.

Rustad LE (2008) The response of terrestrial ecosystems to global climate change: towards an integrated approach. Science of the Total Environment 404:222–235.

Ryan MG, Stape JL, Binkley D, Fonseca S, Loos RA, Takahashi EN, Silva CR, Silva SR, Hakamada RE, Ferreira JM, et al. (2010) Factors controlling *Eucalyptus* productivity: how water availability and stand structure alter production and carbon allocation. Forest Ecology and Management 259:1695–1703.

Sage RF (1994) Acclimation of photosynthesis to increasing atmospheric CO_2: the gas exchange perspective. Photosynthesis Research 39:351–368.

Sala A, Woodruff DR, Meinzer FC (2012) Carbon dynamics in trees: feast or famine? Tree Physiology 32:764–775.

Schulze E-D, Robichaux RH, Grace J, Rundel PW, Ehleringer JR (1987) Plant water balance. BioScience 37(1):30–37.

Schymanski SJ, Or D, Zwieniecki MA (2013) Stomatal control and leaf thermal and hydraulic capacitances under rapid environmental fluctuations. PloS ONE 8(1): e54231.

Sellin A (1999) Does pre-dawn water potential reflect conditions of equilibrium in plant and soil water status? Acta Oecologica 20:51–59.

Sellin A, Kupper P (2007) Effects of enhanced hydraulic supply for foliage on stomatal responses in little-leaf linden (*Tilia cordata* Mill.). European Journal of Forest Research 126:241–251.

Sellin A, Lubenets K (2010) Variation of transpiration within a canopy of silver birch: effect of canopy position and daily versus nightly water loss. Ecohydrology 3:467–477.

Sellin A, Õunapuu E, Kupper P (2008) Effects of light intensity and duration on leaf hydraulic conductance and distribution of resistance in shoots of silver birch (*Betula pendula*). Physiologia Plantarum 134:412–420.

Semchenko M, Zobel K, Heinemeyer A, Hutchings MJ (2008) Foraging for space and avoidance of physical obstructions by plant roots: a comparative study of grasses from contrasting habitats. New Phytologist 179:1162–1170.

Sevanto S, Dickman LT (2015) Where does the carbon go?—Plant carbon allocation under climate change. Tree Physiology 35:581–584.

Shipley B, Meziane D (2002) The balanced-growth hypothesis and the allometry of leaf and root biomass allocation. Functional Ecology 16:326–331.

Smith AM, Stitt M (2007) Coordination of carbon supply and plant growth. Plant, Cell & Environment 30:1126–1149.

SOFR (2013) Australia's State of the Forests Report. Department of Agriculture; Water Resources, Canberra, pp 464.

Stanturf JA, Vance ED, Fox TR, Kirst M (2013) *Eucalyptus* beyond its native range: Environmental issues in exotic bioenergy plantations. International Journal of Forestry Research 2013:1–5.

Strand AE, Pritchard SG, McCormack ML, Davis MA, Oren R (2008) Irreconcilable differences: fine-root life spans and soil carbon persistence. Science 319:456–458.

Sweet GB, Wareing PF (1966) Role of plant growth in regulating photosynthesis. Nature 210:77–79.

Tausz M, Warren CR, Adams MA (2005) Dynamic light use and protection from excess light in upper canopy and coppice leaves of *Nothofagus cunninghamii* in an old growth, cool temperate rainforest in Victoria, Australia. New Phytologist 165:143–156.

Tazoe Y, Von Caemmerer S, Badger MR, Evans JR (2009) Light and CO_2 do not affect the mesophyll conductance to CO_2 diffusion in wheat leaves. Journal of Experimental Botany 60:2291–2301.

Terashima I, Hanba YT, Tazoe Y, Vyas P, Yano S (2006) Irradiance and phenotype: comparative eco-development of sun and shade leaves in relation to photosynthetic CO_2 diffusion. Journal of Experimental Botany 57:343–354.

Thomas SC, Martin AR (2012a) Data from: Carbon content of tree tissues: a synthesis. http://dx.doi.org/10.5061/dryad.69sg2.

Thomas SC, Martin AR (2012b) Carbon content of tree tissues: a synthesis. Forests 3:332–352.

Thomas RB, Strain BR (1991) Root restriction as a factor in photosynthetic acclimation of cotton seedlings grown in elevated carbon dioxide. Plant Physiology 96:627–634.

Thornley JHM (1972) A model to describe the partitioning of photosynthate during vegetative plant growth. Annals of Botany 36:419–430.

Tissue DT, Barbour MM, Hunt JE, Turnbull MH, Griffin KL, Walcroft AS, Whitehead D (2006) Spatial and temporal scaling of intercellular CO_2 concentration in a temperate rain forest dominated by *Dacrydium cupressinum* in New Zealand. Plant, Cell & Environment 29:497–510.

Tjoelker MG, Oleksyn J, Reich PB (1998) Temperature and ontogeny mediate growth response to elevated CO_2 in seedlings of five boreal tree species. New Phytologist 140:197–210.

Tjoelker M, Oleksyn J, Reich PB (1999) Acclimation of respiration to temperature and CO_2 in seedlings of boreal tree species in relation to plant size and relative growth rate. Global Change Biology 5:679–691.

Turnbull TL, Adams MA, Warren CR (2007) Increased photosynthesis following partial defoliation of field-grown *Eucalyptus globulus* seedlings is not caused by increased leaf nitrogen. Tree Physiology 27:1481–1492.

Ubierna N, Marshall JD (2011) Estimation of canopy average mesophyll conductance using $\delta^{13}C$ of phloem contents. Plant, Cell & Environment 34:1521–1535.

Urban L, Alphonsout L (2007) Girdling decreases photosynthetic electron fluxes and induces sustained photoprotection in mango leaves. Tree Physiology 27:345–352.

Valentine HT, Mäkelä A (2005) Bridging process-based and empirical approaches to modeling tree growth. Tree Physiology 25:769–779.

Valentini R, Matteucci G, Dolman AJ, Schulze E-D, Rebmann C, Moors EJ, Granier A, Gross P, Jensen NO, Pilegaard K, et al. (2000) Respiration as the main determinant of carbon balance in European forests. Nature 404:861–865.

Vico G, Manzoni S, Palmroth S, Katul G (2011) Effects of stomatal delays on the economics of leaf gas exchange under intermittent light regimes. New Phytologist 192:640–652.

Vogelman TC, Nishio JN, Smith WK (1996) Leaves and light capture: light propagation and gradients of carbon fixation within leaves. Trends in Plant Science 1:65–70.

Von Caemmerer S, Evans JR (2014) Temperature responses of mesophyll conductance differ greatly between species. Plant, Cell & Environment 38:629–637.

Walter A, Christ MM, Barron-gafford GA, Grieve KA, Murthy R, Rascher U (2005) The effect of elevated CO_2 on diel leaf growth cycle, leaf carbohydrate content and canopy growth performance of *Populus deltoides*. Global Change Biology 11:1207–1219.

Wang D, Heckathorn SA, Wang X, Philpott SM (2012) A meta-analysis of plant physiological and growth responses to temperature and elevated CO_2. Oecologia 169:1–13.

Waring RH (1983) Estimating forest growth and efficiency in relation to canopy leaf area. Advances in Ecological Research 13:327–354.

Warren CR (2008) Stand aside stomata, another actor deserves centre stage: the forgotten role of the internal conductance to CO_2 transfer. Journal of Experimental Botany 59:1475–1487.

Warren CR, Dreyer E, Adams MA (2003a) Photosynthesis-Rubisco relationships in foliage of *Pinus sylvestris* in response to nitrogen supply and the proposed role of Rubisco and amino acids as nitrogen stores. Trees 17: 359–366.

Warren CR, Ethier GJ, Livingston NJ, Grant NJ, Turpin DH, Harrison DL, Black TA (2003b) Transfer conductance in second growth Douglas-fir (*Pseudotsuga menziesii* (Mirb.) Franco) canopies. Plant, Cell & Environment 26:1215–1227.

Warren JM, Iversen CM, Garten CT, Norby RJ, Childs J, Brice D, Evans RM, Gu L, Thornton P, Weston DJ (2012) Timing and magnitude of C partitioning through a young loblolly pine (*Pinus taeda* L.) stand using ^{13}C labeling and shade treatments. Tree Physiology 32:799–813.

Warren CR, Löw M, Matyssek R, Tausz M (2007) Internal conductance to CO_2 transfer of adult *Fagus sylvatica*: variation between sun and shade leaves and due to free-air ozone fumigation. Environmental and Experimental Botany 59:130–138.

Warton DI, Duursma RA, Falster DS, Taskinen S (2012) smatr 3–an R package for estimation and inference about allometric lines. Methods in Ecology and Evolution 3:257–259.

Way DA, Oren R (2010) Differential responses to changes in growth temperature between trees from different functional groups and biomes: a review and synthesis of data. Tree Physiology 30:669–688.

Way DA, Pearcy RW (2012) Sunflecks in trees and forests: from photosynthetic physiology to global change biology. Tree Physiology 32:1066–1081.

Wiley E, Helliker B (2012) A re-evaluation of carbon storage in trees lends greater support for carbon limitation to growth. New Phytologist 195:285–289.

Wilson JW (1965) Stand structure and light penetration. I. Analysis by point quadrats. Journal of Applied Ecology 2:383–390.

Wright IJ, Reich PB, Westoby M (2003) Least-cost input mixtures of water and nitrogen for photosynthesis. The American Naturalist 161:98–111.

Yin X (2002) Responses of leaf nitrogen concentration and specific leaf area to atmospheric CO_2 enrichment: a retrospective synthesis across 62 species. Global Change Biology 8:631–642.

Young IM, Montagu K, Conroy J, Bengough AG (1997) Mechanical impedance of root growth directly reduces leaf elongation rates of cereals. New Phytologist 135:613–619.

Zens MS, Webb CO (2002) Sizing up the shape of life. Science 295:1475–1476.

Zhou R, Quebedeaux B (2003) Changes in photosynthesis and carbohydrate metabolism in mature apple leaves in response to whole plant source-sink manipulation. Journal of the American Society for Horticultural Science 128:113–119.